

---

# Dissecting phospholipid metabolism pathways after glucose stress in *C. elegans*

---



# WPI

**Andre Francisco de Castro Vieira**

In partial requirements for the  
Degree of Doctor of Philosophy, Ph.D. in Biochemistry submitted to the Faculty of  
WORCESTER POLYTECHNIC INSTITUTE  
100 Institute Road, Worcester, Massachusetts 01609

Committee: Professors Carissa Olsen, Suzanne Scarlata, Arne Gericke, Jagan  
Srinivasan, Alonzo Ross.

October 03, 2022 © Copyright

All rights reserved

# Dissecting phospholipid metabolism pathways after glucose stress in *C. elegans*

by

Andre Francisco de Castro Vieira

In partial requirements for the  
Degree of Doctor of Philosophy, Ph.D. in Biochemistry submitted to the Faculty of  
WORCESTER POLYTECHNIC INSTITUTE  
100 Institute Road, Worcester, Massachusetts 01609

APPROVED:

\_\_\_\_\_ Carissa Olsen, PI, WPI CBC

\_\_\_\_\_ Suzanne Scarlata, WPI CBC

\_\_\_\_\_ Arne Gericke, WPI CBC

\_\_\_\_\_ Alonzo Ross, WPI CBC

\_\_\_\_\_ Jagan Srinivasan, WPI BBT

## Table of contents

List of figures .....	7
List of tables .....	9
Dedication .....	10
Dissertation summary.....	11
1. Chapter 1: Introduction .....	14
1.1. Glycerophospholipids: the most abundant component of membranes .....	15
1.1.1. Headgroup synthesis and its importance .....	19
1.1.2. The synthesis of fatty acids .....	21
1.1.3. The different types of fatty acids and their importance .....	23
1.2. Sphingolipids are essential to respond against external stimuli .....	26
1.3. Adopting <i>C. elegans</i> as a model to study membrane regulation .....	30
1.4. Glucose: an important carbohydrate and its multiple effects in the organism .....	32
1.5. Membrane sensors: a group of proteins recently characterized .....	34
1.6. Membranes are a dynamic structure constantly renewed .....	35
1.7. GC/MS and HPLC/MS-MS used in lipidomics .....	37
2. Chapter 2: The variability in the membrane levels of oleic and linoleic fatty acids is associated with high glucose stress response .....	40
2.1. Abstract .....	40
2.2. Introduction .....	41
2.3. Results.....	44

2.3.1. High dietary glucose alters the allocation of oleic acid in the PL membrane.....	44
2.3.2. Recovery period decreases oleic and linoleic fatty acid levels and palmitic acid over accumulates in longer stress periods .....	48
2.3.3. Membrane composition shows better adaptation and recovery after long periods of stress .....	51
2.3.4. Living bacteria is required for the impact of glucose stress on the membrane .....	55
2.4. Discussion .....	58
2.5. Methodologies & Techniques .....	62
2.5.1. Strains maintenance and population synchronization .....	62
2.5.2. Stress conditions, labeling strategy and time-course experiments ..	62
2.5.3. Recovery assay .....	63
2.5.4. Viability Curves and Lifespans .....	64
2.5.5. Heat-killed bacteria .....	64
2.5.6. Lipid Extraction and GC Analysis .....	65
2.5.7. Determining the synthesis of fatty acids .....	66
2.5.8. Phospholipid extraction and analysis using HPLC-MS/MS .....	67
3. Chapter 3: Monomethyl branched-chain fatty acids are critical for <i>Caenorhabditis elegans</i> survival in elevated glucose conditions .....	69
3.1. Abstract .....	69
3.2. Introduction .....	70
3.3. Results .....	74

3.3.1. Quantifying membrane dynamics with elevated dietary glucose .....	74
3.3.2. mmBCFAs are critical for surviving glucose supplementation .....	78
3.3.3. mmBCFAs act in the PAQR-2 network response to glucose stress ...	82
3.3.4. mmBCFAs act in parallel to the fluidity response in glucose stress ...	86
3.4. Discussion .....	89
3.5. Methodologies & Techniques .....	93
3.5.1. Bacteria and nematodes growth media and M9 buffer preparation ...	93
3.5.2. <i>C. elegans</i> and Bacteria Growth and Maintenance .....	95
3.5.3. Altered Dietary Conditions .....	96
3.5.4. RNAi Knockdown .....	97
3.5.5. Viability Curves and Lifespans .....	98
3.5.6. Stable Isotope Labeling Strategy .....	98
3.5.7. qRTPCR testing .....	98
3.5.8. Lipid Extraction and FAME creation .....	99
3.5.9. GC Analysis .....	100
4. Chapter 4: Targeted Lipidomics Reveals a Novel Role for Glucosylceramide in Glucose Response .....	101
4.1. Abstract .....	101
4.2. Introduction .....	102
4.3. Results .....	106
4.3.1. Phospholipid Populations with Glucose Exposure .....	106
4.3.2. Analysis of Phospholipid Classes and the Associated Fatty Acid Tails.....	109

4.3.3. Glycolipid Populations Respond to Glucose Diets .....	113
4.3.4. Ceramide and Glucosylceramide Pools Change with High Glucose Diets .....	116
4.3.5. Sphingolipid Synthesis is Critical for Survival in Elevated Glucose Conditions .....	117
4.4. Discussion .....	118
4.5. Methodologies & Techniques .....	121
4.5.1. Strains and RNAi treatment .....	121
4.5.2. Nematode Growth and Elevated Glucose Feeding Protocols .....	122
4.5.3. Extraction and Detection of Phospholipids by LC-MS/MS .....	122
4.5.4. Extraction and Detection of Sphingolipids by LC-MS/MS .....	124
4.5.5. Phospholipid and Sphingolipidomic Analysis .....	125
4.5.6. Survival Analysis .....	126
5. Chapter 5: Conclusions and future work .....	127
5.1. Overall Conclusion .....	127
5.1.1. Conclusion chapter 2 .....	128
5.1.2. Conclusion chapter 3 .....	129
5.1.3. Conclusion chapter 4 .....	130
5.1.4. Future directions .....	131
6. References .....	134

## List of figures

<b>Figure 1: Canonical structure of a phospholipid molecule.....</b>	<b>16</b>
<b>Figure 2: Chemical structure of headgroups .....</b>	<b>17</b>
<b>Figure 3: Chemical structure of fatty acid tails .....</b>	<b>18</b>
<b>Figure 4: Chemical structure of fatty acid tails .....</b>	<b>20</b>
<b>Figure 5: Fatty acid structure and synthesis pathway .....</b>	<b>22</b>
<b>Figure 6: Ceramide and glucosylceramide chemical structures .....</b>	<b>25</b>
<b>Figure 7: High concentrations of glucose revealed compromised flux of oleic and linoleic FA .....</b>	<b>47</b>
<b>Figure 8: Recovery periods induce significant alterations in membrane composition .....</b>	<b>50</b>
<b>Figure 9: Longer stress periods promote better adaptation of oleic and linoleic FAs .....</b>	<b>54</b>
<b>Figure 10: Glucose stress phenotypes require living bacteria .....</b>	<b>57</b>
<b>Figure 11: Wild-type nematodes under glucose stress maintain optimal membrane composition but have altered membrane dynamics .....</b>	<b>77</b>
<b>Figure 12: mmBCFAs are essential for survival with elevated dietary glucose ....</b>	<b>81</b>
<b>Figure 13: PAQR-2 upregulates mmBCFA production under glucose stress .....</b>	<b>83</b>
<b>Figure 14: elo-5 RNAi alters mmBCFAs dynamics in the membrane .....</b>	<b>85</b>
<b>Figure 15: Saturated fat supplementation promotes larval arrest in PAQR-2 mutants .....</b>	<b>86</b>

<b>Figure 16: mmBCFAs are not required to respond to elevated dietary saturated fatty acid .....</b>	<b>87</b>
<b>Figure 17: Nematodes fed palmitic acid show high levels in PLs and NLs .....</b>	<b>88</b>
<b>Figure 18: mmBCFAs play a role in the membrane's response to glucose stress .....</b>	<b>93</b>
<b>Figure 19: Global phospholipidomics were determined after 100mM glucose exposure .....</b>	<b>108</b>
<b>Figure 20: Glucose feeding impacts fatty acid saturation and length in phospholipids .....</b>	<b>112</b>
<b>Figure 21: RNAi of enzymes sphingolipid pathway in C. elegans compromises the level of GluCer 17:1;O2/22:0;O .....</b>	<b>115</b>
<b>Figure 22: Sphingolipid profile shifts after 100 mM glucose exposure .....</b>	<b>117</b>
<b>Figure 23: elo-3 and cgt-3 RNAi decrease the survival of the nematodes under glucose stress .....</b>	<b>118</b>
<b>Figure 24: Model representation of the findings obtained in this work .....</b>	<b>131</b>



## List of tables

<b>Table 1: Recipes used to prepare all media .....</b>	<b>95</b>
<b>Table 2: Bleach solution .....</b>	<b>96</b>
<b>Table 3: qRT-PCR genes .....</b>	<b>99</b>

*Dedication*

*To my family, friends, and everyone that believed in me, especially*

*Divino Vieira de Campos (In memoriam)*

*&*

*Carmen Lucia Braga de Castro Vieira*

*“Long you live and high you fly; Smiles you'll give and tears you'll cry;  
And all you touch and all you see; Is all your life will ever be”*

*Pink Floyd, 1973.*

## Dissertation Summary

The work presented in this dissertation focuses on understanding the mechanisms that adapt membrane composition in response to glucose stress. An animal undergoes many external and internal stressors throughout life, which require specific cellular responses that are often regulated by biochemical signaling pathways. Different stress conditions can trigger similar effects that are likely responded to by the same pathway. Nowadays, mechanisms responding to glucose stress are receiving good attention, however, information regarding membrane regulation during stress remains unclear. Here we focused our analyses on understanding how *Caenorhabditis elegans* (*C. elegans*) mechanisms regulate the PL membrane composition and dynamics during increasing doses of glucose.

Although a significant amount of evidence has accumulated over the past decades, our understanding of how the membrane composition and dynamics vary during a stress response remains limited. Recently, a mechanism responding to mild concentrations of glucose was shown to regulate the activity of desaturase such as FAT-7 to stabilize membrane composition. Also, the membrane balance between saturated and unsaturated fat in glucose was shown to be important to *C. elegans*' survival. However, the entire mechanism through which this regulation occurs is not completely understood.

**Our first aim characterized the membrane adaptation to different doses of glucose.**

We used gas chromatography-mass spectrometry (GC-MS) to quantify the dynamics of fatty acids (FAs) newly synthesized, elongated, and directly incorporated from the diet in response to glucose stress. Our results showed three important discoveries. First, the membrane regulation to high glucose seems to funnel FAs dynamics toward the

maintenance of PUFAs. Second, membrane composition shows better adaptation to longer periods of stress, and this response seems to be at least partially regulated by *de novo* synthesis. Third, FA species called mono methyl branched-chain fatty acids (mmBCFAs) are produced in response to glucose stress. Our findings are exciting, not just because we were able to fully characterize the membrane response to glucose stress under different conditions, but also because we identified a novel response via mmBCFAs, a fatty acid mostly studied in bacteria but not well characterized in nematodes or mammals.

The presence of mmBCFAs in the PL membrane is considerably low compared to other species such as saturated and polyunsaturated fatty acids. In nematodes, mmBCFAs were shown to be important in the production of a glucosylceramide molecule that is essential to post-embryonic development and foraging. However, the role of mmBCFAs have not been explored in the nematode's response to glucose stress. **Therefore, our second aim investigates the importance of mono methyl branched-chain fatty acids in response to glucose stress.** We directed our RNAi experiments to knockdown the activity of two enzymes (*elo-5* and *elo-6*) responsible for the production of mmBCFAs. Our results showed two important discoveries; first, mmBCFAs are essential to survive glucose stress because *elo-5* knockdown nematodes live significantly shorter compared to controls on glucose plates. Second, we found that the expression of ELO-5 levels is at least partially regulated by PAQR-2 (progesterin and adipoQ receptor).

In *C. elegans*, mmBCFAs are precursors for the production of the backbone of sphingolipids. Recently, the mmBCFAs derived glucosylceramide (GluCer 17:1;O2/22:0;O) were shown important for crucial processes in the nematode via the

nutrient sensor TORC1. Therefore, we hypothesized that mmBCFAs are used to produce the GluCer, to be an essential mediator of the glucose stress response. **Therefore, in our third aim, we investigated the mechanisms that require mmBCFAs to respond against glucose stress.** To investigate this pathway, we assessed the metabolic alterations and survival of nematodes with compromised d17iso GluCer synthesis using RNAi against *elo-3*, *elo-5*, and *cgt-3*. Our first results showed that the impact of the loss of ELO-5 in the membrane's response to glucose is more wide-reaching than the production of mmBCFAs. Next, we confirmed that the knockdown of *elo-3*, *elo-5*, and *cgt-3* compromise the levels of GluCer 17:1;O2/22:0;O. After confirming this impact in glucosylceramide levels, we hypothesized that nematodes lacking the presence of GluCer would not be able to survive glucose stress. To confirm our hypothesis, we tested the survival of nematodes that could not produce GluCer (*cgt-3* and *elo-3* RNAi knockdown) under glucose stress. Our results show a significant decrease in the lifespan of nematodes with reduced levels of GluCer with *cgt-3* knockdown animals having a very short lifespan under glucose stress. Thus, we were able to prove that GluCer is essential for glucose stress survival.

## Chapter 1: Introduction

Initially considered a simple physical barrier used for compartmentalization, it was not long ago that researchers started to deeply study the composition of the cellular membrane and its impact on membrane function. For instance, in 1966 researchers used spectroscopic techniques to study the conformation of proteins from cellular membranes and the intercorrelation between lipids and proteins. Although their work largely concerns protein interaction with the hydrophilic and hydrophobic regions of phospholipids (PL), the conclusion was that "the role of membrane lipids is thus viewed to be more than maintenance of membrane permeability and plasticity" (Wallach & Zahler, 1966). The progress in the research of cellular membranes proves that membranes influence many other cellular activities beyond protein anchoring, such as signaling pathways, molecular channel, osmotic regulation, and others (Hedger & Sansom, 2016); (Koshy & Ziegler, 2015); (Levental et al., 2020).

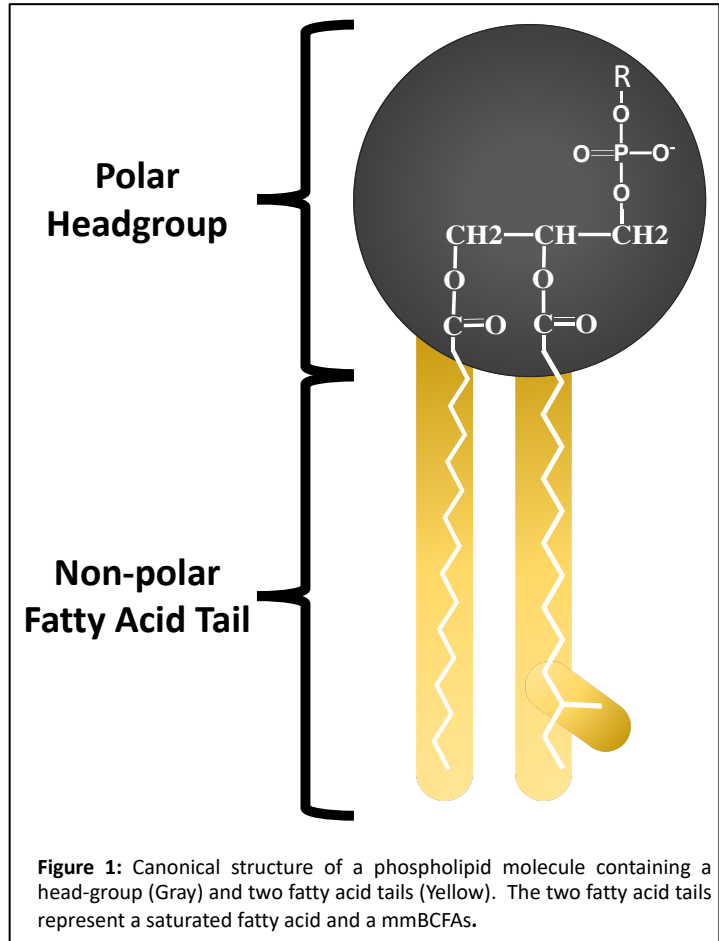
The need to understand membrane composition more thoroughly became increasingly clear when researchers assessing the membrane of patients suffering from various diseases including Alzheimer's disease and diabetes observed that phospholipid (PL) and fatty acid (FA) composition was significantly different from healthy controls (Bandu, Mok, & Kim, 2018) (Borkman *et al.*, 1993) (Snowden, et al., 2017). For instance, in diabetic patients, decreased insulin sensitivity was associated with lower levels of polyunsaturated fatty acids (PUFA) in the membrane of skeletal muscle (Samuel & Shulman, 2012) (Borkman *et al.*, 1993). In addition, the analysis of post-mortem samples, the use of models such as *C. elegans*, and the analyses of metabolites suggested that the dysregulation in the metabolism of unsaturated fatty acids is also present in many

Alzheimer's patients (Fanning et al., 2019) (Snowden, et al., 2017). The dysregulation in these two conditions seems to be related to one specific class of FA, known as polyunsaturated fatty acids (PUFAS) (Pilon, 2016). They are composed of more than one double bond in their chemical structure, and the weakness of the carbon-hydrogen bonds between double bonds makes PUFA molecules more susceptible to damage. To better understand the correlation between this FA species and disease, the details of the PUFA structure and its susceptibility to damage will be discussed later. Although many studies have been trying to understand the role membrane aberrations play in disease, it is still unclear if such alterations are essential for the onset or development of each pathology. Therefore, understanding the complete mechanism used by cells to maintain an adequate membrane composition is critical to the development of new diagnostics and treatments. Here, we use mass spectrometry-based approaches to uncover pathways that respond to external stimuli, specifically glucose stress. To do so, we used *C. elegans* to allow us to monitor the membrane dynamics (explained in detail later) and understand the alterations in the PL and FA composition using the incorporation of stable isotopes.

### **1.1. Glycerophospholipids: the most abundant component of membranes**

Biological membranes are primarily composed of glycerophospholipids, glycolipids, sterols, and proteins. The mutual activity of all these molecules ultimately gives shape and function to the membrane, yet, glycerophospholipids are the most abundant. A canonical glycerophospholipid is formed by a hydrophilic head group and two hydrophobic fatty acid (FA) tails (Figure 1). The amphipathic nature of the PLs allows for the formation of micelles, liposomes, and bilayers with limited energy expenditure (van

Meer, Voelker & Feigenson, 2008). Hundreds of different PL species, derived from different combinations of headgroups and fatty acid tails, are found in a given membrane (Alberts *et al.*, 2002) (Figure 1). The classification of the PLs is based on the structure of the headgroups including phosphatidylcholine (PC), phosphatidylethanolamine (PE), phosphatidylserine (PS), and phosphatidylinositol (PI). The nomenclature of phospholipid



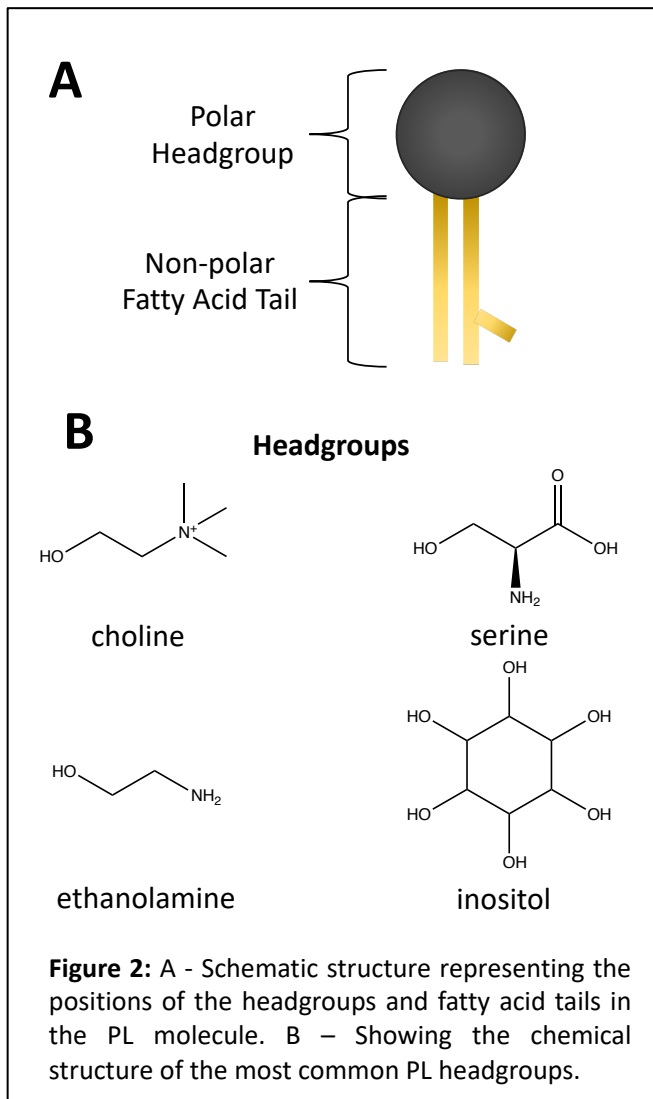
species will contain abbreviations for phospholipid classes (PC, PE, etc), followed by the total number of carbon atoms and double bonds in the molecule (i.e., PC 36:4) (Liebisch *et al.*, 2020). The most abundant polar headgroups found in mammals are PC and PE which comprise about 45% and 30% of total phospholipids, respectively (Van Meer, Voelker & Feigenson, 2008) (Daleke, 2003). While species with PC and PE headgroups build the majority of the lipid bilayer, other less abundant headgroups like PS and PI play key roles in specific cellular activities including signaling, apoptosis, and membrane trafficking pathways (Farine *et al.*, 2015); (Mueller-Roeber & Pical, 2002) (Figure 2). Because each organelle plays a specific role in the organism, its PL composition needs to be assembled in a particular way to perform each respective activity. The endoplasmic



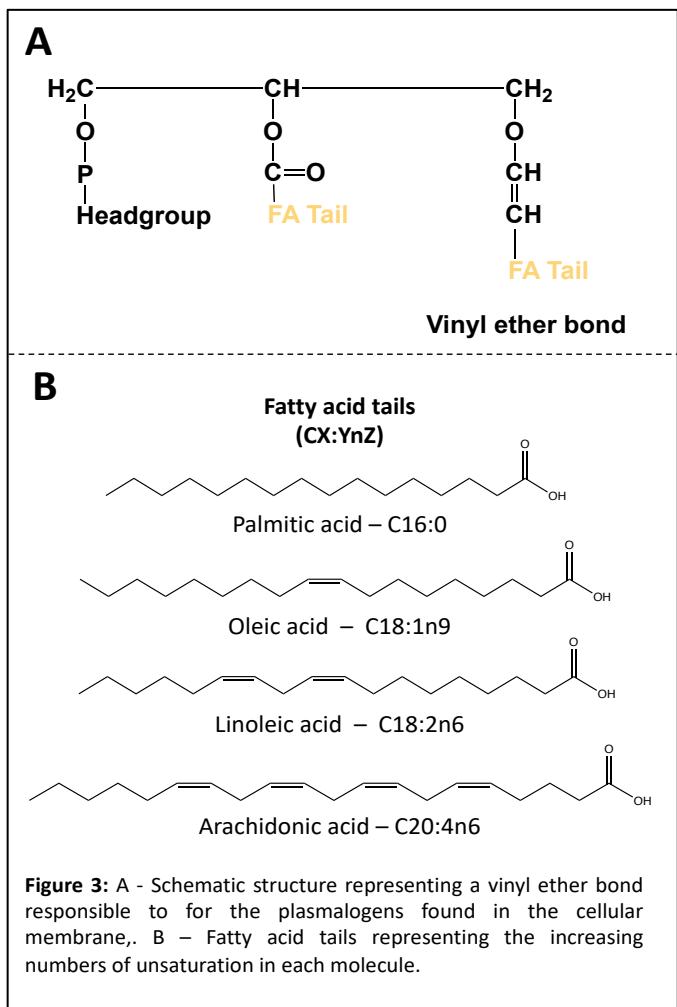
reticulum (ER) is a good example since it has significantly higher levels of PCs compared to the plasma membrane or other organelles (Van Meer, Voelker & Feigenson, 2008). In addition to other activities, phosphatidylcholine plays an essential role in facilitating the transport of lipids such as triacylglycerols out of the liver. Since the ER is constantly producing and transporting molecules, elevated levels of PCs are essential to maintain proper transportation in this organelle (Casares, Escribá & Rosselló, 2019) (Lim, Dial & Lichtenberger, 2013).

Although headgroup variability is essential for regulating physiological

activities and bringing diversity to the PLs forming cellular membranes, the FA tails connected to the glycerol backbone at the *sn-1* and *sn-2* positions have a significant impact on the structure, diversity, and functions of the phospholipid as well. In a typical glycerophospholipid, the incorporated fatty acids vary in length from 12 to 22 carbons and degree of saturation from 0 to 6 double bonds. The nomenclature used to refer to each FA is based on the number of carbons present in the molecule, the number of double bonds, and the position of the first double bond (Figure 3). Differences FA tails in the



membrane can alter the biophysical properties of the bilayer and impact signaling pathways, function as "anchors" to other molecules, or regulate physical properties (Ferguson, 1991) (Svensk *et al.*, 2016) (Papackova & Cahova, 2015). For example, in fish, the regulation of optimal FA composition has been related to the maintenance of membrane viscosity. Specifically, it has been shown that red blood cells and neurons of adult carps can continuously adjust the fluidity of their membranes by controlling the saturation levels in response to changes in temperature (de Carvalho & Caramujo, 2018). In their experiments, Farkas *et al* (2001) demonstrated using steady-state fluorescence that synthetic 18:1/22:6 phosphatidylethanolamine and 16:0/18:1 phosphatidylcholines lipid species have the ability to increase membrane fluidity during adaptation to reduced temperatures. The accumulation of the saturated fat C16:0 was associated with a negative impact on membrane fluidity in mammalian HEK293 cells. The FRAP (fluorescence recovery after photobleaching) analysis of cells supplemented with C16:0 after siRNAi of AdipoR1/2 showed a significant reduction in fluorescence recovery, suggesting a slow movement of molecules inside the membrane (Ruiz *et al.*, 2019). Therefore, the



distribution of PLs and FAs within a membrane directly influence physical properties including thickness, fluidity, and permeability of a bilayer. Hence, any modification in the normal composition of PLs within the cellular membrane can impact many cellular mechanisms including vesicle trafficking, signaling pathways, and cell apoptosis.

### **1.1.1. Headgroup synthesis and its importance**

Lipid headgroups are chemical molecules that attach to the glycerol, sphingosine, or sterol backbones of membrane lipids. Phospho- and glycolipids have headgroups linked to the backbone through a phosphodiester bond. The high structural diversity allows for a large range of functions, including effects on membrane curvature cell signaling, substrate transport, and more. Consequently, the headgroup's crucial role in membrane biology is also tied to a broad range of diseases, from cardiovascular defects to cancer (Tomczyk & Dolinsky, 2020) (Cheng, Bhujwala, & Glunde, 2016).

Lipid composition plays an important role in regulating membrane curvature because the chemical properties of different FA tails or head groups favor the loop formation in different directions. PCs have a neutral curvature due to their cylindrical shape often forming planar bilayers. However, modifying their structure by removing one fatty acid tail forms a new molecule called lyso-PC which lead to a cone-shaped configuration, inducing positive curvature, and therefore, favoring the formation of structures such as micelles (Poojari, Scherer, & Hub, 2021). To counterbalance positive curvatures, the PE headgroup, which is smaller than the PC headgroup, creates negatively curved surfaces (Figure 4A) (Sodt & Pastor, 2014) (McMahon & Boucrot, 2015). Because of that, PC and PE predominantly reside on the outer and inner leaflets

of the plasma membrane bilayer, respectively (Poojari, Scherer, & Hub, 2021). The correct synthesis and combination of these PLs varying their headgroups will play essential roles in regulating pathways such as *de novo* lipogenesis, and membrane delineation of cells and organelles (van der Veen *et al.*, 2017). For instance, in *C. elegans* the reduction of PC synthesis triggers negative feedback inducing the activity of SBP-1, a homologous of the mammalian sterol regulatory element-

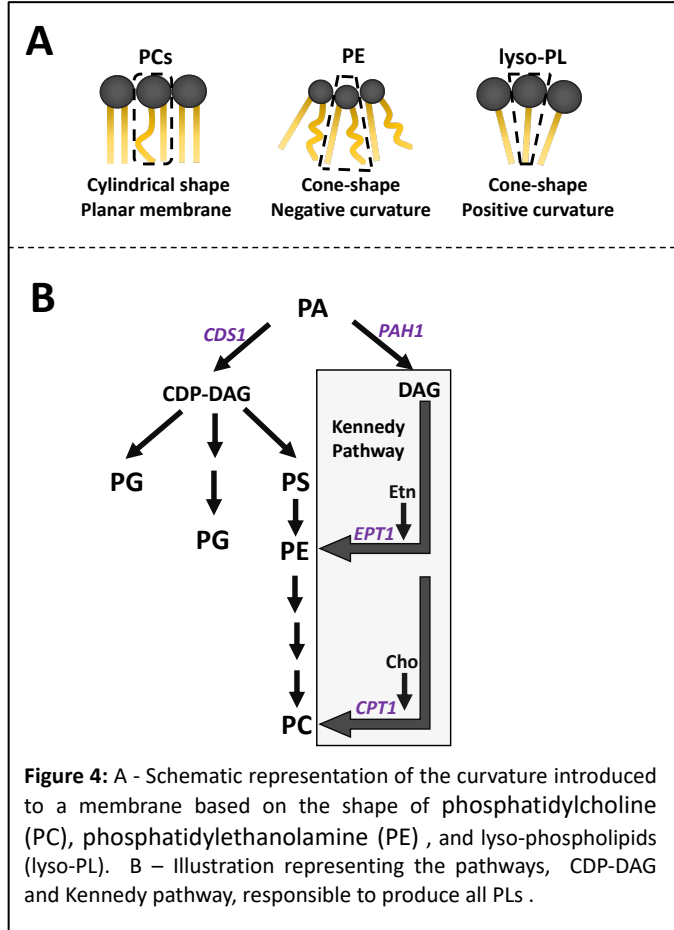


**Figure 4:** A - Schematic representation of the curvature introduced to a membrane based on the shape of phosphatidylcholine (PC), phosphatidylethanolamine (PE), and lyso-phospholipids (lyso-PL). B – Illustration representing the pathways, CDP-DAG and Kennedy pathway, responsible to produce all PLs.

binding proteins (SREBP), to increase the activity of its targeted genes such as choline/ethanolamine palmitoyltransferase (CEPT-1) and desaturases (FATs) (Walker *et al.*, 2011). In several mouse models and human studies, a change in not only the absolute concentrations of these phospholipids, but more critically in the molar ratio between PCs and PEs, is a key determinant of liver health being linked to the development of non-alcoholic fatty liver disease (NAFLD) and liver failure (Li *et al.*, 2006) (Ling *et al.*, 2012).

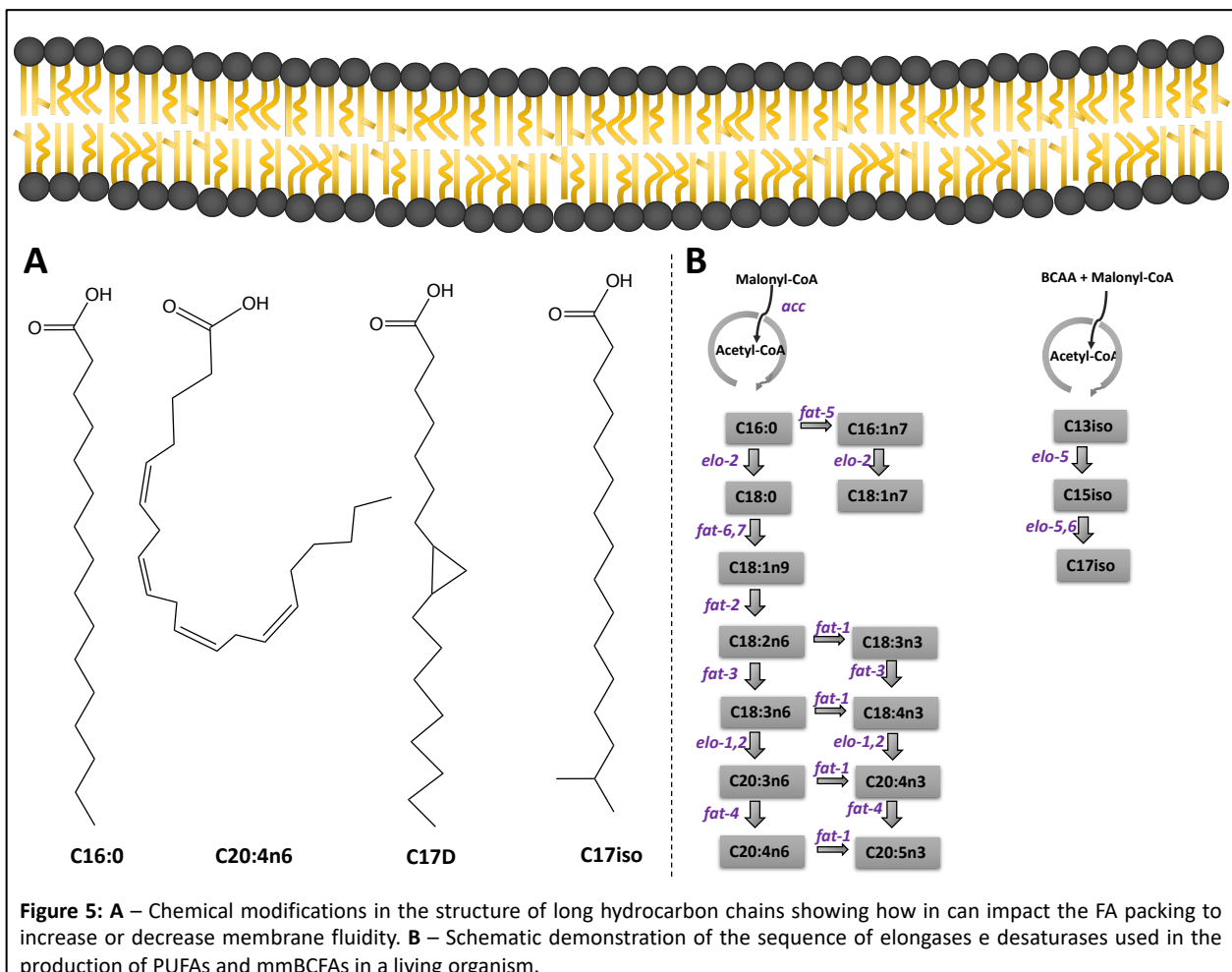
Enzymes such as Phosphatidate cytidyltransferase 1 (CDS-1), Phosphatidic acid phosphohydrolase 1 (PAH1), choline/ethanolamine palmitoyltransferase 1 (CEPT1), and others are essential in the production of PC, PE, PS and PIs (Figure 4B). The initial step in PL headgroups production starts with the conversion of phosphatidic acid (PA) into

CDP-diacylglycerol (CDP-DAG) and diacylglycerol (DAG), which will enter the CDP-DAG pathway and the Kennedy pathway, respectively (Carman & Han, 2011); (Gibellini & Smith, 2010). The activity of the CDP-DAG pathway will synthesize all major PLs including cardiolipin which is exclusively located in the mitochondrial membrane. On the other hand, the Kennedy pathway will be favorable only to the production of PC and PE species (Gibellini & Smith, 2010). As mentioned before, PCs make up a high proportion of the lipids in the outer leaflet of the plasma membrane and because of the generally cylindrical shape of the molecule, they are not capable of inducing large amounts of curvature to membranes. In humans, PCs are the main surface-active component of human lung surfactant, and it has the essential role to provide alveolar stability. Additionally, it is believed that the lateral pressure applied by PEs to create membrane curvature is essential to promote membrane protein stabilization (van der Veen *et al.*, 2017). Thus, the formation of a functional membrane structure directly depends on the proper activity of each one of these and other pathways.

### **1.1.2. The synthesis of fatty acids**

The diversity of PLs and FAs forming membranes is extremely important to the maintenance of the organism's health. The variability introduced by FAs is related to the molecular shape that the long hydrocarbon chain receives after the incorporation of chemical alterations such as double bonds and methyl groups (Figure 5A). The pathway for FA biosynthesis, called *de novo* fatty acid synthesis, is highly conserved from rudimentary organisms to highly developed ones such as mammals. The initial step in FA synthesis is the conversion of acetyl-CoA to malonyl-CoA, which is catalyzed by the

enzyme acetyl-CoA carboxylase (ACC) (Figure 5B). A repetitive cycle catalyzed by the enzyme fatty acid synthase (FASN) will extend the resulting chain by two carbons until a saturated hydrocarbon chain with 16 carbon (palmitate or C16:0) is released. The C16:0 can enter the elongation/desaturation pathway to generate fatty acid precursors needed for PL production and other FA metabolism pathways. C16:0 can be modified by a series of desaturases and elongases, into FAs with very long carbon chains and multiple double bonds (Watts & Ristow, 2017) (Figure 5). Elongases introduce more carbons to the fatty acid molecule, for instance, *elo-2* in *C. elegans* introduces another malonyl-CoA to the C16:0 creating C18:0. Desaturases are responsible for adding double bonds at specific positions of the hydrocarbon chains. Depending on the chemical modification, the FAs



are classified into different classes such as saturated fatty acids (SFAs), unsaturated fatty acids (UFAs), cyclopropane fatty acids (CFAs), and monomethyl-branched chain fatty acids (mmBCFAs) (Figure 5) (Watts & Browse, 202). It is important to note that the presence of polyunsaturated fatty acids (PUFAs) such as arachidonic acid (C20:4n6) and eicosapentaenoic acid (C20:5n3) play an essential role in increasing the fluidity of the membrane. The activity of these enzymes and the production of many different FAs will play an important role in determining the biophysical properties of the membrane.

### **1.1.3. The different types of fatty acids and their importance**

Saturated fatty acids have a long hydrocarbon chain formed exclusively by single bonds, giving this type of fatty acids a straight structure that allows for tight packing. Saturated fatty acids are essential to maintain optimal membrane composition by balancing other FAs and tuning the appropriate level of membrane fluidity. Moreover, the single bonds are less susceptible to damage than double bonds; therefore, they remain in the membrane when responding to external stimuli such as oxidative stress, while other species are consumed. Although these FAs are present in the membrane of many organisms, in *C. elegans* the excess saturated fat was mostly associated with conditions such as early aging, membrane alteration, and reduced survival (Lee *et al.*, 2015) (Devkota *et al.*, 2017). In fact, the elevation of C16:0 saturated fat caused by glucose exposure was shown to elevate toxicity by disrupting membrane fluidity and decreasing survival (Svensk *et al.*, 2016) (Devkota *et al.*, 2017). To counter-balance, the toxicity caused by SFA and help regulate membrane physical properties, another species of fatty acids called unsaturated fatty acids (UFAs) are essential. This regulation happens

because the double bonds in the cis configuration present in the hydrocarbon chain create kinks in the structure. In fact, the higher the number of double bonds in the hydrocarbon chain, the more it disturbs the membrane packing, and consequently, the higher the level of fluidity. Epidemiological evidence suggests that dietary consumption of UFAs commonly found in fish or fish oil may modify the risk for certain degenerative or neuropsychiatric disorders (Lunn & Theobald, 2006) (Snowden *et al.*, 2017). The dysregulation in UFA was associated with abnormal fatty acid profiles, increase and selective lipoxidative damage, and an increase in advanced glycation and products (AGE) and AGE receptors (RAGE) expression in the frontal cortex in cases with early stages of parkinsonian neuropathology without treatment (Dalfó *et al.*, 2005).

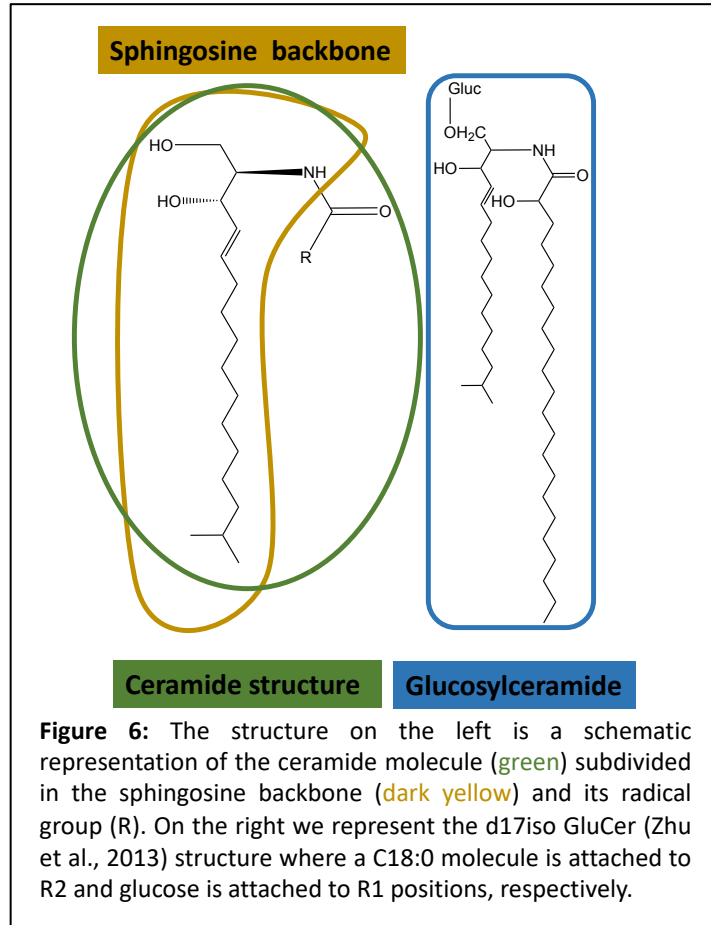
Other less abundant fatty acid species like cyclopropane and monomethyl-branched chain fatty acids are present in the membrane. Cyclopropane fatty acids are broadly distributed in a variety of organisms, in particular bacteria such as *Escherichia coli*, *Streptococcus*, and *Salmonella*. Organisms such as *C. elegans* do not produce these fatty acids because they do not have the enzymes required for the process; therefore, the existence of cyclopropane FA content in their cellular membrane is exclusively due to diet incorporation (Watts & Browse, 2002) (Cao & Mak, 2020). It has been suggested that cyclopropane fatty acids may reduce the fluidity of membranes, thereby limiting their permeability to undesirable compounds ranging from a single proton to butan-1-ol and possibly even some antibiotics (Valderrama *et al.*, 1998) (Bianco *et al.*, 2019). Cyclopropane fatty acids have also been shown to play a role in pathogenesis. Cyclopropanation of mycolic acids, a major component of the cell envelope in *M. tuberculosis*, is correlated with the persistence of the pathogen (Glickman, Cahill &



Jacobs, 2001) (Rao et al., 2005). Although significant variations in the membrane content of cyclopropane fatty acids have been identified in a multitude of physiological situations, little is known regarding the actual role that these fatty acids play in the membranes of more developed organisms.

About three decades ago, mmBCFAs emerged as an essential fatty acid participating in important cellular activities such as fluidity

regulation in bacteria and post-embryonic development in nematodes. mmBCFAs are endogenous products of fatty acid synthase (FASN) and their in vivo synthesis is influenced by mitochondrial BCAA catabolism. These FAs are primarily synthesized in mammalian adipose depots and decreased in the context of diet-induced obesity, in which adipose-specific hypoxia potently suppresses BCAA catabolism and lipogenesis (Wallace et al., 2018). mmBCFAs are found in different organisms from bacteria to mammals with a methyl branch located on the penultimate carbon of their FA chain (Figure 5). In humans, they have been detected in the skin, adipose tissue, blood, and cancer cells (Kniazeva, Euler & Han, 2008) (van de Vossenberget al., 1999). In *C. elegans*, the two mmBCFAs presents in the membrane are 13-methyltetradecanoic acid (C15iso) and 15-



methylhexadecanoic acid C17iso. *C. elegans* possess a system for mmBCFA biosynthesis that includes a fatty acid synthase (FASN-1) cycle, and two FA elongation enzymes, ELO-5 and ELO-6, which are regulated at least in part by the nematode homolog of SREBP-1c (Ipd-1). The nematodes may also obtain mmBCFAs from their diet (bacteria) (Kniazeva et al., 2004). In OP50 (*E. coli*) the nematode's regular diet in the laboratory, polyunsaturated fatty acids (PUFAs) and mmBCFAs are not present; therefore, all of the mmBCFAs content presented in the membrane comes from the elongase pathway (Vieira et al., 2022) (Figure 5B). The most common branched-chain fatty acids found in *C. elegans* membranes are methylated at the iso position of saturated hydrocarbon chains containing 14 (yielding C15iso) or 16 (yielding C17iso) (Kniazeva, Euler & Han, 2008). These methyl branches in membranes increase the area per lipid, reduced the bilayer thickness, lowered chain ordering, and favored the formation of kinks at the branching point; taken together, these effects manifest themselves as increasing membrane fluidity (Kniazeva et al., 2004). However, mmBCFAs have not been found to regulate membrane fluidity in multicellular organisms such as nematodes or mammals. Recently, these FAs were reported as the main structures in the production of sphingolipids, a lipid class that is particularly important in signaling pathways. Therefore, these FAs open a wide avenue for future research to understand their main activity in multicellular organisms.

## **1.2. Sphingolipids are essential to respond against external stimuli**

Sphingolipids like ceramides, sphingomyelins, and sphingosine are far less abundant than glycerophospholipids, typically representing 2–15% of the total cellular

lipidome. These lipids constitute a very diverse group including hundreds of different species. Their basic structure contains a variety of membrane-associated molecules that contain a long-chain sphingoid base (Figure 6), which can be acylated, glycosylated, and phosphorylated to produce a variety of structures with important and unique biological functions (Delgado et al., 2013); (Hannun & Obeid, 2011). Sphingolipids are normally recognized as regulators of cellular events because of their ability to form microdomains (rafts and caveolae) in the plasma membrane (Bieberich, 2018). In nematodes, a sphingolipidomic assay using mass spectrometry coupled with multiple reaction monitoring mode (LC-MS-MRM) showed that they are important to normal development and nutrition (Cheng et al., 2019). This investigation showed that sphingolipids accumulated after serine supplementation (Cheng et al., 2019). Also, the supplementation of 18 different amino acids to nematodes has been shown to increase lifespan (Edwards et al., 2015). Therefore, they believe that the extension of *C. elegans*' lifespan might be connected to mitochondrial metabolism-mediated stress response enhancing sphingolipid production (Cheng et al., 2019).

After recent findings in our laboratory, we became interested in the sphingolipid class, glucosylceramides (Vieira et al., 2021). The ceramide is a sphingolipid that constitutes the basal building block for the more complex sphingolipids and consists of a long-chain sphingoid base (LCB), sphinganine or sphingosine, with a fatty acid attached via an amide bond at the R2 position. More complex sphingolipids are generated by attaching various headgroups in the R1 position of ceramides (Olsen Anne & Færgeman Nils, 2017); (Chaurasia & Summers, 2021) (Figure 6). For instance, if a molecule of glucose is attached to the R1 position this new structure will become a glucosylceramide.

Mass spectrometry has improved the characterization of ceramides in human serum, tissue samples, and model organisms. These methods have helped to associate alterations in the circulating sphingolipids with diseases such as diabetes and coronary diseases (Thorens et al., 2019); (Poss et al., 2020). Besides the essential role played in the nervous systems, ceramides are also deeply associated with pro-apoptotic functions, oxidative stress response, differentiation, senescence, and others (Bandet et al., 2019). Animal studies including in the nematode have identified specific roles for sphingolipids including a specific glucosylceramide called d17iso-glucosylceramide. D17iso-GluCer was found to play an essential role in the development and survival of nematodes. The synthesis of this molecule requires C15iso to form the long-chain base (LCB), which is attached to a molecule of C18:0 in the R2 position, and a molecule of glucose will later be attached to the R1 position (Kniazeva, Euler & Han, 2008) (Zhu et al., 2013). Sphingolipids like ceramides, sphingomyelins, and sphingosine are far less abundant than glycerophospholipids, typically representing 2–15% of the total cellular lipidome. These lipids constitute a very diverse group including hundreds of different species. Their basic structure contains a variety of membrane-associated molecules that contain a long-chain sphingoid base (Figure 6), which can be acylated, glycosylated, and phosphorylated to produce a variety of structures with important and unique biological functions (Delgado et al., 2013); (Hannun & Obeid, 2011). Sphingolipids are normally recognized as regulators of cellular events because of their ability to form microdomains (rafts and caveolae) in the plasma membrane (Bieberich, 2018). In nematodes, a sphingolipidomic assay using mass spectrometry coupled with multiple reaction monitoring mode (LC-MS-MRM) showed that they are important to normal development

and nutrition (Cheng *et al.*, 2019). This investigation showed that sphingolipids accumulated after serine supplementation (Cheng *et al.*, 2019). Also, the supplementation of 18 different amino acids to nematodes has been shown to increase lifespan (Edwards *et al.*, 2015). Therefore, they believe that the extension of *C. elegans*' lifespan might be connected to mitochondrial metabolism-mediated stress response enhancing sphingolipid production (Cheng *et al.*, 2019).

After recent findings in our laboratory, we became interested in the sphingolipid class, glucosylceramides (Vieira *et al.*, 2021). The ceramide is a sphingolipid that constitutes the basal building block for the more complex sphingolipids and consists of a long-chain sphingoid base (LCB), sphinganine or sphingosine, with a fatty acid attached via an amide bond at the R2 position. More complex sphingolipids are generated by attaching various headgroups in the R1 position of ceramides (Olsen Anne & Færgeman Nils, 2017); (Chaurasia & Summers, 2021) (Figure 6). For instance, if a molecule of glucose is attached to the R1 position this new structure will become a glucosylceramide. Mass spectrometry has improved the characterization of ceramides in human serum, tissue samples, and model organisms. These methods have helped to associate alterations in the circulating sphingolipids with diseases such as diabetes and coronary diseases (Thorens *et al.*, 2019); (Poss *et al.*, 2020). Besides the essential role played in the nervous systems, ceramides are also deeply associated with pro-apoptotic functions, oxidative stress response, differentiation, senescence, and others (Bandet *et al.*, 2019). Animal studies including in the nematode have identified specific roles for sphingolipids including a specific glucosylceramide called d17iso-glucosylceramide. D17iso-GluCer was found to play an essential role in the development and survival of nematodes. The

synthesis of this molecule requires C15iso to form the long-chain base (LCB), which is attached to a molecule of C18:0 in the R2 position, and a molecule of glucose will later be attached to the R1 position (Kniazeva, Euler & Han, 2008) (Zhu et al., 2013).

### **1.3. Adopting *C. elegans* as a model to study membrane regulation**

To maintain proper membrane composition, both proteins and lipids must be coordinated to provide efficient feedback to signaling pathways and ensure membrane homeostasis. To properly study these pathways, it is important to choose a model that allows for easy manipulation and shows powerful genetic tools to support human application. *Caenorhabditis elegans* (*C. elegans*), the organism used in this dissertation, present these characteristics with about 41% of homology when compared to the human genome, and easy diet manipulation feeding of *E. coli* seeded to agar media (Lai et al., 2000). So far, studies analyzing the membrane adaptation to cold temperature and glucose stress using *C. elegans* were key to important discoveries in understanding part of these pathways (Svensk et al., 2013) (Svensk et al., 2016) (Vieira et al., 2022).

To be able to regulate the type of lipid present in the membrane, the glycerophospholipids biosynthesis is regulated by transcription factors like Ino2-4 and NHRs responding to internal and external signals like the alteration in phospholipid or fatty acid pools, and oxidative stress (Carbon & Calderon, 1995). These responses happen in the endoplasmic reticulum, golgi complex, and mitochondria that are stimulated to decrease or increase lipid production and degree of saturation. The transcription factors are responsible for initiating the signaling cascade stimulating these organelles to establish a proper response to each stimulus (Watts & Ristow, 2017). NHR is a class of

transcription factors that can coordinate metabolic pathways through the activity of the ligand-binding domain and the DNA-binding domain. Although larger amounts of genes encoding NHRs are present in nematodes, some important regulators of lipid synthesis like NHR-49 and NHR-80 are conserved in both humans and *C. elegans*. These receptors were shown to act in combination with membrane sensors like PAQR-2, regulating the activity of enzymes such as desaturases (e.g.: FAT-6, FAT-7) and elongases (e.g.: ELO-1, ELO-2) playing a key role in the regulation of the saturation levels. Trials were made in an attempt to rescue the unhealthy phenotypes seen in PAQR-2 mutants such as larval arrest and small body size. These trials used *gain-of-function* and *loss-of-function* of proteins responsible for membrane homeostasis and included meticulous analysis of membrane composition (Svensk *et al.*, 2013) (Svensk *et al.*, 2016). PAQR-2 mutants submitted to *nhr-80 loss-of-function* showed amelioration in the overall phenotypes, partially suppressing the growth defect seen in cold temperatures (Svensk *et al.*, 2013). Because *nhr-80* and *nhr-49* are binding partners, it was believed that the same would happen in *nhr-49 loss-of-function*. However, the opposite was seen in *paqr-2;nhr-49* double mutant (Svensk *et al.*, 2013). Furthermore, it was tested the *gain-of-function* of two different *nhr-49* alleles and they were able to suppress the growth defect caused by cold temperature by inducing the activity of FAT-7 to produce UFAs regulating membrane fluidity (Svensk *et al.*, 2013) (Svensk *et al.*, 2016).

Studying the activities of both, *nhr-49*, which is remarkably similar to the mammalian Peroxisome Proliferator-Activated Receptor (PPAR), and PAQR-2, which is homologous to the human protein AdipoR2 have disclosed important routes to elucidate the mechanisms adapting membrane composition. Although there is a limitation in the

correlation between human metabolism and pathologies to *C. elegans*, assays using these nematodes have the power of emulating certain human metabolic aspects. These help to elucidate molecular mechanisms and deliver new approaches for therapeutic strategies in different diseases (Kaletta & Hengartner, 2006).

#### **1.4. Glucose: an important carbohydrate and its multiple effects in the organism**

Like proteins and fats, carbohydrates are an important part of a healthy diet because they perform vital roles in the organism. For instance, the monosaccharides ribose and deoxyribose play an essential role in the backbone structure of the genetic materials RNA and DNA, respectively. Except for dietary fiber, when carbohydrates are consumed, they are digested and broken down into monosaccharides, which serve as an energy source for most tissues in the human body. To produce energy, it enters a pathway called glycolysis in the cytoplasm which breaks down glucose into pyruvic acid, and the continuous breakdown generates free energy that is used to form the high-energy molecule adenosine triphosphate (ATP). If the organism has an excess of energy production associated with low energy expenditure, it will be stored in different forms such as glycogen and fat. Evidence shows that the excess consumption of glucose leads to conditions such as fat accumulation causing obesity (Warner *et al.*, 2020). Indeed, lipid metabolism is closely related to glucose levels, because, in fed states, glycolytic products are used to synthesize fatty acids through *de novo* lipogenesis. It starts with the transport of citrate from the mitochondria to the cytosol and converting it into acetyl-CoA molecules and ultimately palmitic acid (C16:0) (Rui, 2014) (see section 1.1.2). Moreover, when carbohydrates are abundant, *de novo* synthesized FAs can be esterified and combined



with glycerol 3-phosphate generating triacylglycerol (TAG) (Rui, 2014). Many transcription factors and co-regulators such as SERBP and PPAR $\gamma$  participate in the regulation of this process depending on the availability of substrates (Horton, Goldstein & Brown, 2002).

Lately, studies using *C. elegans* are helping to create a full understanding of mechanisms responding to glucose exposure (Jung *et al.*, 2020) (Devkota *et al.*, 2017) (Schlotterer *et al.*, 2009). In nematodes, glucose was shown to directly affect body length, membrane dynamics, survival, and others (Schlotterer *et al.*, 2009) (Vieira *et al.*, 2022) (Wang *et al.*, 2020). For instance, long-term supplementation of glucose reduces body length in wildtype nematodes showing a dose-dependent decrease in size (Wang *et al.*, 2020). The decrease in nematode survival is also aggravated in a dose-dependent manner, indicating strong damage caused by long-term exposure to glucose (Alcántar-Fernández *et al.*, 2018). Glucose was shown to modify membrane dynamics even in mild concentrations of glucose, suggesting that stronger and longer effects could promote accentuated responses (Vieira *et al.*, 2022). Furthermore, nematodes with defective response mechanisms show an elevation in SFA levels and reduced survival when exposed to glucose; but, the supplementation of UFA such as arachidonic acid and linoleic acid was shown to increase lifespan and elicited protective effects against glucose toxicity in *lpin-1(RNAi)* worms (Jung *et al.*, 2020) (Svensk *et al.*, 2016). Thus, regulatory mechanisms must exist to properly respond to membrane challenges such as glucose stress.

### **1.5. Membrane sensors: a group of proteins recently characterized**

As discussed before, regulatory mechanisms exist within each cell and are responsible to adjust membrane composition and maintain correct physical properties. For instance, healthy animals can restore or adjust their membrane composition when facing conditions that increase the amount of saturated fat in the membrane including cold temperatures and glucose exposure. These adjustments require the regulation of pathways that sense and respond to the shift in the saturation level (Dancy *et al.*, 2015); (Devkota *et al.*, 2017). Despite their obvious importance, it was only in recent years that molecular regulators of membrane composition have been identified. Transcriptional factors such as NH-49 were known to respond against high levels of free SFA in the cytosolic environment by signaling desaturases to produce more UFA and consequently control the saturation balance (Van Gilst *et al.*, 2005). Increased levels of saturated fat can occur in specific sites such as the PL membrane without affecting the free fat in the cell, suggesting mechanisms that sense and regulate the saturation levels directly from the membrane structure. Recently, the discovery of the bacterial fluidity regulator DesK, a kinase that activates fatty acid desaturases upon reduced membrane fluidity, was found to restore membrane fluidity during adaptation to low temperatures (Cybulski *et al.*, 2015). After this remarkable discovery, membrane researchers became interested in understanding how multicellular organisms respond to alterations in saturation levels, and if these fluidity sensors are present in more complex organisms.

Diseases such as diabetes and Alzheimer's were associated with important dysregulation in key mechanisms responsible to maintain membrane composition, and it consequently alters the normal levels of PL and FA in patients compared to healthy

individuals (Ruiz-Gutierrez *et al.*, 2015); (Fabiani & Antollini, 2019). Recently, studies done in *C. elegans* indicated that the transmembrane protein, PAQR-2, plays an important role in the regulation of membrane composition. PAQR-2 is a transmembrane protein conserved in mammals and homologous to the human protein AdipoR-2. PAQR-2 acts as a sensor to regulate the level of saturated fat present in the membrane through the regulation of proteins including *sbp-1*, *nhr-80*, and *nhr-49* (Svensk *et al.*, 2016); (Devkota *et al.*, 2017). Environmental conditions capable of increasing the levels of saturated fat such as cold temperatures and high glucose diets directly influence the health of PAQR-2 mutants. These two conditions increased the level of saturated FAs and caused unhealthy phenotypes including a withered tail, shorter lifespan, and smaller size (Svensk *et al.*, 2016). As mentioned before, PAQR-2 mutants with *nhr-80 loss-of-function* show amelioration in the overall phenotypes partially suppressing the growth defect seen in cold temperatures. On the other hand, *nhr-49*, a binding partner of *nhr-80*, was effective in recovering unhealthy phenotypes after *gain-of-function* (Svensk *et al.*, 2013); (Svensk *et al.*, 2016); (Devkota *et al.*, 2017). Likely, membrane sensors are mediators in the signaling pathways to control membrane adaptation, and understanding all the networks participating in it becomes very important to develop ways to treat abnormal membrane composition in diseases.

## **1.6. Membranes are a dynamic structure constantly renewed**

Lipids forming membranes are constantly replaced. These lipids are normally consumed by cellular processes including vesicle trafficking, damage, and signaling pathways; therefore, to preserve the overall membrane integrity, consumed and damaged

lipids must be replaced. This constant movement of PL and FA through the membrane is called membrane dynamics. Techniques using microscopy and isotopes have been used to evaluate and quantify the turnover of membrane lipids (Perez & Van Gilst, 2008) (Dawidowicz, 1987) (Svensk et al., 2016). Past studies were limited to the incorporation of one or a few radiolabeled or stable isotope-labeled tracers into the membrane, which restricted this analysis to the single or few molecules incorporated (Dawidowicz, 1987). To simultaneously analyze the turnover of all FA species at the same time, a technique introducing stable isotopes to the nematode's diet was developed (Perez & Van Gilst, 2008) (Dancy et al. 2015). This strategy has demonstrated that FA replacement rates are very significant; for example, analysis done with the stable isotopes identified that the fatty acids of membrane phospholipids are renewed about 1.7 times faster than those in neutral lipids in the same organism. In addition, it was found that at least 60% of the PL membrane structure is renewed every day by combining  $^{13}\text{C}$  labeling of fatty acid tails and  $^{15}\text{C}$  of phospholipid head groups (Dancy et al. 2015). The mechanisms that organize and regulate this constant composition throughout the continual flux are largely unknown.

The study of membrane dynamics using stable isotopes is more complicated than it appears. Specific conditions need to be controlled; for example, the isotope used cannot affect the normal metabolism of the organism after consumption, the equipment used to detect the isotope incorporation needs to be efficient, and the model organism must allow maximum isotope incorporation. Therefore, *C. elegans* emerged as a good study model. These nematodes allow a significant enrichment of  $^{13}\text{C}$  and  $^{15}\text{N}$  stable isotopes in a cost-effective manner due to their small size which makes it possible to evaluate the majority of fatty acid species simultaneously. The dietary  $^{13}\text{C}$  is

incorporated in the fatty acid tails allowing for comprehensive quantification of fatty acid dynamics. However, carbon isotopes cannot be used in the same way to quantify phospholipid turnover, because incorporating  $^{13}\text{C}$  at multiple positions and the presence of many PL species with similar compositions leads to a significant overlap in molecular weights that cannot be separated computationally. In order to overcome this problem,  $^{15}\text{N}$  isotopes can be incorporated into the single nitrogen position of the phospholipid headgroup, making the total mass vary +1 which can be quantified by HPLC and tandem mass spectrometry avoiding any molecular weight overlap (Perez & Van Gilst, 2008); (Dancy et al. 2015). Together, the  $^{13}\text{C}$  and  $^{15}\text{N}$  incorporation will allow us to quantify the intact phospholipid and fatty acid dynamics in the membrane and ultimately contribute to understand mechanisms that regulate overall membrane maintenance under normal and stress conditions.

### **1.7. GC/MS and HPLC/MS-MS used in lipidomics**

Mass spectrometry has become the technique of choice for the definitive identification of a wide variety of molecules including small molecules, proteins, and lipids. In general, this is an analytical technique that identifies compounds using the mass-to-charge ( $m/z$ ) ratio, which consists of a molecular ionization by giving it a positive or negative charge (Thurnhofer & Vetter, 2005) (Zhang *et al.*, 2011). This ionization can be generated differently based on the type of ion sources; for instance, electron ionization can cause extensive fragmentation of molecules, but gentler sources such as chemical ionization or electron spray are more favorable to the analysis of intact molecules (Poole, 2015). Although the ionized molecules can be separated using the  $m/z$  ratio when

accelerated into a magnetic field, often mass spectrometers are coupled to other separation techniques such as gas chromatography (GC) and high-pressure liquid chromatography (HPLC). If coupled with GC, the samples must be vaporized to be carried by an inert gas such as helium. Alternatively, HPLC coupling allows the samples to be carried in a liquid mobile phase. The stationary phase needs to be carefully chosen based on sample properties like polarity to allow for appropriate separation (Chiu & Kuo, 2020). In fact, to promote high-resolution separation of lipids, stationary phases such as biscyanopropyl cyanopropylphenyl polysiloxane and C18 columns are good choices for GC and HPLC, respectively (Delmonte, 2016) (Cajka & Fiehn, 2014).

The analyses of lipids by GC/MS require prior hydrolysis from their glycerol backbone and derivatization to a respective ester form for separation on capillary chromatographic columns (Perez & Van Gilst, 2008) (Chiu & Kuo, 2020). The detection and quantification of a wide range of ions with different sizes will generate a chromatogram that represents the quantification of each molecule in your sample. Because the detection system is highly sensitive, we can track the dynamics of new fatty acids containing  $^{13}\text{C}$  being incorporated into the PL membrane (Dancy *et al.*, 2015) (Perez & Van Gilst, 2008).

The preparation of samples to be analyzed by HPLC/MS-MS is simpler because it does not require extra preparation to allow quantification. After proper extraction and solubilization, this method combines the separating power of liquid chromatography with the highly sensitive and selective mass analysis based on static or dynamic fields, and magnetic or electric fields. The accuracy of this equipment is usually extremely high with a mass accuracy on the scale of 1 ppm, making this technique ideal for lipidomic analysis.

Studies using both methods (GC/MS and HPLC/MS-MS), observed that the replacement of FA and PL in the membrane of *C. elegans* is extremely high. Using GC/MS and stable isotopes it was found that membrane phospholipids are renewed about 1.7 times faster than neutral lipids used to store fat in the same organism. In addition, it was also shown that at least 60% of the PL membrane structure is renewed every day (Dancy *et al.*, 2015) (Perez & Van Gilst, 2008). The use of mass spectrometry was also essential to characterize the pathway responsible for the synthesis of PUFAs in *C. elegans*. GC/MS was used to assess the FA composition of *C. elegans* mutants defective in specific desaturases and elongases. Therefore, they were able to observe, for example, that *fat-2* mutation induces the accumulation of C18:1n9 which is the precursor of C18:2n6 when this desaturase is not working properly (Watts & Browse, 2002) (Figure 5B). The membrane regulation to external stimuli was also characterized using mass spectrometry, more specifically LC/MS-MS. A relative analysis of PLs in the membrane of PAQR-2 nematodes submitted to glucose stress showed that both PCs and PEs have elevated levels of C16:0, a SFA, but other SFAs such as C14:0 followed the same elevation in PCs and C18:0 in PEs. These results showed that mechanisms are constantly and carefully regulating membrane adaptation in response to environmental and dietary changes that can challenge optimal membrane composition. Therefore, it is clear that the combination of these techniques allows for a precise understanding of mechanisms that orchestrated the regulation of membrane composition and dynamics.

## Chapter 2: Monitoring Oleic Acid Metabolism after Glucose Stress in *C. elegans*

Andre F. C. Vieira<sup>1</sup>, Mark A. Xatse<sup>1</sup>, Sofi Murray<sup>1</sup> and Carissa Perez Olsen<sup>1</sup>

Submitted to *Lipids in Health and Disease* October 2022

<sup>1</sup>From the Department of Chemistry and Biochemistry, Worcester Polytechnic Institute,  
Worcester, Massachusetts, USA

**Note:** The mass spectrometry data analyzing composition and dynamics in N2 stressed with high glucose was generated by Andre Vieira, as well as the lifespan analysis. The recovery period analyzed by GC/MS and the heat-killed bacteria experiments were conducted in collaboration between Andre and Mark. Finally, the experiments made during longer stress periods were conducted by Andre and Sofi.

### 2.1. Abstract

The response against glucose stress is orchestrated by a series of proteins including membrane sensors such as PAQR-2. This response involves regulating the activity of enzymes such as *fat-7* to achieve proper balance between saturated and unsaturated fatty acids in the membrane. Here, we used <sup>13</sup>C stable isotopes incorporated into the nematode's diet, GC/MS, and HPLC/MS-MS to track the entire response to glucose stress. Previous work has analyzed the membrane composition of *C. elegans* when responding to mild glucose stress, not showing many alterations. Therefore, a careful evaluation of high glucose stress could reveal responses more accurate to extreme conditions. We found here a decrease in the membrane levels and dynamics of oleic acid and linoleic acid responding to 100mM and 200mM of glucose. Furthermore, the decrease in this species is present only in animals stressed for short periods but it



shows normal levels in longer stress. The *de novo* synthesis showed the same response to short and long stress periods. Finally, the supplementation of glucose in heat-killed bacteria did not alter membrane composition. Taken together, the regulation of membrane levels depends on the proper activity of *de novo* synthesis and requires enough time to promote the correct allocation of fatty acids.

## **2.2. Introduction**

As animals encounter a change in their environment or their diet, there is often a rewiring of metabolic pathways that tune or adjust membrane composition to the new conditions (Chen *et al.*, 2019) (Svensk *et al.*, 2013). In certain circumstances such as temperature changes, a different phospholipid content is established that promotes membrane function with the altered biophysical properties of the membrane (Chen *et al.*, 2019) (Farkas *et al.*, 2001). There are also situations as with the addition of moderate glucose stress where the membrane composition remains relatively stable; however, this stability requires a rewiring of metabolic pathways specifically through the membrane sensor PAQR-2 (Vieira *et al.*, 2022) (Svensk *et al.*, 2016). The PAQR-2 response network is directly dependent on the activity of enzymes including FAT-7 which is essential in the production of polyunsaturated fatty acids (PUFAs) and ELO-5 that is responsible for monomethyl-branched chain fatty acids (mmBCFAs) (Devkota *et al.*, 2017) (Vieira *et al.*, 2022). Recently, it has been shown that mmBCFAs play a critical role in providing fatty acid backbones for glucosylceramide production (Zhu *et al.*, 2013).

To promote the correct balance of saturated fatty acids (SFAs) and unsaturated fatty acids (UFAs), fatty acids incorporated from the diet and produced by *de novo*

synthesis must be proportionately incorporated into the membrane of organisms (Perez & Van Gilst, 2008) (Dancy et al., 2015). In *C. elegans*, FAT-7 introduces the first double bond to stearic acid (C18:0) producing oleic acid (C18:1n9), which is further elongated and desaturated to produce PUFAs such as linoleic acid (C18:2n6) and the C20 PUFAs including eicosapentaenoic acid (C20:5n3) (Watts, 2016). It is important to note that the FA composition of *E. coli* (OP50), the standard laboratory diet used to feed *C. elegans* nematodes, consists primarily of saturated FAs and cyclopropane FAs (Vieira et al., 2022). Therefore, to produce and incorporate polyunsaturated fatty acids (PUFAS) in a given membrane, enzymes such as FAT-7 must work in the conversion of C18:0 to C18:1n9 (Watts, 2016) (Devkota et al., 2017). This step is critical to survival and essential in the regulation of membrane composition, and the supplementation of C18:1n9 in PAQR-2 mutants was shown capable of restoring short lifespan (Svensk et al., 2016) (Devkota et al., 2017). In addition, quantification of *de novo* synthesis analysis in *C. elegans* showed that overall lipid production is compromised after FAT-7 RNAi knockdown (Dancy et al., 2015). Together, both findings reinforce the hypothesis that the C18:0 to C18:1n9 conversion is essential to membrane homeostasis.

To promote membrane adaptation, mechanisms to adjust the production and the allocation of different lipid molecules must be present. Techniques using stable isotopes have been used to evaluate and quantify the dynamics of lipids in the PL membrane. These stable isotope labeling strategies incorporate <sup>13</sup>C or <sup>15</sup>N into the nematode's diet and allow for the analysis of FA species simultaneously. The evaluation of <sup>13</sup>C presence in FAs showed that membrane renovation is extremely fast in nematodes (Perez & Van Gilst, 2008) (Dancy et al., 2015). Recently, we showed that to maintain composition nearly

stable during mild glucose stress (15mM), the dynamics of fatty acids like C16:0 and C17:iso are modified (Vieira *et al.*, 2022). However, it remains unclear how fatty acid dynamics respond against higher levels of glucose, and how FAs adapt to longer stress periods.

The diet is also an important component, helping in the regulation and adaptation of membrane composition. Many fatty acids present in nematodes are partially obtained intact from the diet; therefore, modification in bacterial composition also influences membrane adaptation in nematodes. The incorporation of glucose was previously shown to alter the overall FA composition in the bacteria, increasing the levels of C16:0 (Svensk *et al.*, 2016). We recently found that *E. coli* growing in High Growth (HG) media enriched with glucose presented lower levels of vaccenate acid (C18:1n7), suggesting a direct influence on the membrane composition assessed in the nematodes (Vieira *et al.*, 2022). Furthermore, recent studies have also shown that altering the bacterial diet provided to *C. elegans* by adding lower doses of fructose (~55mM) increased the lifespan of nematodes (Diot *et al.*, 2022) (Zheng *et al.*, 2017). Based on these evidences it is clear the essential role played by the diet in membrane adaptation to stress response. However, we still need to understand if the beneficial or harmful effects are dependent on the bacteria digesting the carbohydrates to produce reactive metabolites or serving as a vector transferring intact glucose molecules from the media to the nematode's organism.

As mentioned before, in our first study we found that lower levels of glucose promote few significant changes in the membrane composition, not showing a complete picture of the metabolic responses orchestrated by the organism. On the other hand, isotope incorporation revealed alterations in FA dynamics responding to glucose stress.

Researchers have also shown that the gradual elevation in glucose stress has an inverse proportion to the nematode's survival (Wang *et al.*, 2020) (Alcántar-Fernández *et al.*, 2018). Because of the relationship between glucose stress and membrane adaptation, we believe that higher levels of glucose can stimulate and disclose other mechanisms not seen previously. Here we assessed the membrane response to higher concentrations of glucose using GC-MS and HPLC-MS/MS to completely evaluate the response delivered by the nematode's organism.

### **2.3. Results**

Here we present all the results proving the importance of mmCBFAs to respond against glucose stress. In the text, we showed all the figures seen in the body of our publication; however, the supplementary tables and figures will not be included in this Thesis due to the size of the material. To see the supplementary material, you can access the page of the official publication.

#### **2.3.1. High dietary glucose alters allocation of oleic acid in the PL membrane**

Because the stable isotope feeding strategy employed here showed varied production of fatty acids depending on species, we further probed the kinetics of fatty acid metabolism with a focus on C18:1n9 and C18:2n6. First, the stable isotope labeling technique used here introduces  $^{13}\text{C}$  - OP50 on agarose media, which is free of nutrients to prevent the labeled bacteria from incorporating  $^{12}\text{C}$  from the plate. A consequence of this protocol is that the nematodes are submitted to a "recovery period" of 6 hours when there is no glucose stress. It was previously shown that removing nematodes from short

glucose stress allows for recovery of development in PAQR-2 mutants (Devkota *et al.*, 2017). In order to understand if membrane composition and dynamics are affected by these 6 hours of recovery, we used GC-MS to quantify the saturated and unsaturated fatty acids under three different conditions: nematodes stressed for 12 hours and frozen immediately following the stress (+gluc 12h(NoRecovery)); nematodes stressed for 12 hours followed by 6 hours of "recovery period" (+gluc 12h (Recovery)); and third, nematodes were stressed during 18 hours and frozen immediately after stress (+gluc 18h (NoRecovery)).

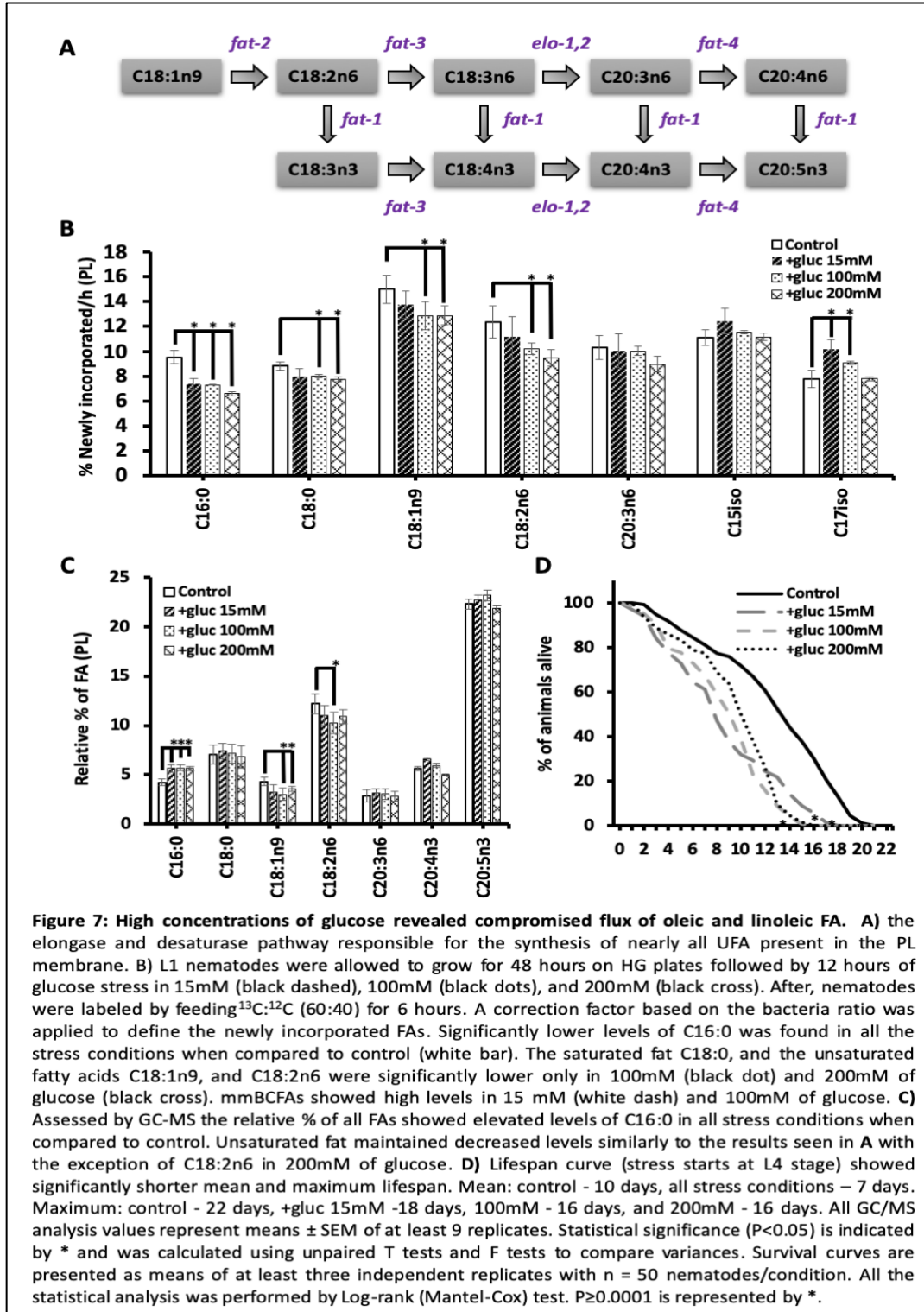
To induce the glucose stress, we selected 100mM of glucose which caused the most significant alterations in membrane dynamics and composition. We first quantified the abundance of C16:0 in the three conditions and found a significant increase in all glucose treatment groups regardless of the timing and recovery period. Interestingly, the increase in C16:0 with the recovery period was significantly less than in either of the treatment groups without a recovery period of time (Figure 8A). This trend suggests that metabolic rewiring can adjust the membrane composition back to baseline relatively quickly following glucose stress. The amount of C16:0 does continue to significantly rise between 12 hours and 18 hours of glucose feeding (Figure 8A). Because the glucose survival assays are done with constant glucose exposure, this suggests that the larger accumulation of SFA during longer periods of glucose stress could play an important role in raising toxicity levels and shortening the nematode's lifespan.

Because the recovery period reduced the overall changes we see in C16:0, we analyze the relative levels of C18:1n9 and C18:2n6 in the PL membrane. We focused on these two fatty acid species since they both showed significant changes in dynamics only

at the higher glucose concentrations. In addition, they are the precursor of all PUFAs synthesized by the elongase and desaturase pathways; therefore, alterations in these two FAs could promote major changes in membrane arrangement (Figure 7A). These fatty acids were analyzed from the same animals described above with and without a recovery period. If the nematodes are not submitted to a recovery period, oleic acid (C18:1n9) and linoleic acid (C18:2n6) levels are not significantly different in 12 hour glucose-stressed animals versus controls (Figure 8B). When submitted to a recovery period, +gluc 12h (Recovery) showed a significant decrease when compared to control 12h (Recovery). The levels of both C18:1n9 and C18:2n6 decreased from  $5.2\% \pm 0.6$  to  $4\% \pm 0.3$ , and from  $9.1\% \pm 1.2$  to  $6.9\% \pm 0.8$ , respectively (Figure 8B). Since the reduction in C18:1n9 and C18:2n6 may require longer than 12 hours, we also examined these fatty acid species after 18 hours of glucose stress and still saw no change in overall levels (Figure 8B).

We next examined whether the reduction in C18:1n9 and C18:2n6 abundance after recovery was specific to these fatty acid species. We quantified the relative fatty acid abundances for all major species in the nematode in the three glucose treatment groups versus their respective controls (Figure 8C, Supplement Fig. 1A). Some fatty acids that had significant changes were previously described: increased levels of C16:0 in all treatment groups, decreased C18:1n9 abundance in the 12h plus recovery and decreased C18:2n6 abundance in the 12h plus recovery treatment group. In addition, there was a small but significant decrease in C18:0 in the 12 h group without recovery. Because of reduced C18:1n9 and C18:2n6 levels, we were particularly interested in examining whether the C20 PUFAs would also show altered levels. We found that there are no significant modifications in the relative abundance of any C20 PUFAs in any stress

conditions (Figure 8C). Taken together, our data suggest that the reduction in C18:1n9 and C18:2n6 occurs as these fatty acids are converted to C20 PUFAs in the period following glucose exposure.



### **2.3.2. The recovery period decreases oleic and linoleic fatty acid levels and palmitic acid over accumulates in longer stress periods**

Because the stable isotope feeding strategy employed here showed varied production of fatty acids depending on species, we further probed the kinetics of fatty acid metabolism with a focus on C18:1n9 and C18:2n6. First, the stable isotope labeling technique used here introduces  $^{13}\text{C}$  - OP50 on agarose media, which is free of nutrients to prevent the labeled bacteria from incorporating  $^{12}\text{C}$  from the plate. A consequence of this protocol is that the nematodes are submitted to a "recovery period" of 6 hours when there is no glucose stress. It was previously shown that removing nematodes from short glucose stress allows for recovery of development in PAQR-2 mutants (Devkota *et al.*, 2017). In order to understand if membrane composition and dynamics are affected by these 6 hours of recovery, we used GC-MS to quantify the saturated and unsaturated fatty acids under three different conditions: nematodes stressed for 12 hours and frozen immediately following the stress (+gluc 12h(NoRecovery)); nematodes stressed for 12 hours followed by 6 hours of "recovery period" (+gluc 12h (Recovery)); and third, nematodes were stressed during 18 hours and frozen immediately after stress (+gluc 18h (NoRecovery)).

To induce the glucose stress, we selected 100mM of glucose which caused the most significant alterations in membrane dynamics and composition. We first quantified the abundance of C16:0 in the three conditions and found a significant increase in all glucose treatment groups regardless of the timing and recovery period. Interestingly, the increase in C16:0 with the recovery period was significantly less than in either of the treatment groups without a recovery period of time (Figure 8A). This trend suggests that



metabolic rewiring can adjust the membrane composition back to baseline relatively quickly following glucose stress. The amount of C16:0 does continue to significantly rise between 12 hours and 18 hours of glucose feeding (Figure 8A). Because the glucose survival assays are done with constant glucose exposure, this suggests that the larger accumulation of SFA during longer periods of glucose stress could play an important role in raising toxicity levels and shortening the nematode's lifespan.

Because the recovery period reduced the overall changes we see in C16:0, we analyze the relative levels of C18:1n9 and C18:2n6 in the PL membrane. We focused on these two fatty acid species since they both showed significant changes in dynamics only at the higher glucose concentrations. In addition, they are the precursor of all PUFAs synthesized by the elongase and desaturase pathways; therefore, alterations in these two FAs could promote major changes in membrane arrangement (Figure 7A). These fatty acids were analyzed from the same animals described above with and without a recovery period. If the nematodes are not submitted to a recovery period, oleic acid (C18:1n9) and linoleic acid (C18:2n6) levels are not significantly different in 12 hour glucose-stressed animals versus controls (Figure 8B). When submitted to a recovery period, +gluc 12h (Recovery) showed a significant decrease when compared to control 12h (Recovery). The levels of both C18:1n9 and C18:2n6 decreased from  $5.2\% \pm 0.6$  to  $4\% \pm 0.3$ , and from  $9.1\% \pm 1.2$  to  $6.9\% \pm 0.8$ , respectively (Figure 8B). Since the reduction in C18:1n9 and C18:2n6 may require longer than 12 hours, we also examined these fatty acid species after 18 hours of glucose stress and still saw no change in overall levels (Figure 8B).

We next examined whether the reduction in C18:1n9 and C18:2n6 abundance after recovery was specific to these fatty acid species. We quantified the relative fatty acid

abundances for all major species in the nematode in the three glucose treatment groups versus their respective controls (Figure 8C, Supplement Fig. 1A). Some fatty acids that had significant changes were previously described: increased levels of C16:0 in all

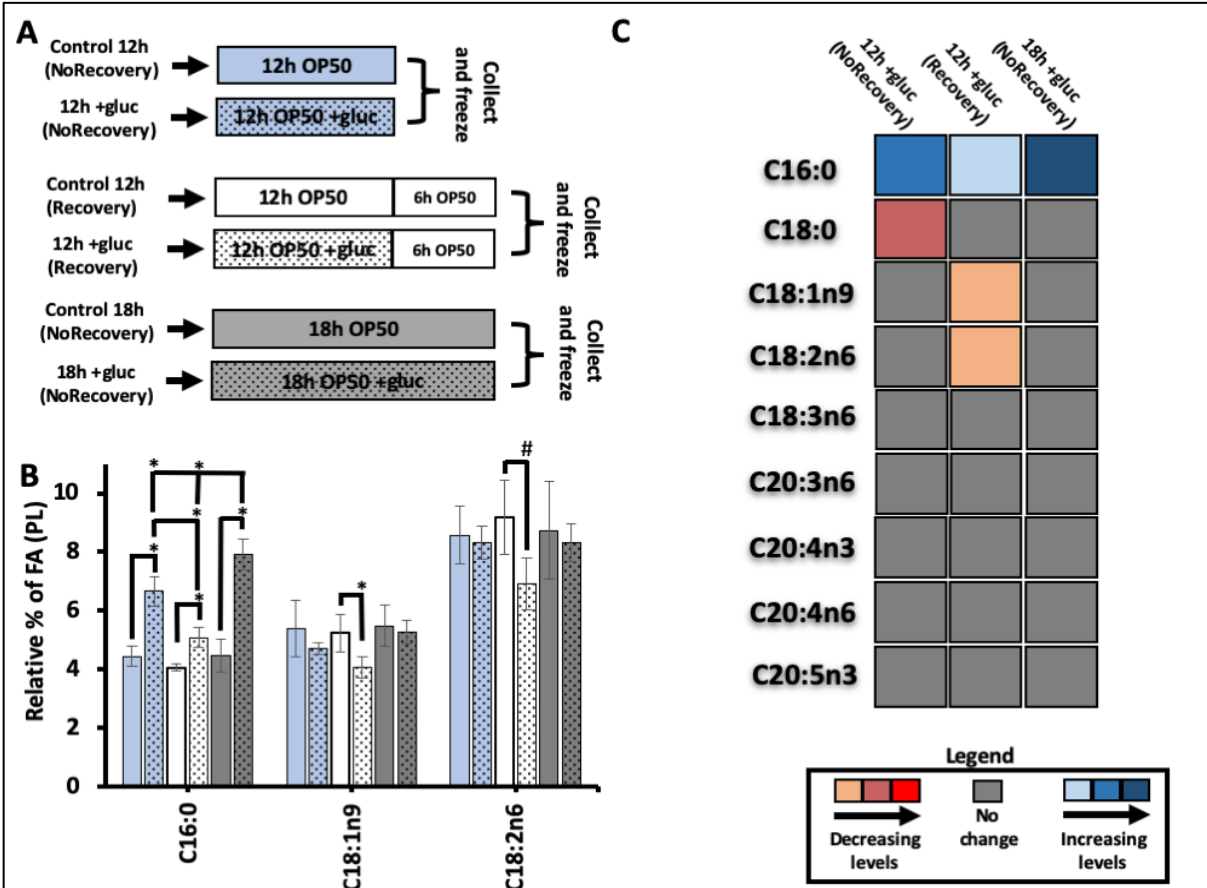


**Figure 8: Recovery periods induces significant alterations in membrane composition.** **A**) Bar scheme representing each control and stress condition. The blue bars represent nematodes collected immediately after 12 hours of stress, control 12h (NoRecovery)(solid blue) and +gluc 12h (NoRecovery)(black dot). The white bars represent nematodes allowed to recover for 6 hours in agarose plates seeded 0.15mg/mL of OP50, control 12h (Recovery)(solid white) and +gluc 12h (Recovery)(black dot). The gray bars represent nematodes collected immediately after 18 hours of stress, control 18h (NoRecovery)(solid gray) and +gluc 18h (NoRecovery)(black dot). **B**) C16:0 SFA showed significant increase in all glucose stressed animals relative to its controls (solid blue, solid black, and solid orange bars), and nematodes stressed for a longer period (18h) showed significantly larger accumulation of C16:0 compared to all other two stress conditions. UFA maintained stable levels in “NoRecovery” animals, but showed significant decrease in +gluc 12h (Recovery) compared to its respective control. C18:1n9 decreased from 5.2% ± 0.6 in control 12h (Recovery) to 4% ± 0.3 in +gluc 12h (Recovery), and C18:2n6 decreased from 9.1% ± 1.2 in control 12h (Recovery) to 6.9% ± 0.8 in +gluc 12h (Recovery). **C**) Heat map representing the alteration in FA levels comparing stressed animals to controls (+gluc/controls). Significant decreases are shown in light orange (little), dark orange (intermediate), and red (substantial). Significant increases are shown in light blue (little), median blue (intermediate), and dark blue (substantial). Gray bars indicate FAs that did not have significant alteration. For all GC/MS analysis, values represent means ± SEM of at least 9 replicates. Statistical significance, P<0.05 indicated by \* and P<0.1 is indicated by #, was calculated using unpaired T tests and F tests to compare variances.

treatment groups, decreased C18:1n9 abundance in the 12h plus recovery and decreased C18:2n6 abundance in the 12h plus recovery treatment group. In addition, there was a small but significant decrease in C18:0 in the 12 h group without recovery. Because of reduced C18:1n9 and C18:2n6 levels, we were particularly interested in examining whether the C20 PUFAs would also show altered levels. We found that there are no significant modifications in the relative abundance of any C20 PUFAs in any stress conditions (Figure 8C). Taken together, our data suggest that the reduction in C18:1n9 and C18:2n6 occurs as these fatty acids are converted to C20 PUFAs in the period following glucose exposure.

### **2.3.3. Membrane composition shows better adaptation and recovery after longer periods of stress**

In order to determine if changes in fatty acid abundance would occur with longer durations of glucose stress, nematodes were subjected to 100 mM glucose for 12 hours, 24 hours, 48 hours, and 72 hours. All treatment groups had a 6 hour recovery period to elicit the reduction in C18:1n9 and C18:2n6 as well as to allow for stable isotope labeling. First, C16:0 abundance was considered, and, with all durations of glucose stress, there was a significant increase in C16:0 (Figure 9A). Interestingly, the longer periods of glucose stress did not lead to further increases in C16:0 abundance. The lack of correlation between length of exposure and C16:0 levels suggests that there are mechanisms in place to maintain a maximum saturated fatty acid level consistent with previous work.

We next quantified the abundance of C18:1n9 with different lengths of 100mM exposure. Here, we found a decrease of C18:1n9 from  $4.4\% \pm 0.1$  in control 12h to  $3.9 \pm 0.1$  in +gluc 12h, and a greater decrease from  $5.6\% \pm 0.6$  in control 24h to  $4.3 \pm 0.2$  in +gluc 24h. However, the 48h and the 72h treatments did not lead to significant changes in C18:1n9 (Figure 9A). In order to interpret this data, we considered the oleic acid populations in the control populations which revealed that the baseline C18:1n9 levels increased in the 24h and the 48h controls (Figure 9A). The longer glucose exposure dictates that the lipid populations are being examined in older animals, and, although 24 h is a relatively short period of time, the first three days of adulthood are the peak reproductive period within the nematodes and are associated with metabolic changes (Byerly *et al.*, 1976) (Muschiol *et al.*, 2015).

To determine the impact of the altered C18:1n9 levels on fatty acid elongation and desaturation pathway, we next examined C18:2n6, the immediate product of C18:1n9 desaturation (Figure 9A). The trends in C18:2n6 were similar to C18:1n9 with significantly decreased abundance from  $10.8\% \pm 1$  in control 24h to  $7.5 \pm 0.3$  in +gluc 24h (Figure 9A). Similar to C18:1n9, there is no significant change within 48 hours of glucose feeding. However, the 72h analysis revealed significantly higher levels of C18:2n6 in control animals compared to the young 12 h stressed controls and a significant decrease in C18:2n6 with 72h glucose exposure (Figure 9A). We next examined if the reduction in C18:2n6 and C18:1n9 impacted the abundance of the C20 PUFAs downstream. To do so, we examined the levels of the major C20 PUFAs with 24 hours of glucose stress as that treatment had the greatest impact. For C20:3n6 and C20:5n3, there was no significant change in these pools despite a compromised precursor population supporting

the hypothesis that the C18:1n9 produced by FAT-7 upregulation is funneled to preserve C20 PUFAs (Figure 9B).

The C18:1n9 pool may be ultimately generated from dietary fat or *de novo* synthesized fatty acids. We implemented a stable isotope labeling strategy to determine whether the origin of the oleate pool is altered with glucose supplementation. Under basal conditions,  $14.8\% \pm 0.3$  of C18:1n9 is derived from *de novo* fatty acid synthesis consistent with past reports (Perez & Van Gilst, 2008). The contribution of synthesis to C18:1n9 production falls to  $13.2 \pm 0.3$  in +gluc 12h (Figure and from  $13.6\% \pm 0.4$  in control 24h to  $11 \pm 0.1$  in +gluc 24h when comparing the levels of C18:1n9 and C18:2n6, respectively (Figure 9B). The levels of linoleic acid were also decreased in +gluc 48h from  $12.9\% \pm 0.2$  to  $11.1 \pm 0.06$  when compared to the control 48h (Figure 9B). Interestingly, the levels of newly incorporated FAs in the control 72h started significantly lower when compared to all controls (12h, 24h, and 48h) (Figure 9B). This decrease was seen previously in our lab (data not published) during aging experiments testing the dynamics of PLs and FAs. Even though there is a 24 hours difference between our aging (Day 4) experiments compared to the data seen here (Day 3), we believe that this decrease might be related to the end of the nematode's fertile period. But comparing control 72h to +gluc 72h we see a significant increase in the dynamics of C18:1n9 and C18:2n6 in stressed animals, from  $10.1\% \pm 0.3$  to  $11.9 \pm 0.2$  and  $6.5 \pm 0.3$  to  $7.9 \pm 0.2$ , respectively.

To further evaluate the mechanisms responding to high glucose stress, and understand how the levels of UFA are controlled, we did a synthesis analysis based on the incorporation of stable isotopes (described in the methods section). We found a significant decrease in the synthesis of C16:0 and C18:1n9 only when comparing control

12h to +gluc 12h. Essentially, C16:0 decreased from  $11\% \pm 0.3$  to  $9.2 \pm 0.2$  and C18:2n9 from  $19.7 \pm 0.4$  to  $14.3 \pm 2.9$  (Figure 9C-D). We also noticed that the synthesis of both FAs showed a significant increase over time from 12 hours to 48 hours (Figure 9C-D).

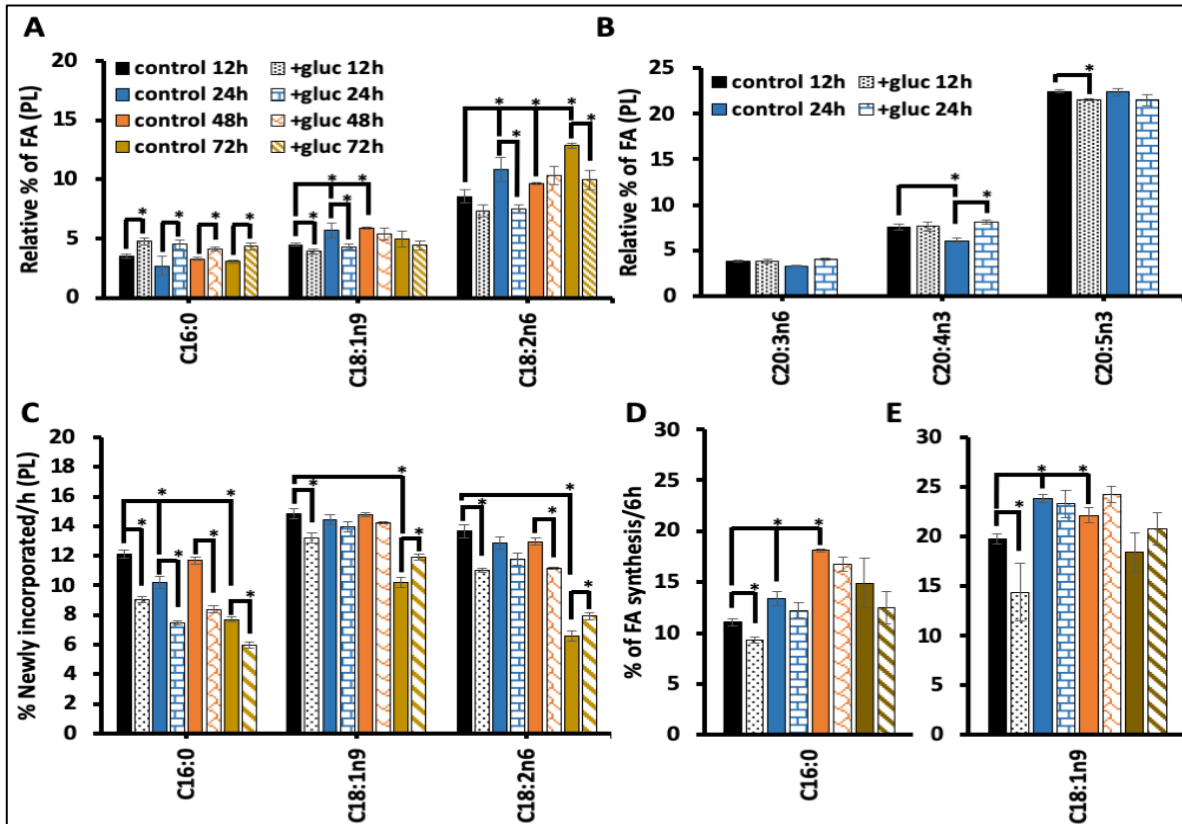


**Figure 9: Longer stress periods promotes better adaptation of oleic and linoleic FAs.** **A)** Analyzing the relative % of FA we found that C16:0 is significantly increased in all glucose stressed animals relative to its controls. C18:1n9 was significantly decrease comparing +gluc 12h (black dot) to control 12h (black bar), and 24h +gluc (blue horizontal brick) to control 24h (blue bar). Linoleic acid was significantly decreased comparing +gluc 24h to control 24h, and 72h +gluc (gold diagonal stripes) to control 72h (gold bar). The levels of oleic acid were significantly increased in control 24h and control 48h when compared to control 12h. The levels of linoleic acid in all controls (24h, 48h, and 72h) were significantly higher when compared to 12h control. **B)** The relative % of PUFAs assessed in 12h and 24h nematodes showed maintenance almost all FAs with the exception of a significant decrease in the levels of C20:4n3 comparing control 24h (blue bar) to control 12h (black bar), and in C20:5n3 comparing +gluc 12h (black dot) to control 12h (black bar). We also observed an increase in C20:4n3 comparing +gluc 24h (blue horizontal brick) to control 24h (blue bar). **C)** The % of newly incorporated FA showed significantly decreased of C16:0 in all glucose stressed animals relative to its controls. C18:1n9 significantly decrease in +gluc 12h compared control 12h, and increase in control 72h compared to control 72h. C18:2n6 decreased in +gluc 12h and +gluc 48h compared to their respective controls, and increase in +gluc 72h compared to control 72h. Control 72h and +gluc 72h showed significant decrease in the dynamics of all species compared to other conditions. **D)** FA synthesis was calculated based on the incorporation of isotopomers and corrected by a normalization factor that translates the probability of incorporation of each isotopomer. We noticed a significant decrease only in the synthesis of C16:0 in control 12h (solid black) compared to +gluc 12h (black dot). There was also a significant increase in the synthesis of C16:0 in control 24 (solid blue) and control 48h (black orange) compared to control 12h nematodes. **E)** Similarly, to C16:0, C18:1n9 there was a decrease in synthesis in +gluc 12h compared to control 12h, and increase in control 24 and control 48h compared to control 12h nematodes. For all GC/MS analysis, values represent means  $\pm$  SEM of at least 4 replicates. Statistical significance ( $P < 0.05$ ), is indicated by \* and was calculated using unpaired T tests and F tests to compare variances.

Thus, this data suggested that the organism uses FA synthesis, raising the production of new FAs, to respond to prolonged periods of stress.

Consistent with our previous data, the levels of newly incorporated SFA significantly decrease in all stressed animals when compared to their respective control (Figure 9B). But we did not find an extra decrease in the dynamics of nematodes stressed for a longer time. Similarly to UFA, the levels of C16:0 in the control 72h showed significant decrease when compared to all other controls (12h, 24h, and 48h) (Figure 9B). Taken together, our data suggest that after longer periods of stress the mechanisms adapting membrane composition behave more efficiently compared to short periods. Perhaps, because the longer stress periods allow the organism to understand exactly how to deal with the stress, avoiding excessive reactions. Also, it seems that young adults require higher dynamics of FAs to the membrane in order to compensate for the fatty acids that will be used in the production of eggs.

#### **2.3.4. Living bacteria is required for the impact of glucose stress on the membrane**

In the dietary glucose supplementation experiment, glucose was added to the agar media. Because the bacterial food source for the nematode (OP50) is also present in the media, during glucose exposure, glucose is in contact with both the bacteria and the worms. Thus, the bacteria can metabolize glucose and contribute to the effects of glucose stress. Bacteria may use glucose to synthesize excess saturated fatty acids, and thus impact the diet of the worms. Alternatively, a recent study shows that bacteria metabolizing glucose can cause oxidative stress through increased production of advanced glycation agents (Kingsley *et al.*, 2021). To test the impact of bacteria

processing glucose on the membrane composition, we set up an experimental design shown in the scheme (Figure 10A). Briefly, the OP50 bacteria was grown in LB broth media. After the bacteria were separated into two groups- living and heat-killed bacteria. Living bacteria was resuspended into fresh LB (OP50) and LB media containing 100 mM glucose (OP50 +gluc). In the other treatment group, bacteria was heat killed at 65 °C for 20 mins and resuspended into fresh LB media (OP50 HK) and LB media containing 100 mM glucose (OP50 HK + gluc). First, to establish the impact of heat killing on the bacteria's food source, we analyzed the fatty acid composition using GC/MS. Notably, we found that heat killing significantly increased the level of saturated fatty acids and decreased the level of unsaturated fatty acids. The level of C16:0 (the most abundant saturated fatty acid in the bacteria) increased from 33.7%  $\pm$  1 in OP50 to 52%  $\pm$  4.5 in OP50 HK. The level of C18:1n7 (the most abundant unsaturated fatty acid in the bacteria) decreased from 28.4  $\pm$  4.5 in OP50 to 6.7%  $\pm$  2.1 in OP50 HK. Interestingly, glucose did not impact the composition of living bacteria. However, glucose led to changes in OP50 HK + gluc, with a significant decrease in the level of C14:0 (Figure 10B).

To assess the impact of bacteria processing glucose on the lipid composition of the nematodes, the animals were fed a bacteria diet from the four treatment groups outlined in Figure 4A for 12 hours (+ recovery). The phospholipid composition was analyzed using HPLC/MS-MS. Here we focus on the main phospholipid class, phosphatidylcholine (PC) and phosphatidylethanolamine (PE) which constitute the major membrane phospholipid (See supplement table 1 for full list). Because the GC/MS analysis revealed distinct changes in the unsaturation levels of specific fatty acids, the phospholipids were binned according to the total number of double bonds present in the



two fatty acid tails (i.e., 0-1, 2-3, 4-5, 6-7 and 8 or more). In analyzing the PC population, we found that feeding the animals with OP50+ gluc led to a significant decrease in the level of species with 2-3 double bonds and an increase in species with 4-5 double bonds

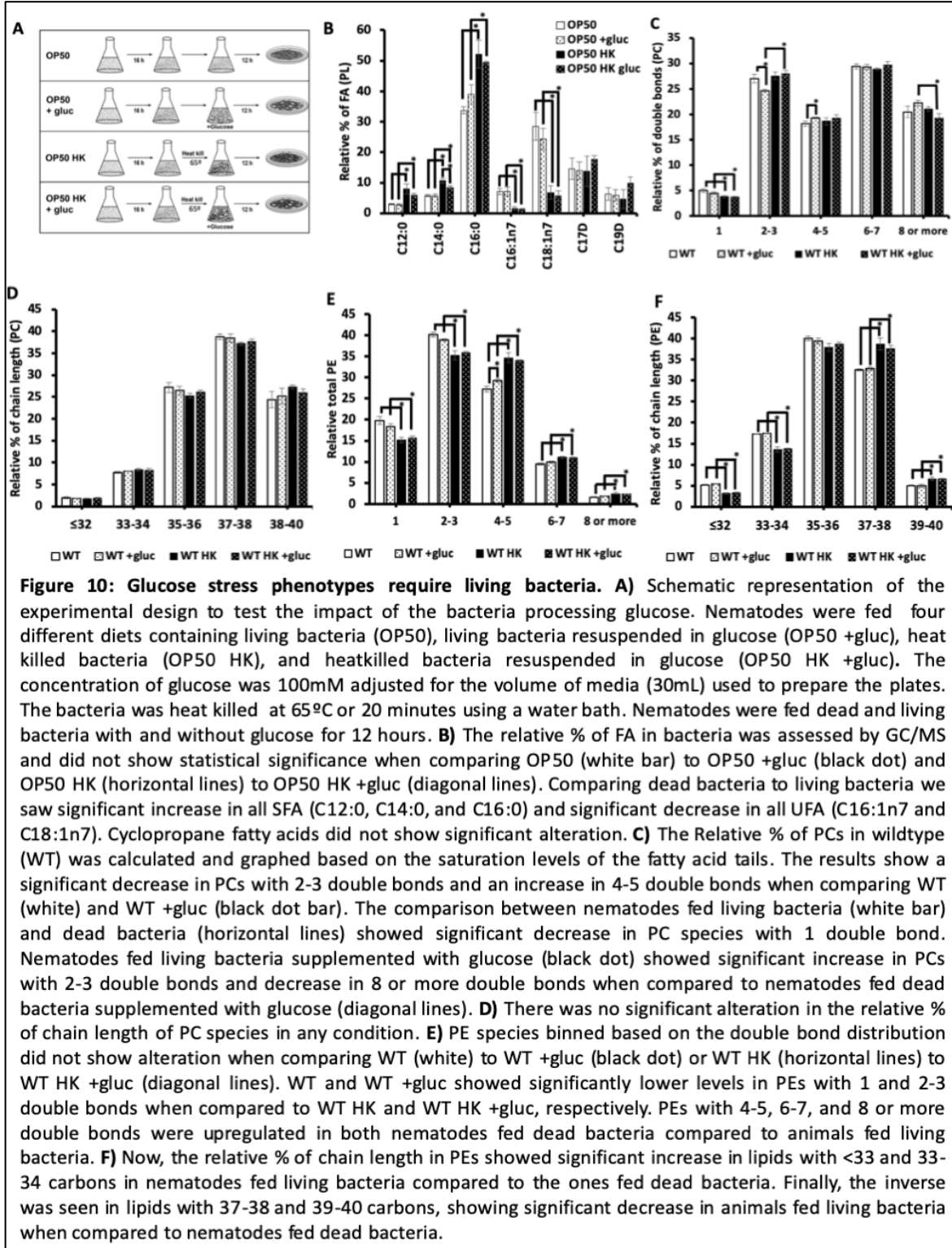


(Figure 10C). The decrease in lipid species with 2-3 double bonds is consistent with GC/MS data as the fatty acids C18:1n9 and C18:2n6 are mostly present in this population. Contrastingly, worms that were fed a HK OP50 +gluc did not have any significant change in their degree of unsaturation. The phospholipid was also binned according to their chain length (total number of carbon present) as the length of phospholipids can influence the biophysical property of the membrane such as thickness. However, there were no significant changes in the chain length of PC lipids when the worms were fed either living bacteria or heat-killed bacteria (Figure 10D).

In analyzing the double bond distribution of the PL population, the results show fewer changes in PC lipids when the animals were fed OP50 + gluc diet with only a significant increase in phospholipids with 4-5 double bonds (Figure 10E). Again, there were no significant alterations in the level of unsaturation when the nematodes were fed a HK OP50 +gluc diet. Furthermore, there was no significant impact on the chain length when the animals were fed glucose via living or heat-killed bacteria (Figure 10F). Notably, there were significant changes in the chain length distribution of OP50 compared with OP50 HK. These changes reflect the difference in the dietary composition of living bacteria and heat-killed bacteria. In summary, these results show that living bacteria is required to observe the effects of glucose stress on the membrane lipid composition.

## **2.4. Discussion**

Here, we used increasing concentrations of glucose along with different feeding windows to map the metabolic responses to glucose stress. In doing so, we established that the main feature of the glucose stress response is in regulating the saturation balance

in the PL membrane (Svensk *et al.*, 2016) (Devkota *et al.*, 2017). We hypothesize that this response is largely mediated by PAQR-2, a membrane sensor homologous to the mammalian protein AdipoR2. PAQR-2 plays a similar role in regulating membrane fluidity in the membrane of HEK 293 cells (Ruiz *et al.*, 2019). Additionally, the activity of AdipoR2 also promotes the regulation of UFA by controlling the activity of desaturases such as SCD ( $\Delta$ -9-desaturase) (Pilon, 2016). The data shown here reveals an important regulation of UFA responding to high glucose stress, and this regulation appears to start on the levels C18:1n9 and C18:2n6.

This research aimed to understand how the PL and FA levels are regulated during elevated concentrations of glucose and different periods of stress. We know that proteins like PAQR-2 play an important role in the proper adaptation of membrane composition during stress (Devkota *et al.*, 2017). Although regulation of membrane saturation was shown by controlling the activity of FAT-7, the majority of the data testing membrane composition used mild concentrations (15 to 20mM) of glucose (Vieira *et al.*, 2022) (Devkota *et al.*, 2017). These concentrations were enough to show an accumulation of SFA in healthy nematodes, but species like C18:1n9 and C18:2n6 maintained stable levels (Svensk *et al.*, 2016). In order to have a more complete understanding of PL and FA regulation, we tested the membrane composition and dynamics in higher (100 and 200mM) concentrations of glucose. Our labeling technique indicated a decreased renewal of C16:0 in all concentrations of glucose, but C18:0 renewal became affected only in 100 and 200mM. Likewise, UFA species showed a decrease in C18:1n9 and C18:2n6 renewal only when submitted to the higher concentrations of glucose. There was no reduction in the fatty acids downstream of C18:2n6 indicating that C20 PUFA synthesis is prioritized.

Each double bond is responsible to create "kinks" in the FA structure disrupting the tight packing of more linear molecules such as saturated fat. Previous fluorescence studies in cell culture have shown that the incorporation of fatty acids with four or more double bonds such as AA, EPA, and DHA increases membrane fluidity (Ruiz *et al.*, 2018) (Yang *et al.*, 2011). We hypothesize that the decreased levels in all precursor FAs and the strict maintenance of PUFAs are a funneling process towards the maintenance of highly unsaturated fat to control membrane fluidity.

Although we can map the response to elevated glucose in the diet, it is not clear how the excess glucose is driving those changes. Here, we find that this response requires living bacteria as we do not see the same changes with heat-killed bacteria. Furthermore, we find only a moderate increase in saturated fatty acid abundance in the diet. Taken together along with finding that glucose can promote oxidative damage in molecules, we hypothesize that high levels of glucose stress result in an elevated oxidative burden in the nematodes (Volpe *et al.*, 2018). Several groups have associated glucose accumulation with the increase of oxidative stress ultimately affecting cell migration and promoting inflammation in human tissues (Wu *et al.*, 2016) (Oguntibeju *et al.*, 2019) (Peng *et al.*, 2013). In the membrane, the FAs form a major target of oxidation, resulting in the production of peroxidation products (Ayala *et al.*, 2014). This happens because the double bonds are particularly susceptible to ROS attack allowing for hydrogen abstraction from the carbon atoms (Assies *et al.*, 2014). Therefore, PUFAs' susceptibility to damage is high, also being capable of causing chain reactions of oxidative degradation. In our experiments, we substantially increased glucose concentration, which could have raised the levels of oxidative damage in the PUFAs.

Thus, the maintenance of PUFAs may be an effort to correctly replace damaged lipids avoiding membrane dysregulation and consequently apoptosis. In support of this model, the decrease in lifespan seen in nematodes exposed to alive bacteria fed glucose does not happen in dead bacteria supplemented with glucose (Alcántar-Fernández *et al.*, 2018).

To better understand the importance of C18:1n9 and C18:2n6 in the overall response to high levels of glucose, we proposed to test the effectiveness of recovery mechanisms in restoring membrane composition after removal from the stress source. It was previously shown that removing PAQR-2 mutants from glucose stress allows for full development to adulthood if the stress does not last longer than 12 hours (Devkota *et al.*, 2017). Clearly, mechanisms responding to the glucose stress help in the amelioration until basal conditions are restored (Ayala *et al.*, 2014) (Assies *et al.*, 2014). However, little is now about the influence of these mechanisms in the membrane adaptation to recovery. In our experiments, the labeling techniques submit the nematodes to a 6 hours recovery period after stress, which becomes a great opportunity to further understand the process of membrane recovery. Interestingly, the decrease seen in C18:1n9 and C18:2n6 is only seen during recovery periods, which suggests either a continuous activity of enzymes consuming or reduced activity of enzymes producing this species. Analyzing the recovery response to longer stress periods made clear that the effectiveness of the recovery is time-dependent.

In conclusion, our findings indicate that: the regulation of oleic and linoleic fatty acids is essential to respond against high concentrations of glucose; also, that this

response is time-dependent and relay on the proper synthesis and dynamics of these FAs to the membrane; and lastly that the stress is caused only by alive bacteria.

## **2.5. Methodologies & Techniques**

### **2.5.1. Strains maintenance and population synchronization**

All experiments were conducted using wildtype N2 nematodes obtained from the *C. elegans* Genetics Center (CGC; MN, USA). To synchronize the population and allow development at the same life stage, we submitted gravid adults to 20% bleach solution for 6 minutes. The eggs recovered from the bleach were washed at least 3 times and left rotating overnight at 20°C in M9 solution. Unless specified, OP50 bacteria on HG plates was used to feed the nematodes.

### **2.5.2. Stress conditions, labeling strategy and time-course experiments**

The preparation of glucose stress plates (+gluc) followed the protocol that we published previously in Vieira *et al.*, 2022. Shortly, the +gluc plates were made to a final concentration of 15mM, 100mM, and 200mM of glucose by adding a filtered glucose solution to cooled autoclaved HG media. All the plates were seeded using regular OP50 bacteria and the +gluc plates were seeded at least 4 days before plating the worms. To start the stress, synchronized L4 stage worms growing on HG plates were transferred to +gluc plates and kept for 12, 24, 48, and 72 hours.

Our label strategy followed the protocols established by Perez & Van Gilst, 2008. Briefly, isogro media (<sup>13</sup>C) and LB media (<sup>12</sup>C) were inoculated with OP50 colonies to allow the growth of bacteria for 16 hours at 37°C. Next, the bacteria were harvested and

resuspended in M9 at a concentration of 0.15g/mL. A mixture containing enriched bacteria  $^{13}\text{C}:^{12}\text{C}$  (60%:40%) was transferred to agarose plates and allowed to dry. Nematodes from +gluc plates were harvested, washed three times using M9, and plated onto stable isotope labeling plates containing 800uL of bacteria mixture for 6 hours. Labeled worms were harvested, washed, and stored at  $-80^{\circ}\text{C}$  until lipid extraction and analysis by GC/MS.

Labeling with stable isotopes ( $^{13}\text{C}$ ) allows for the analysis of the percentage of all newly incorporated FA species simultaneously. Briefly, to calculate the MPE the isotopomers were normalized and corrected to the incorporation of natural isotopes. % Newly Incorporated Fatty Acids considers all newly modified fat independent of its source (*de novo* synthesized, elongated, or directly absorbed) as described in Dancy et al. Error bars of the  $^{13}\text{C}$  labeling show the standard error of the mean, and *t-tests* were used to identify significant differences between the fatty acids.

### **2.5.3. Recovery assay**

The glucose plates (+gluc) were made to a final concentration of 100mM of glucose by adding a filtered glucose solution to cooled autoclaved HG media. OP50 bacteria was used to seed control and +gluc plates at least 4 days before transferring the worms. To start the stress, synchronized L4 stage worms growing on HG plates were transferred to +gluc plates and followed the stress as described below:

- 12 hours NoRecovery: Nematodes spent 12 hours on glucose plates and were collected and washed three times before immediately snap-freeze for further

GC/MS analysis. This condition was labeled +gluc 12h (NoRecovery) in the text and figures.

- 12 hours Recovery: Nematodes spent 12 hours on glucose plates and 6 hours of "recovery period" in agarose plates seeded with concentrated OP50 (0.15mg/mL) to mimic the conditions in labeling plates. After recovery, they were collected and frozen to further analysis by GC/MS. This condition was labeled +gluc 12h (Recovery) in the text and figures.
- 12 hours NoRecovery: Nematodes spent 18 hours on glucose plates and were collected and washed three times before immediately snap-freeze for further GC/MS analysis. This condition was labeled +gluc 18h (NoRecovery) in the text and figures.

#### **2.5.4. Viability Curves and Lifespans**

To quantify survival on +gluc plates, L4440 bacteria were seeded onto 3cm NGM +CI plates, and L1 worms were grown for 48 hours. Approximately 50 L4 stage nematodes were then transferred to fresh NGM +CI +gluc plates each day, and the number of dead animals was determined by gently prodding with a pick.

#### **2.5.5. Heat-killed bacteria**

Concentrated OP50 *E. coli* stocks were generated from OP50 stock plates by inoculating 2-3 colonies in each of 4 flasks of 50 mL LB media. These flasks were left to shake overnight (16-18 hours) at 250 rpm and 37°C. Each flask of 50 mL was put into an individual 50 mL centrifuge tube, labeled live OP50 (LOP50), live OP50 plus glucose (LOP50 gluc), heat-killed OP50 (HK), and heat-killed OP50 plus glucose (HK gluc), and



spun at 3900 rpm for 10 minutes to pellet the bacteria. All four pellets were resuspended in M9 according to the pellet's mass at a concentration of .015g/mL. After heating a water bath to 65°C, two of the four resuspended pellets were heat-killed for 20 minutes (HK and HK gluc). All four tubes of living and dead bacteria were centrifuged at 3900 rpm for 10 minutes again. Considering the volume of media in each HG plate as 30 mLs, to prepare a 100mM stress plate, we measured 0.54g of glucose and dissolved it in 1mL of M9 1x. Two tubes containing glucose solution were transferred to two bacterial pellets of either living or dead bacteria (LOP50 gluc and HK gluc). The two remaining tubes of living and dead bacteria pellets were resuspended in pure M9 1x (LOP50 and HK). The heat-killed tubes of M9 and M9 glucose resuspensions were streaked on LB plates and left overnight in a 37°C incubator to confirm death. All tubes were kept at room temperature for about 12-14 hours until needed for seeding plates. Before plates were seeded, the tubes containing heat-killed bacteria were placed again in a 65°C water bath for 20 minutes to ensure no survival of bacteria. Before transferring nematodes, the plates received a large volume of liquid and were allowed to dry for about 20-40 minutes at room temperature inside the fume hood. Nematodes in the L4 stage were transferred to each plate condition (LOP50, LOP50 gluc, HK, and HK gluc) right after the plates were completely dry, and allowed to feed for 12 hours before they were frozen and saved for analysis.

#### **2.5.6. Lipid Extraction and GC Analysis**

Total lipid was extracted using a chloroform:methanol solution (2:1 mixture) and the PL population was separated using solid phase chromatography before GC-MS analysis (Perez & Van Gilst, 2008) (Dancy et al., 2015). Lipid standards, 1,2-diundecanoyl-sn-glycero-3-phosphocholine (Avanti Polar Lipids) and tritridecanoin (Nu-

Chek Prep) were added to each sample and used as an internal control to ensure proper separation. Dried total lipids resuspended in 1mL of chloroform were loaded onto HyperSep Silica SPE columns (100mg capacity, Thermo Scientific), and after a sequence of chloroform (3 mL), and acetone:methanol(9:1 (5mL)); pure methanol was used to elute PLs from the column. Purified PLs were dried and resuspended in 1mL of 2.5% H<sub>2</sub>SO<sub>4</sub> in methanol, then incubated for 1 hour at 80°C to create fatty acid methyl esters (FAMES) to run on GC-MS (Thermo trace 1310, ISQ LT single quadruple).

The relative % of FAs in each sample was calculated by using the integrated area under the peaks seen in the gas chromatograph and as defined here:  $\text{Relative FA Abundance} = \frac{\text{FA area}}{\text{Total FA area}} * 100$  as in (Perez & Van Gilst, 2008). Error bars of the lipid composition show the standard error of the mean, and *t-tests* were used to identify significant differences between the fatty acids.

### **2.5.7. Determining the synthesis of fatty acids**

To determine the percentage of synthesized fatty acids we followed the protocol published by Perez & Van Gilst, 2008 and Dancy et al., 2015. Briefly, using the mass variation in the parent ion ( $m+1$ ,  $m+2$ , etc) analyzed by GC/MS, we excluded peaks directly incorporated from the diet and elongated from dietary content. For instance, the molecular weight of C<sub>16:0</sub> can vary from 270 to 286 depending on if 0 or 16 stable isotopes (<sup>13</sup>C) were incorporated into the molecule. Based on the examination of bacterial data and the normalization for the natural incorporation of <sup>13</sup>C, peaks between 270-272 and 284-286 were considered directly incorporated or elongated from the diet. Therefore, to calculate the synthesis of FA, peaks between 273-283, after normalization, were

selected. The percentage calculation takes into consideration the sum of 273-283 peaks over the sum of total peaks 270-286 multiplied by 100%, as represented in the equation below.

$$\text{Synthesis \% of FA} = (\Sigma 273-283) / (\Sigma 270-286) \times 100$$

#### **2.5.8. Phospholipid extraction and analysis using HPLC-MS/MS**

The phospholipid analysis was conducted based on previous studies (Dancy Drechsler papers). Briefly, total phospholipids were extracted from frozen nematodes based on the Folch procedure using 2:1 chloroform: methanol. Extracted lipids were resuspended in 200  $\mu$ L of acetonitrile/2-propanol/water (65:30:5 v/v/v) and 10  $\mu$ L was injected into the Dionex UHPLC UltiMate 3000. The phospholipids were separated on a reverse-phase LC column (C<sub>18</sub> Hypersil Gold 2.1 x 50mm, 1.9 $\mu$ m column) at a flow rate of 300  $\mu$ L/min. The phospholipids were eluted using gradient solvents A and B containing 10 mM ammonium formate (NH<sub>4</sub>COOH) and 0.1% formic acid (FA). Solvent A was composed of 60/40, water/acetonitrile, and solvent B was composed of 90/10, isopropyl alcohol/acetonitrile. The schedule for the gradient was 32% B over 0-1.5 min; 32-45% B from 1.5-4 min; 45-52% B from 4-5 min; 52-58% B from 5-8 min; 58-66% B from 8-11 min; 66-70% B from 11-14 min; 70-75% B from 14-18 min; 75-97% B from 18-21 min; 97% B up to 25 min; 97-32% B from 25-26 min; 32% B is maintained until 30 min for column equilibration.

Mass spectrometry of PLs was performed on a Qexactive mass spectrometer (Thermo Fisher Scientific). The analysis was performed in the negative ion mode and Full scan data-dependent MS<sup>2</sup> (ddMS<sup>2</sup>) mode. The scan range for MS analysis was 300-1200 m/z with a maximum injection time of 100 ms and an AGC target of 10<sup>6</sup>. The capillary


spray voltage was set at 3.2 kV and the capillary temperature was set at 325°C The sheath gas flow rate at 45 units and the auxiliary gas flow at 10 units. For MS1 profiling, scans were run at a resolution of 70k. MS2 analyses were performed at NCE of 35 using 6 scan events, with the top five ions chosen from an initial MS1 scan.

Analysis of the LC-MS/MS data was conducted using the software Lipid Data Analyzer (LDA) Version 2.8.1. A 0.1% relative peak cutoff value was applied to the RAW files in order to focus on the major phospholipid species.

## Chapter 3: Monomethyl branched-chain fatty acids are critical for *Caenorhabditis elegans* survival in elevated glucose conditions

Received for publication, March 10, 2021, and in revised form, November 12, 2021  
Published, Papers in Press, November 23, 2021,

<https://doi.org/10.1016/j.jbc.2021.101444>

Andre F. C. Vieira<sup>1</sup>, Mark A. Xatse<sup>1</sup>, Hamide Tifeki<sup>1,2</sup>, Cédric Diot<sup>3</sup> , Albertha J. M. Walhout<sup>3</sup>, and Carissa Perez Olsen<sup>1, \*</sup>

From the <sup>1</sup>Department of Chemistry and Biochemistry, Worcester Polytechnic Institute, Worcester, Massachusetts, USA; <sup>2</sup>Department of Chemistry, University of Alaska Anchorage, Anchorage, Alaska, USA; <sup>3</sup>Program in Systems Biology and Program in Molecular Medicine, UMASS Medical School, Worcester, Massachusetts, USA

**Note:** The mass spectrometry data analyzing composition and dynamics in bacteria, N2, PAQR2, and *elo-5* RNAi was completed by Andre Vieira, as well as the *elo-5* and *elo-6* lifespan curves in glucose and C16:0 stress. The lifespan curves in *elo-5* mutants (*gk208*) and PAQR-2 mutants was a collaboration of replicates carried by Andre Vieira and Mark Xatse. The qRT-PCR was conducted and plotted by Cedric Diot.

### 3.1. Abstract

The maintenance of optimal membrane composition under basal and stress conditions is critical for the survival of an organism. High-glucose stress has been shown to perturb membrane properties by decreasing membrane fluidity, and the membrane sensor PAQR-2 is required to restore membrane integrity. However, the mechanisms required to respond to elevated dietary glucose are not fully established. In this study, we used a <sup>13</sup>C stable isotope-enriched diet and mass spectrometry to better understand the impact of glucose on fatty acid dynamics in the membrane of *Caenorhabditis elegans*. We found a novel role for monomethyl branched-chain fatty acids (mmBCFAs) in mediating the ability of the nematodes to survive conditions of elevated dietary glucose.

This requirement of mmBCFAs is unique to glucose stress and was not observed when the nematode was fed elevated dietary saturated fatty acid. In addition, when worms deficient in *elo-5*, the major biosynthesis enzyme of mmBCFAs, were fed *Bacillus subtilis* (a bacteria strain rich in mmBCFAs) in combination with high glucose, their survival rates were rescued to wild-type levels. Finally, the results suggest that mmBCFAs are part of the PAQR-2 signaling response during glucose stress. Taken together, we have identified a novel role for mmBCFAs in stress response in nematodes and have established these fatty acids as critical for adapting to elevated glucose.

### **3.2. Introduction**

In many disease states, including diabetes, cancer, and neurodegenerative diseases, defects in membrane structure and composition have been identified (Gianfrancesco, *et al.*, 2018) (Pilon, 2016) (Samuel & Shulman, 2012) (Bandu, Mok, & Kim, 2018) (Fanning *et al.*, 2019) (Fecchio, Palazzi, & de Laureto, 2018). Biological membranes are essential barriers between the intracellular and extracellular environment and are also crucial in the compartmentalization of subcellular organelles. Membranes are not limited to establishing passive barriers, but they also influence numerous and diverse cellular bioactivities such as signaling and regulation (Budin *et al.*, 2018) (Hedger & Sansom, 2016) (Koshy & Ziegler, 2015) (Levental *et al.*, 2020) (Spector & Yorek, 1985). Although membranes allow a certain degree of variation in their makeup, it is critical to maintain a membrane composition within an acceptable range for optimal cellular function. Several studies have shown that there are regulatory mechanisms, including membrane sensors, that detect perturbations in the biophysical properties of the

membrane and can allow membranes to adapt to variations in environmental cues including temperature and dietary composition (Siliakus, van der Oost, & Kengen, 2017) (Svensk et al., 2016).

Model systems including the nematode, *Caenorhabditis elegans*, have been established in order to probe the regulation of membrane composition and the response to perturbations. In addition to the genetic tools available, *C. elegans* has the added advantage of being small enough to allow for high isotope enrichment and subsequent detailed measurements of membrane flux. Our lab has developed stable isotope feeding strategies in *C. elegans* to track the incorporation of new fatty acid molecules into the membrane (Perez & Van Gilst, 2008) (Dancy *et al.*, 2015). Using this technique, we established that the majority of the membrane lipids are replaced or modified within a 24-h period in young animals. This replacement is significantly greater in the phospholipids showing 1.7-fold faster renewal than in neutral lipids used to store fat in the same animals (Dancy *et al.*, 2015) (Sultana, & Olsen, 2020). Thus, in addition to responding to external and internal stimuli, the phospholipid membrane is a highly dynamic structure with tremendous flux of lipids in and out of the membrane even under basal conditions. Not only is the turnover greatly abundant in membrane lipids, but the rates differ depending on the specific type of lipid, thus allowing for the maintenance of overall membrane composition and adjustment of that content when needed.

Monomethyl branched-chain fatty acids (mmBCFAs) are present in plants, bacteria, and animals, and decreased levels of mmBCFAs in humans have been linked to obesity and insulin resistance (Su *et al.*, 2015). In *C. elegans*, mmBCFAs are found within the membrane at significant concentrations, accounting for about 5.5% of the

relative abundance of FAs. They are synthesized from branched-chain amino acids particularly leucine through the activity of the branched-chain ketoacid dehydrogenase complex (BCKDH), fatty acid synthase (FASN-1), and acetyl-coA carboxylase (POD-2) ultimately resulting in the production of C13iso, which is elongated by elo-5 and elo-6 to make C15iso and C17iso; (Kniazeva et al., 2004) (Kniazeva, Euler & Han, 2008). mmBCFAs are critical for post embryonic growth facilitated in part by activating TORC1 signaling pathway to facilitate nutrient sensing and metabolism in nematodes (Kniazeva et al., 2015) (Zhu et al., 2013) (Wallace et al., 2018).

In bacteria, the presence of mmBCFAs impacts the packing of the membrane and influences overall membrane fluidity (Mercier, Dominguez-Cuevas, & Errington, 2012) (Jones et al., 2002). In fact, two branched-chain fatty acid classes, referred to as iso and anteiso, contain a methyl group at either the penultimate or the antepenultimate carbon, respectively, and are the most prominent fatty acids of cell membranes of some bacteria, especially of the genus *Bacillus*. The presence of these branched fatty acids has a different impact on membrane properties such as packing, since they mimic properties of both straight-chain saturated and cis- monounsaturated fatty acids (MUFAs). The ratio iso/anteiso fatty acids is reduced when the growth temperature is decreased, indicating that anteiso species strongly affect membrane fluidity compared with iso species (Eibler et al., 2017) (Rilfors, 1984). However, the participation of mmBCFAs in the response to other external stress such as high glucose diet has not yet been described.

Altered conditions such as temperature changes require that the membrane composition is adjusted in order to maintain the membrane's properties. For instance, lower temperatures reduce overall membrane fluidity in poikilotherms and, thus, require



an increase in the amount of unsaturated fatty acids provided to the membrane to maintain membrane function (Holthuis & Menon, 2014) (Watts & Ristow, 2017). The presence of double bonds in the cis configuration causes kinks or bends in the acyl chain, affecting the overall fatty acid packing and consequently the membrane structure increasing fluidity (van Meer, Voelker & Feigenson, 2008). The amount of saturated fat within a membrane must be balanced with monounsaturated (MUFA) and polyunsaturated (PUFA) fatty acids to tune the biophysical properties of the membrane (Farine et al., 2015). Other fatty acids including mmBCFA contribute to overall membrane fluidity and permeability as well.

Glucose homeostasis is critical, and organisms have multiple regulatory mechanisms that allow them to maintain optimum membrane composition when challenged with glucose. For example, PAQR-2 is a protein capable of sensing and responding to the accumulation of saturated fat within the endoplasmic reticulum induced by cold temperature. Additionally, PAQR-2 is required for survival in other conditions that perturb the membrane properties including excess dietary glucose (Devkota *et al.*, 2017). In the absence of PAQR-2, nematodes fed glucose accumulate SFAs, have a withered tail, and reduced viability. The most well-characterized role for PAQR-2 is to provide UFA to the membrane through the FAT-7 desaturase, which incorporates the first double bond into the saturated fatty acids. However, it is unclear if PAQR-2 influences the activity of other metabolic pathways that contribute to survival in elevated glucose diets. Although it is clear that membrane composition is impacted by glucose stress, the mechanisms involved in responding to perturbations in membrane properties have not been completely defined. In our studies, we use stable isotope labeling under elevated glucose conditions

to monitor the fatty acid populations of the membrane after stress. Our results unveiled a novel role for mmBCFAs in surviving elevated glucose conditions. We have probed these relationships to find that nematodes not producing mmBCFAs show decreased survivorship when stressed with glucose.

### **3.3. Results**

Here we present all the results proving the importance of mmCBFAs to respond against glucose stress. In the text, we showed all the figures seen in the body of our publication; however, the supplementary tables and figures will not be included in this Thesis due to the size of the material. To see the supplementary material, you can access the page of the official publication.

#### **3.3.1. Quantifying membrane dynamics with elevated dietary glucose**

While it has been established that high-glucose diets require a compensatory metabolic shift in lipid pathways, the specific alterations in the membrane lipids of animals exposed to excess glucose have not been identified. To define the response to dietary glucose, we transferred larval (L4) *C. elegans* to 15 mM glucose supplementation plates (referred to as “+gluc plates”), which is the concentration where phenotypes are observed in *paqr-2* mutant animals with minimal lethality (Svensk et al., 2016). After 12 h on +gluc plates, animals were collected, fatty acid methyl esters were created from the major lipid classes (i.e., phospholipids, neutral lipids, glycolipids) and analyzed by gas chromatography–mass spectrometry (GC-MS) to quantify the relative abundance of associated fatty acids ((see Experimental procedures) Perez and Van Gilst, 2008). We will use the standard nomenclature (CX:YnZ) to describe the fatty acid populations where

X indicates the number of carbons in the fatty acid, and Y shows the number of double bonds at position Z for our analysis.

We first examined the changes in phospholipids on +gluc plates focusing on the major fatty acid populations (>1.5% of the total pool). Here, we do not report the fatty acid analysis for the polyunsaturated fatty acids, because they contain more than two double bonds and fragment extensively in the mass spectrometer making them incompatible with the stable isotope studies reported later. We found that there were no significant changes in any major fatty acid species with the exception of a decrease in vaccenate (C18:1n7) from  $18.1 \pm 0.8\%$  to  $15.7 \pm 0.6\%$  and a slight increase in palmitate (C16:0) from  $3.7 \pm 0.2\%$  to  $4.8 \pm 0.3\%$  (Fig. 11A). The reduction in C18:1n7 levels is likely due to the reduced presence of this species in the bacteria exposed to glucose. The lack of major changes in the phospholipid populations has been previously demonstrated by HPLC-MS-based studies as well (Svensk et al., 2016). The result further supports the presence of maintenance mechanisms to specifically control the fatty acid composition of the membrane lipids under elevated glucose concentrations.

These maintenance pathways may be specific to membrane lipids or may regulate lipid metabolism pathways in general. Therefore, to determine whether glucose supplementation impacts the other pools within the nematode, we evaluated the neutral lipid fraction, which represents the stored fat. After extraction and analysis by GC-MS, we found more significant changes in the overall fatty acid profile from neutral lipids. Specifically, there are significant decreases of multiple fatty acid populations including a reduction of vaccenate (C18:1n7) by 22%, oleate (C18:1n9) by 17%. The mmBCFAs, 13-methyl myristic acid (C15iso), and 15-methyl hexadecanoic acid (C17iso) were decreased

by 23% and 17% respectively (Fig. 11B). These alterations support the conclusion that glucose supplementation drives changes in lipid metabolism pathways and that the neutral lipid pools are regulated less than phospho- lipid populations.

One potential issue using the GC/MS to analyze the membrane composition is that changes in lipid pools might be diluted by the preexisting large quantities of lipids at the start of the glucose stress. Therefore, we incorporated a global dietary stable isotope tracer to monitor the different types of lipids provided to the membrane immediately following glucose supplementation. The nematodes were fed bacteria enriched with  $^{13}\text{C}$  - isotopes by growing the standard laboratory diet (OP50) in Isogro  $^{13}\text{C}$  -enriched media (>99%  $^{13}\text{C}$  from Sigma-Aldrich) (Dancy *et al.*, 2015). After the appropriate corrections (defined in the Experimental procedures), the stable isotope labeling was examined in the palmitate (C16:0) population, as previous studies have observed high levels of palmitate in the absence of corrective pathways. There is a significant reduction in the provision of C16:0 to the membrane with  $8.6 \pm 0.6\%$  of C16:0 being newly incorporated in glucose-fed worms compared with  $11.5 \pm 0.3\%$  in control animals (Fig. 11C). To determine if this decrease is a common feature of saturated fatty acids, we examined C18:0 and found no significant decrease in C18:0 stable isotope patterns. Thus, we conclude that the downregulation of flux is specific to C16:0 and not all saturated fatty acids.

Because of the use of a general stable isotope tracer, we can probe the remaining fatty acid species in the same animals with the exception of the C20 PUFAs that fragment extensively in the mass spectrometer. The dynamics of the C18 mono- and polyunsaturated fatty acids, namely oleate (C18:1n9) and linoleate (C18:2n6), were not impacted by the glucose supplementation (Fig. 11C). However, we identified a

significant increase in the provision of vaccenate (C18:1n7) and the mmBCFA, C17iso, to the membrane (Fig. 11C). This mmBCFA species is not significant component of the

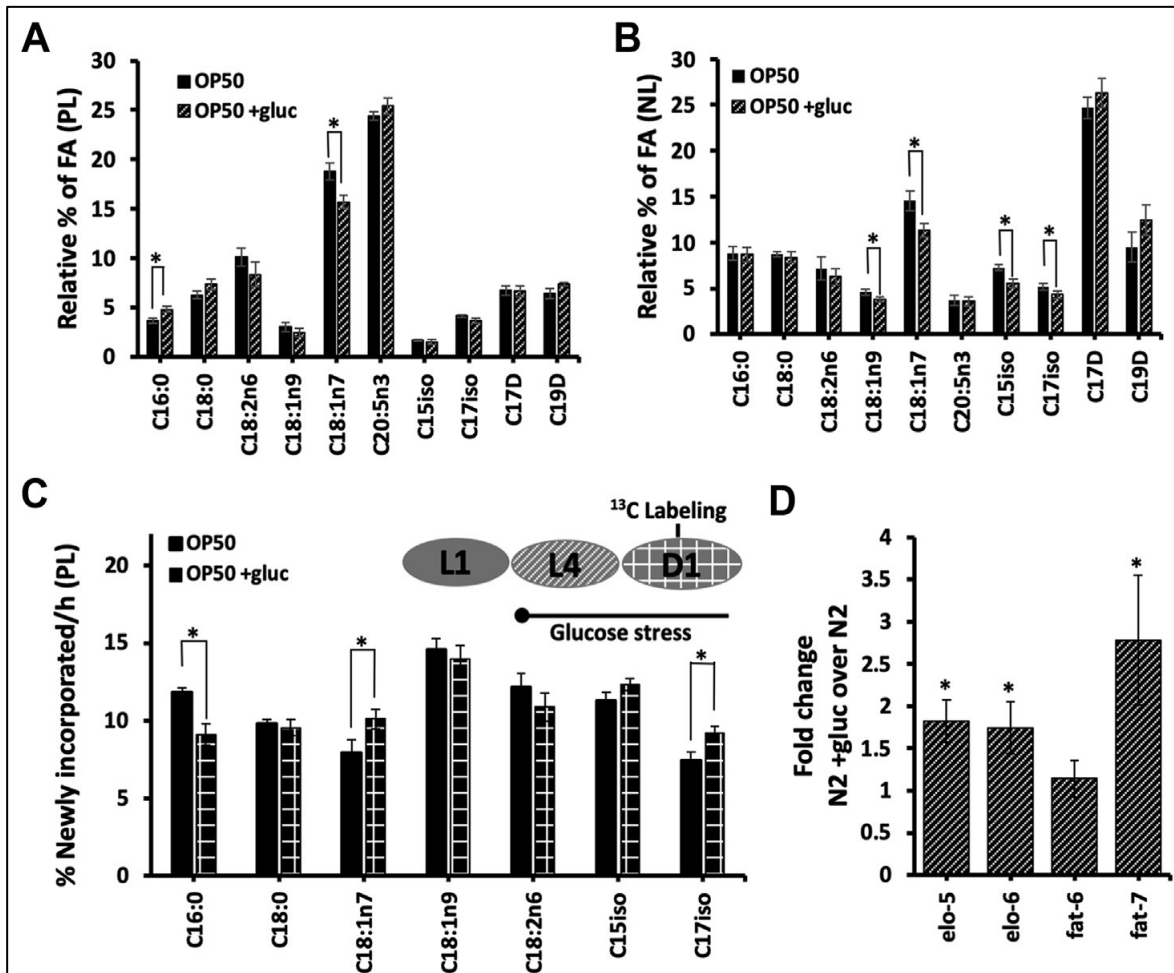


**Figure 11: Wild-type nematodes under glucose stress maintain optimal membrane composition but have altered membrane dynamics.** L1 animals were fed OP50 bacteria on HG plates for 48 h followed by 12 h of OP50 feeding on 15 mM glucose plates (+gluc; indicated throughout with stripes) and an additional 6 h of stable isotope labeling required for part C. **A**, FAMES from the PL population were analyzed by GC/MS and the relative abundance of each fatty acid species was quantified. Here, the major FA species of interest are shown with significant alterations observed only in C16:0 and C18:1n7 of glucose-fed animals (striped) versus controls (black). **B**, in the isolated neutral lipid (NL) fraction, there were alterations in the relative abundance of four FAs: C18:1n9, C18:1n7, C15iso, and C17iso. **C**, after 15 mM glucose supplementation, animals were fed OP50 bacteria enriched with <sup>13</sup>C stable isotope in the proportion of 60:40 (13C:12 C) for 6 h on agarose plates (isotope labeling on +gluc is shown throughout as checkered). The <sup>13</sup>C-label was used to quantify the newly incorporated fatty acids during the labeling window. Because a 60:40 mixture was used, an adjustment factor was used to define the entire newly incorporated population of lipids and is shown here. There were significantly lower levels of labeled C16:0 and higher levels of labeled C18:1n7 and C17iso in +gluc animals. For all GC/MS analysis, values represent means ± SEM of at least nine replicates. Statistical significance ( $p < 0.05$ ) is indicated by \* and was calculated using unpaired T tests and F tests to compare variances. **D**, qRT-PCR was conducted on N2 +gluc and normalized to untreated animals. The expressions of *elo-5*, *elo-6*, and *fat-7* were significantly upregulated as evaluated by applying a One-Sample t test (hypothetical value = 1) on GraphPad Prism (v9.0.0). FAMES, fatty acid methyl esters.

diet, and thus this increase likely represents de novo synthesis of these fats. Specifically, the labeled population in C18:1n7 increases by 27% and by 23% in C17iso. Overall, most unsaturated membrane lipids are unchanged from control populations, but there is an overall reduction in the labeling of saturated fatty acids and an increase in mmBCFAs following glucose feeding. We hypothesize that these changes may be important responses to the elevated glucose levels.

In order to determine if there is an increase in mmBCFA production, we next examined the expression of the fat-6 and fat-7 desaturases and the mmBCFA elo-5 and elo-6 elongases after glucose feeding. In previous reports, fat-7 has been shown to be upregulated with glucose diets, and the qRT-PCR analysis completed here shows a significant increase in expression with glucose feeding (Fig. 11D). This upregulation is specific to fat-7 as fat-6 mRNA levels are unchanged. There is a significant increase of both elo-5 and elo-6 expression by 1.8 and 1.7-fold indicating that these genes are transcriptionally upregulated to promote mmBCFA synthesis in elevated glucose conditions (Fig. 11D).

### **3.3.2. mmBCFAs are critical for surviving glucose supplementation**

Because the stable isotope labeling shows increased mmBCFA provision to the membrane following glucose supplementation, we tested if mmBCFAs play a role in responding to the elevated glucose conditions. We compromised their production with elo-5 RNAi because ELO-5 is the elongase essential for the synthesis of both significant mmBCFA species, C15iso and C17iso (Fig. 12A). A 12-h feeding period before elo-5 RNAi treatment was used to prevent the smaller size and shorter life span seen with elo-

5 RNAi initiated immediately at L1. After 48 h of growth, L4 animals were placed on 15 mM +gluc plates as in the previous lipid studies or a higher 45 mM +gluc plate to ensure sufficient glucose exposure. At both glucose concentrations, there was significantly more death in the *elo-5*-treated animals than the controls. Here, we report the highest concentration of glucose where only  $6 \pm 5\%$  of the *elo-5*-treated animals were alive at day 4 compared with  $82 \pm 6\%$  of the controls (Fig. 12B).

The fatty acid data generated from labeled N2 animals fed glucose showed a significant change in the provision of C17iso but not C15iso to the membrane. We therefore investigated whether depleting C17iso alone would result in altered survival in high-glucose conditions. To do so, we examined the role of ELO-6, which is only required for C17iso production (Fig. 12A). The *elo-6* RNAi-treated animals survived the glucose treatment similarly to wild-type animals with  $81 \pm 5\%$  alive at day 4 (Fig. 12B) suggesting that the depletion of C17iso at least by 73% is not sufficient to cause death (Fig 12C). In support of this conclusion, the *elo-6* RNAi treatment reduces overall mmBCFA levels by 50%, while *elo-5* RNAi nearly eliminates the mmBCFAs completely (Fig 12C).

To confirm the role of mmBCFAs in directly impacting the response to glucose, we fed nematodes a diet containing 50% *Bacillus subtilis*, because this bacterial strain contains high levels of mmBCFAs. Consistent with our results indicating a role for mmBCFAs in responding to elevated dietary glucose, *B. subtilis* feeding restored the survival rates of animals on +gluc plates back to wild-type levels (Fig 12D). The levels of mmBCFAs in *B. subtilis* are  $11.2 \pm 0.3\%$  C15iso and  $5.2 \pm 0.1\%$  C17iso (Fig 12E) compared with OP50 where mmBCFAs are completely absent (Fig 12E). Additionally, *B. subtilis* contains a high percentage of anteiso mmBCFA species that terminates in an

isobutyl and not an isopropyl as in the iso species. Consistent with our results indicating a role for mmBCFAs in responding to elevated dietary glucose, *B. subtilis* feeding restored the survival rates of animals on +gluc plates back to wild-type levels (Fig. 12D). To ensure that this rescue of nematode viability with *B. subtilis* supplementation was not due to *elo-5* RNAi bacteria dilution, we fed wild-type nematodes a L4440/*elo-5* mixture to confirm sufficient RNAi knockdown with a diluted RNAi bacterial diet. Animals fed the L4440/*elo-5* mixture show high mortality under glucose stress, confirming our data presented previously (Fig. S1). Thus, *B. subtilis* can rescue phenotypes caused by the absence of ELO-5, and we conclude that the incorporation of new mmBCFAs from synthesis or from the diet is critical for glucose stress survival.

To further examine the relationship of mmBCFA in survival with glucose stress, we tested whether mmBCFA production was actively needed on +gluc plates or simply the presence of mmBCFAs synthesized prior to glucose exposure. We tested it by compromising mmBCFA synthesis only during adulthood and assessed the viability on +gluc plates. The *elo-5* knock-down was initiated concurrently with the glucose stress in day 1 adults. In the adult-only *elo-5* RNAi treatment, there is significantly reduced survival compared with controls with treated animals showing 50% of viability in day 9 as opposed to controls reaching 50% of viability in day 11 (Fig. 12F). The reduced survival on +gluc plates demonstrates that there is an active role for mmBCFA synthesis in responding to glucose that is independent of the abundance of mmBCFAs accumulated during development.



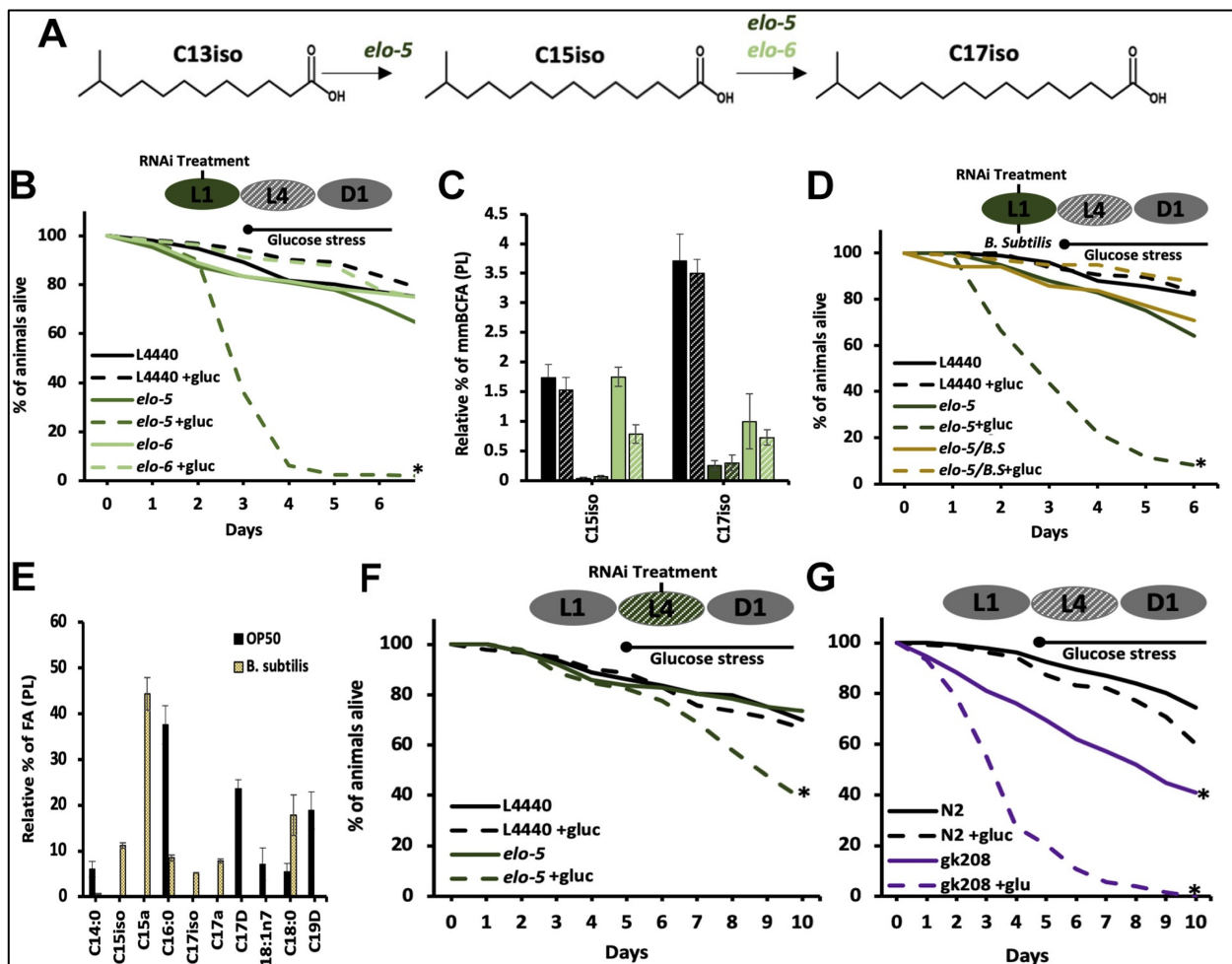


**Figure 12: mmBCFAs are essential for survival with elevated dietary glucose.** **A**, the elongases, *elo-5* (dark green) and *elo-6* (light green), produce the two mmBCFAs (C15iso and C17iso) by elongation steps shown here. **B**, RNAi knockdown of *elo-5* (dark green) and *elo-6* (light green) in N2 worms started from L1 along with control empty vector RNAi (L4440) (black). At the L4 stage, animals were transferred to 45 mM glucose (dashed lines), and the percent of animals alive was assessed daily. On day 4, we observed that 94% of the nematodes were dead in *elo-5* RNAi +gluc plates. **C**, The levels of mmBCFAs confirm efficient knockdown with animals fed *elo-5* RNAi on +gluc plates having almost no detected C15iso or C17iso. In *elo-6* animals, there was a significant decrease in the levels of C15iso with on +gluc but no significant difference in C17iso (light green striped). **D**, To confirm the role of mmBCFAs in survival on +gluc plates, L1 animals were fed a bacteria strain rich in mmBCFAs (*B. subtilis*) (yellow). A ratio of 1:1 (RNAi bacteria to *B. subtilis* ratio) was used to ensure sufficient knockdown of *elo-5*. **E**, FAMES were analyzed by GC/MS to generate an FA profile of the diet. *B. subtilis* (yellow) compared to OP50 (black). There are significant differences including elevated C15iso, C15a (anteiso mmBCFA), C17iso, and C17a. **F**, RNAi knockdown of *elo-5* was initiated later and simultaneously with the transfer to +gluc plates. On day 9, 53% death was seen in *elo-5* +gluc animals. **G**, *elo-5(gk208)* mutants (purple) were grown on +gluc plates (dashed line) and monitored for death daily. *elo-5* mutants have dramatically reduced viability on +gluc plates similar to the *elo-5* RNAi feeding. Survival curves are presented as means of at least three independent replicates with  $n = 50$  nematodes/condition. All the statistical analysis was performed by Log-rank (Mantel-Cox) test.  $p \geq 0.0001$  is represented by \*. The lipid composition values represent means  $\pm$  SEM of at least four replicates. Statistical significance ( $p < 0.05$ ) was calculated using an unpaired t test and F test to compare variances.

Finally, we confirmed that *elo-5* (*gk208*) mutants also died prematurely on +gluc plates with  $27\% \pm 10\%$  alive at day 4 compared with  $76 \pm 5\%$  alive in control animals (Fig. 12G). These experiments demonstrate for the first time a critical role for mmBCFAs in surviving glucose stress and elucidate a novel function for these unique fatty acids in adult animals.

### **3.3.3. mmBCFAs act in the PAQR-2 network response to glucose stress**

Previous studies characterize this seven-transmembrane protein PAQR-2 as an important membrane sensor that responds to decreased membrane fluidity resulting from excess glucose. Because of the high mortality of *elo-5* knockdown animals on +gluc plates (Fig. 12B), we hypothesized that the *elo-5* elongase could be activated by PAQR-2 as part of the metabolic response to glucose stress. To probe this relationship, we assessed the membrane composition of *paqr-2* (*tm3410*) mutants immediately after glucose stress and analyzed their mmBCFAs abundance with GC/MS. We found significantly less mmBCFAs (C15iso and C17iso) in the membranes of *paqr-2* animals on +gluc plates compared with *paqr-2* animals on control plates (Fig. 13A). Specifically, C15iso was depleted from  $1.7 \pm 0.1\%$  to  $1.1 \pm 0.1\%$  and C17iso from  $5.3 \pm 0.3\%$  to  $3.0 \pm 0.2\%$  with glucose treatment, demonstrating that PAQR-2 may be required to maintain mmBCFA levels under glucose stress.

To further investigate the impact of PAQR-2 in the response to elevated glucose, we analyzed the membrane dynamics of *paqr-2* mutants with stable isotope labeling as previously described. In *paqr-2* mutant animals, there is a significant reduction in the labeling of mmBCFAs with C15iso levels decreasing from  $8.6 \pm 0.6\%$  to  $5.6 \pm 0.7\%$  and

C17iso from  $6.1 \pm 0.3\%$  to  $2.5 \pm 0.3\%$ , indicating that PAQR-2 may be required for the upregulation of ELO-5. Furthermore, the analysis of the other fatty acid species in the

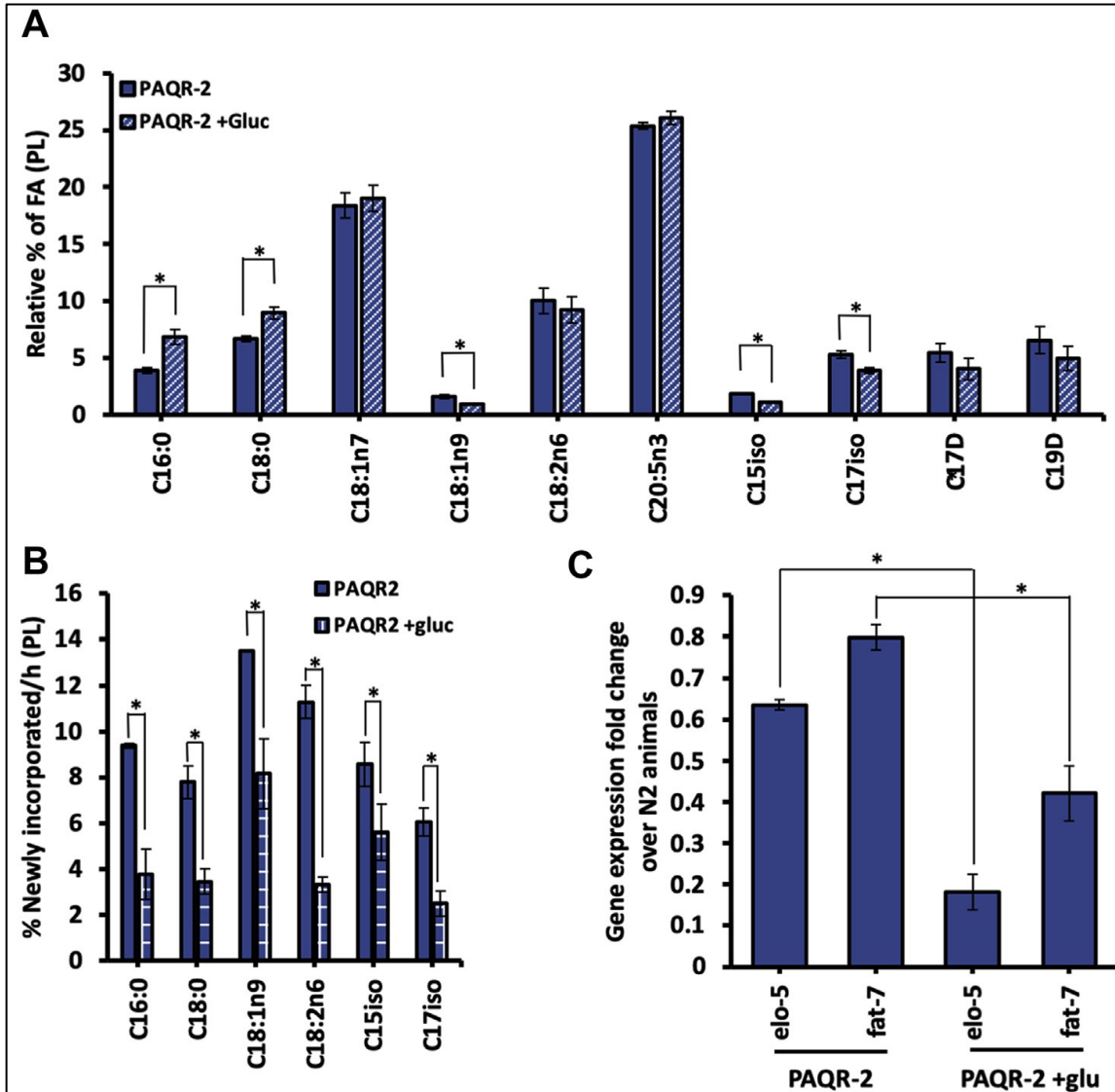


**Figure 13. PAQR-2 upregulates mmBCFA production under glucose stress.** A, *paqr-2(tm3410)* mutants in the L4 stage (48 h old) were fed for OP50 bacteria seeded onto HG plates with (blue stripe) or without 15 mM of glucose (blue) for 12 h. Using GC/MS, the FA composition of PLs was assessed and significant changes were found in C16:0, C18:0, C18:1n9, C15iso, and C17iso as indicated by the \*. B, a 6 h-period of isotope labeling shows a significant decrease in the amount of newly incorporated FAs (marked by  $^{13}\text{C}$ -isotopes) in all species quantified in *paqr-2* animals fed glucose (blue checked). The relative % of FA and the % newly incorporated FA/h represent means  $\pm$  SEM of at least three independent replicates. Statistical significance ( $p < 0.05$ ) was calculated using unpaired t test and F test to compare variances. C, quantitative real-time PCR was implemented to quantify the transcript levels of *elo-5* and *fat-7* in *paqr-2* mutants compared with controls. Fold changes were quantified using the  $2^{-\Delta\Delta\text{Ct}}$  method, and significance was assessed by applying a One-Sample t test (hypothetical value = 1) on GraphPad Prism (v9.0.0). There is a significant reduction in expression of both *elo-5* and *fat-7* compared with N2 controls as denoted by \*. mmBCFAs, monomethyl branched-chain fatty acids.

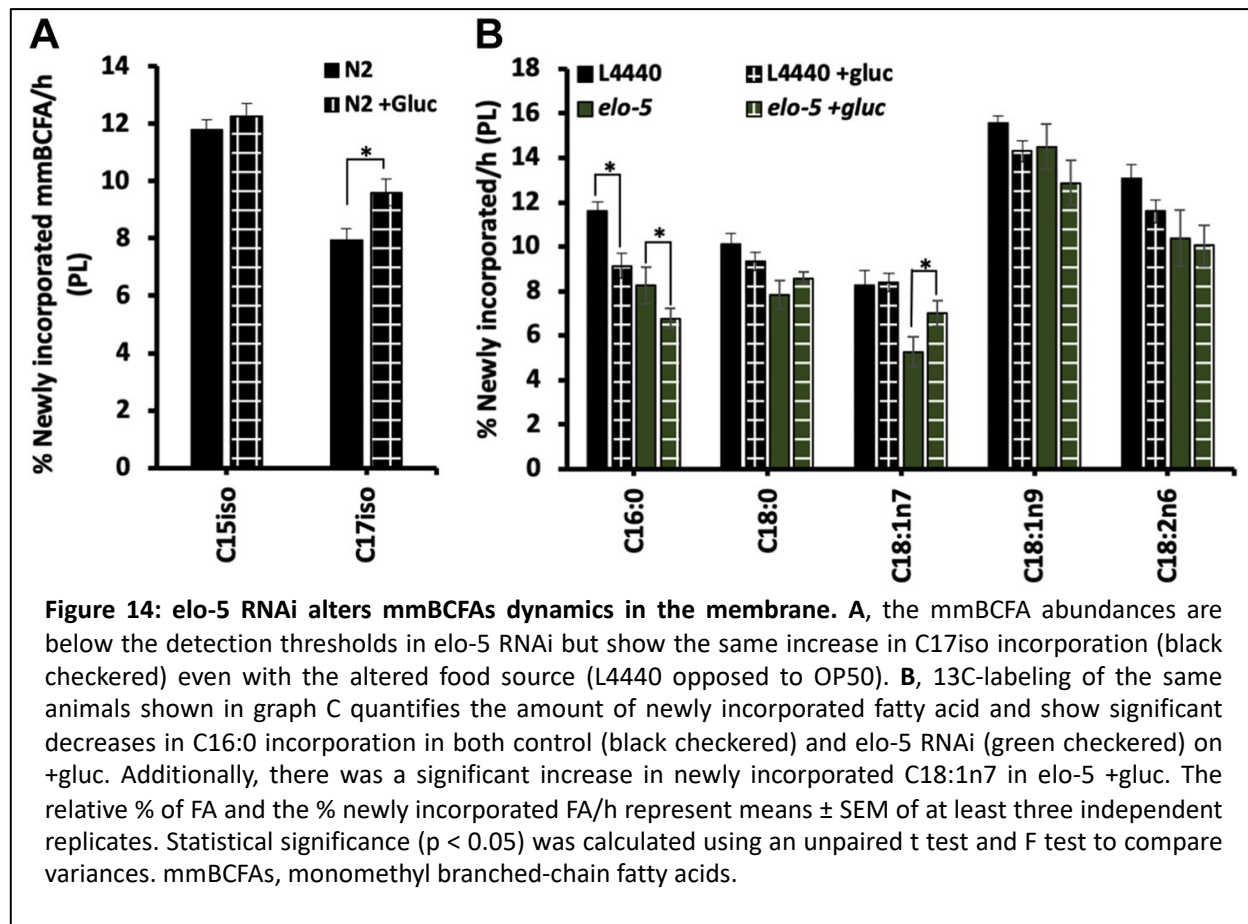
membrane indicates a global reduction in the turnover of all species in *paqr-2* mutant animals on +gluc plates with the greatest decrease observed in linoleate (C18:2n6) (71% reduction) (Fig. 13B). It is important to note that the *paqr-2* mutants are unhealthy on glucose plates, so the reduction in turnover may be a consequence of their compromised health (Svensk et al., 2016). However, PAQR-2 has been found to regulate *fat-7* expression, and reduction of *fat-7* by RNAi results in a global reduction of fatty acid flux, presumably to mitigate the impact of the compromised fatty acid pool on the membrane (Dancy et al., 2015).

Since PAQR-2 is known to impact transcription of metabolic genes, we sought to examine the expression of *elo-5* in these mutants with and without glucose. First, we confirmed the requirement of PAQR-2 to induce *fat-7* expression with glucose and found that *fat-7* is expressed at 0.4 the levels of control animals (Figure 13C). Interestingly, *fat-7* in PAQR-2 animals is at approximately 80% of wild-type expression in the absence of glucose. Next, we found that *elo-5* is only expressed at 60% of wild-type levels without glucose and 20% of wild-type levels with glucose (Figure 13C). Overall, the qRT-PCR analysis demonstrates that *elo-5* is regulated by PAQR-2 and indicates that mmBCFA synthesis is a major factor in the PAQR-2 response.

Finally, we used stable isotope labeling to confirm that the perturbation in mmBCFA production in the *elo-5* depleted animals does not impact the turnover of the other fatty acid species. The control for the RNAi studies is L4440 bacteria, which can carry the RNAi vector, and has a slightly different fatty acid composition. Therefore, we first confirmed the elevated mmBCFA turnover on +gluc with this diet and found that the wild-type animals fed L4440 showed high levels of turnover of C17iso on glucose compared with

controls, confirming the mmBCFAs response seen previously in OP50-fed animals (Fig. 14A). In *elo-5* RNAi-treated animals, there is also a reduction in labeled C16:0 on +gluc plates, and although the initial abundance is lower, the decrease of 17.9% is consistent with control animals at 21.2% (Fig. 14B). Therefore, the nematode responds to the accumulation of SFA from glucose stress by downregulating the flux of C16:0 to the membrane but not through a pathway that requires ELO-5. Interestingly, unstressed *elo-5* animals start off with lower replenishment of C16:0 (Fig. 14B), indicating that the absence of *elo-5* enzymes impacts the flux of this SFA to the membrane even in control conditions.

In addition, the replacement of the MUFA, vaccinate (C18:1n7), which is mostly provided by the diet, was significantly increased in *elo-5* knockdown nematodes (Fig.



14B). Because these animals lack mmBCFAs, the increase in C18:1n7 may alleviate the impact of this loss on the properties of the membrane. Taken together, our results indicate that a rewiring of FA metabolism pathways including mmBCFAs upregulation is essential to respond to glucose stress, and that C18:1n7 is a potential compensatory FA participating in the overall response.

### 3.3.4. mmBCFAs act in parallel to the fluidity response in glucose stress

The major established role of PAQR-2 is to correct the reduced membrane fluidity that occurs with excess dietary glucose or excess dietary saturated fat. Because both C15iso and C17iso contain a branch within the hydrocarbon chain, these fatty acids disrupt lipid packing and promote fluidity within a membrane. In order to determine if

mmBCFAs play a general role in restoring membrane fluidity, nematodes were fed excess SFA (2 mM C16:0) and examined for altered development and survival. First, we investigated whether ELO-5 is required for growth and development on plates with excess SFA (2 mM C16:0), which we refer to as +SFA plates. There was no impact on larval development in *elo-5* RNAi fed animals on +SFA in

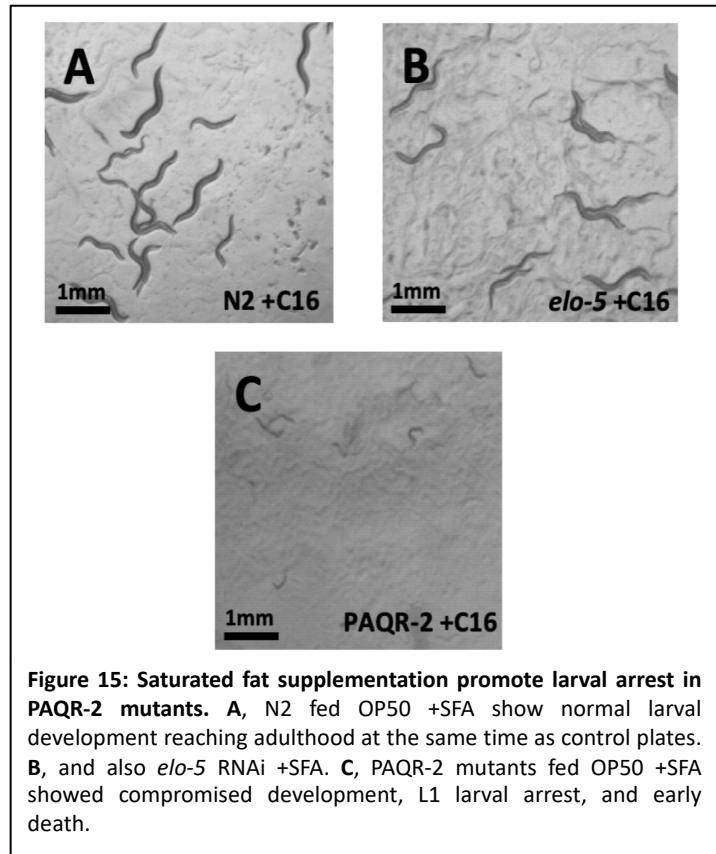
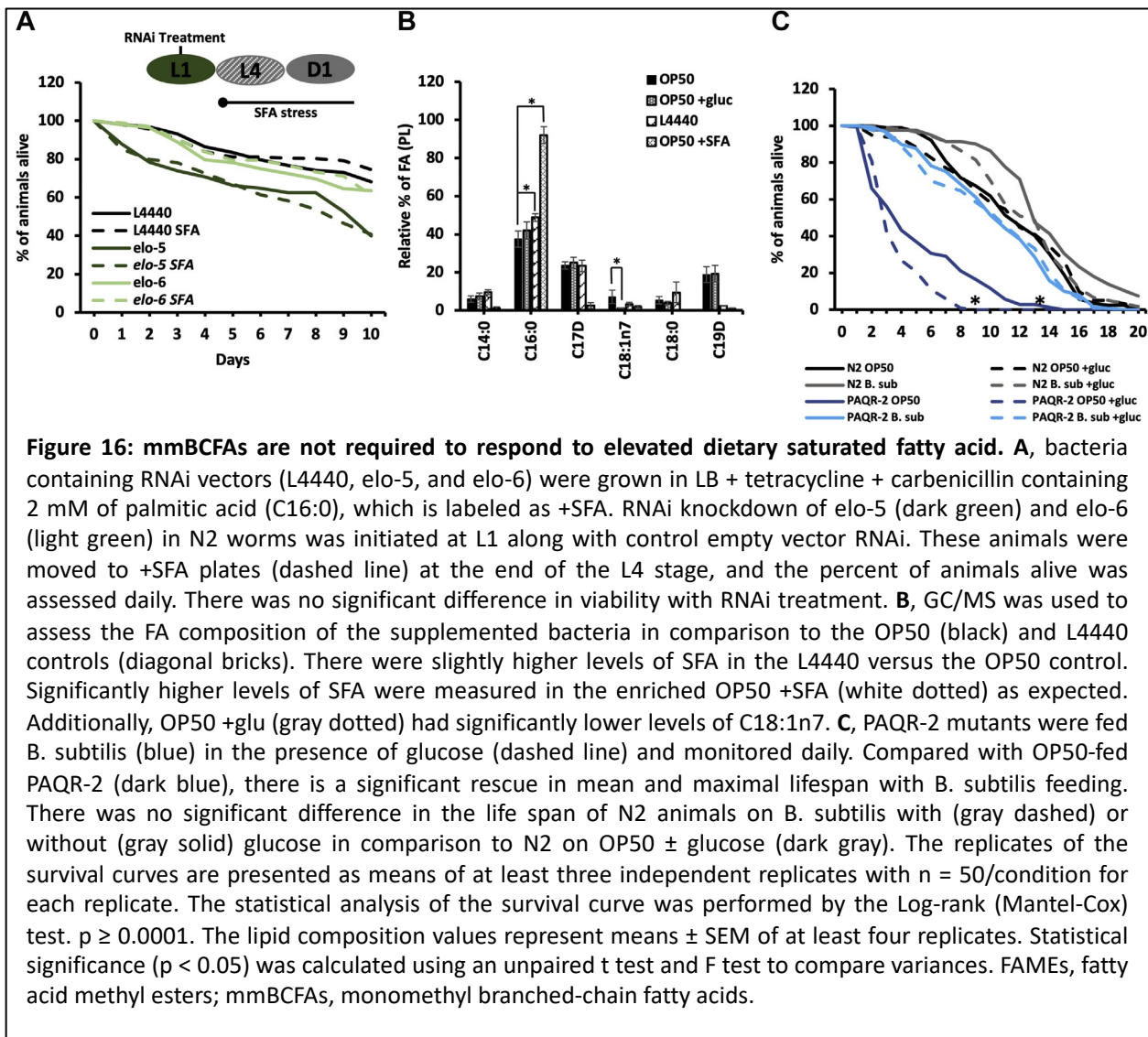


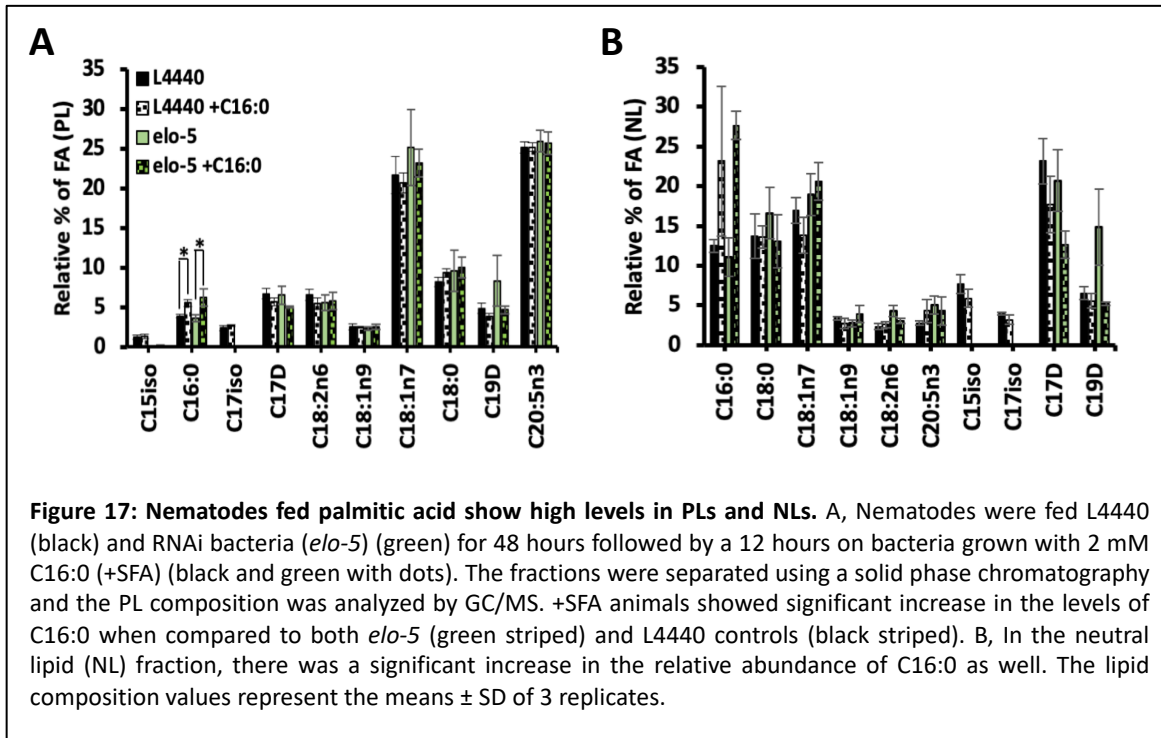
**Figure 15: Saturated fat supplementation promote larval arrest in PAQR-2 mutants.** A, N2 fed OP50 +SFA show normal larval development reaching adulthood at the same time as control plates. B, and also *elo-5* RNAi +SFA. C, PAQR-2 mutants fed OP50 +SFA showed compromised development, L1 larval arrest, and early death.

contrast to the arrest seen in *paqr-2* (*tm3410*) animals (Figure 15). Next, the mortality rates of *elo-5* and *elo-6* RNAi-treated animals were compared with controls. The incorporation of exogenous SFA did not impact viability of *elo-5* or *elo-6* RNAi-treated animals (Fig. 16A). The lack of impact with SFA supplementation demonstrates that the role of mmBCFAs is not in a general response to membrane saturation but specific to certain conditions such as high glucose.

To confirm SFA incorporation, we quantified the amount of C16:0 in the phospholipid population of the supplemented animals and found a significant increase in C16:0



abundance from 3.8% to 5.5% in wild type and from 3.6% to 6.2% in *elo-5* RNAi knockdown (Fig. 17A). We also confirmed a significant increase of C16:0 in the bacteria on the +SFA plates and found that this diet contains 92% SFA (Fig. 16B). In order to determine how the C16:0 was incorporated into the nematode, the fatty acid population of neutral lipids was also measured, and there was an increase from  $7.7 \pm 0.8\%$  to  $15.6 \pm 9.3\%$  in wild-type animals (Fig. 17B). Not only does this data confirm that significant C16:0 is available for the nematodes, but it also demonstrates active mechanisms to protect the membrane from excess saturated fat. We can also conclude that the role of mmBCFAs is not in reestablishing membrane fluidity.



Because our earlier experiments suggest that PAQR-2 may coordinate the response in mmBCFAs, we tested whether the mmBCFA-enriched *B. subtilis* could improve survival of *paqr-2* animals on +gluc plates. We found that the *B. subtilis* diet dramatically extended the life span of *paqr-2* animals on +gluc, further suggesting that the mmBCFAs are a critical component to the metabolic response to elevated glucose (Fig. 16C). Moreover,



we observed that paqr-2 animals had a compromised lifespan even in the absence of glucose with a mean life span of  $3.5 \pm 1$  days compared with N2 on OP50 with a lifespan of  $11.5 \pm 2$  days. A shortened life span has been reported for paqr-2 animals previously; however, the difference was not as dramatic as shown here perhaps due to changes in the dietary fatty acid composition. Despite the short life span, we find that the addition of +gluc plates further compromises the life span of paqr-2 animals to 8 days. Taken together, these experiments strongly implicate mmBCFAs as part of the PAQR-2-driven response to elevated dietary glucose.

### **3.4. Discussion**

We aimed to identify mechanisms that provide an effective response to elevated dietary glucose conditions that perturbs the optimal membrane composition when unaddressed. Although it is known that the PAQR-2 membrane sensor responds to glucose stress through the FAT-7 desaturase, we utilized a stable isotope labeling approach to identify a new component of the PAQR-2 response (Fig. 18). Specifically, our labeling studies identified that under glucose stress, the membrane receives significantly lower levels of palmitic acid and higher levels of C17iso. The upregulation of mmBCFA production through ELO-5 is critical for survival on glucose as elo-5 RNAi results in severely compromised survival on +gluc plates. Our results confirm that we have identified mmBCFAs in a novel and essential response to elevated glucose.

Previous FRAP studies have shown that elevated glucose decreases membrane fluidity and have found an increased incorporation of saturated fat into the membrane lipids (Devkota et al., 2017). It has been suggested that the elevated saturated fat is

produced by the bacteria fed surplus glucose through de novo fatty acid synthesis. However, we quantified the saturated fat abundance from the glucose-fed bacteria (OP50+gluc) and found it has a slight but insignificant increase in C16:0, suggesting that the increase in SFA may be occurring in the nematode. In addition, glucose-stressed animals have a distinct response and life span compared with SFA stress, because we found ELO-5 is required for survival on glucose but not SFA. It is possible that the decreased fluidity in glucose stress could be due to an imbalance between the SFA and UFA, because the OP50 + gluc diet has significantly lower levels of C18:1n7. Since this fatty acid is mostly obtained from diet (Perez & Van Gilst, 2008), the nematode would incorporate a disproportionately lower amount of MUFA, which would impact the membrane fluidity. However, the data thus far favors the hypothesis that the surplus glucose is influencing the animals independent of saturated fatty acid accumulation.

In nematodes, mmBCFAs have been shown to be involved in postembryonic growth (Kniazeva et al., 2004), sensory neuron maturation, and foraging (Kniazeva *et al.*, 2015). However, mmBCFAs can impact the membrane directly, as mmBCFAs influence overall membrane fluidity since the branch in their structure prevents tight lipid packing. Because excess dietary SFA decreases membrane fluidity but the loss of *elo-5* does not exacerbate this phenotype, we hypothesize that the role of mmBCFAs is not in regulating membrane fluidity. Instead, a study conducted by Zhu et al found that the mmBCFA-derived sphingolipid d17iso-Glucosylceramide was linked to the target of rapamycin-1 (TORC1) (Zhu et al., 2013). The GluCer/Torc1 pathway was proposed to coordinate metabolic status in the intestine with growth and postembryonic development (Rachdi *et al.*, 2008) (Laplante & Sabatini, 2012). Therefore, the elevated levels of mmBCFAs

observed in high-glucose diet may serve to increase the induction of TORC1 signaling to then increase the uptake and metabolism of glucose, which will be a direction of future study.

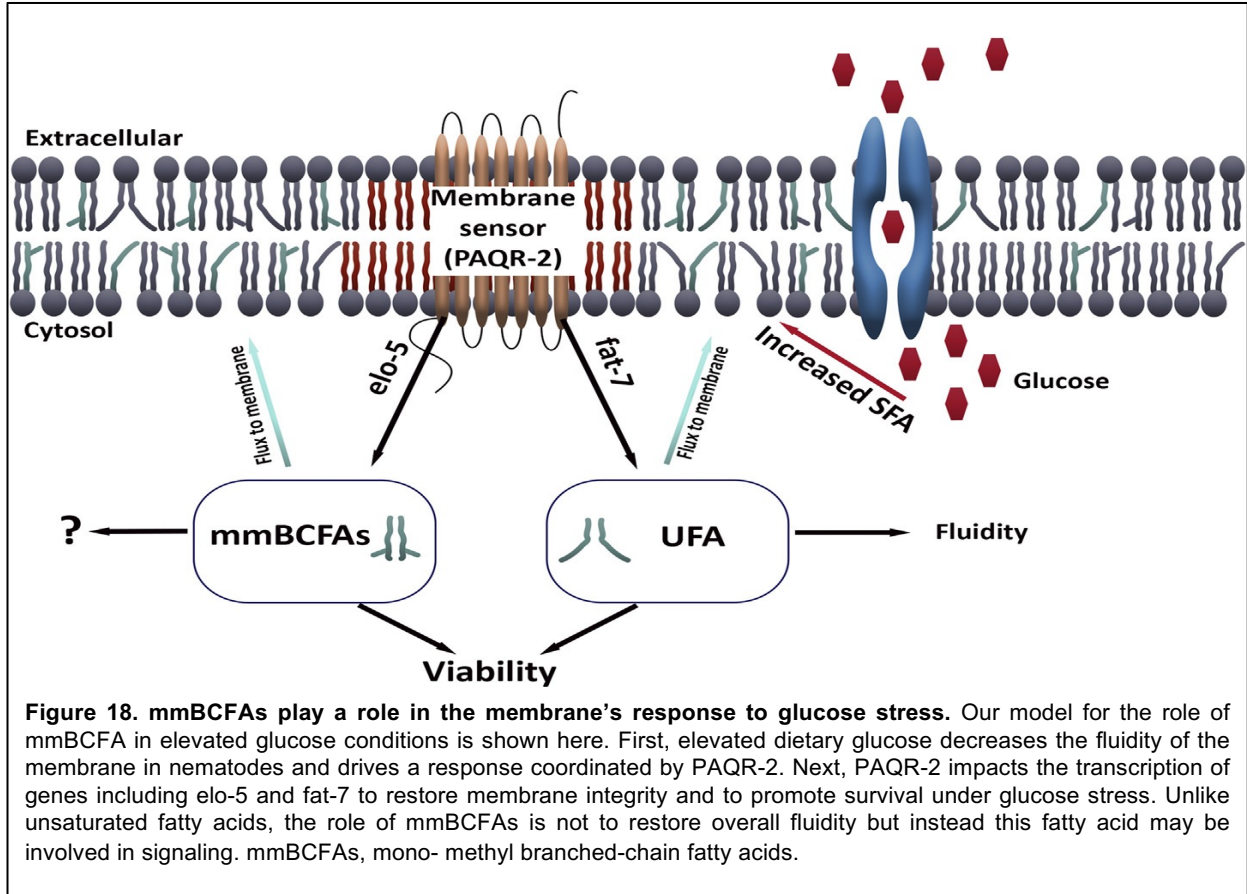
In wild-type animals, there is a significant upregulation of C17iso but not C15iso as revealed by stable isotope tracing. Interestingly, on +gluc plates, there are no glucose sensitivity in the *elo-6* RNA, which depletes C17iso but not C15iso levels. The lack of *elo-6* phenotypes may indicate a compensatory response by C15iso when C17iso synthesis is not available as there are still significant levels of C15iso in those treated animals. We propose that the role of mmBCFAs is not specific to one type of fatty acid but to the overall abundance of the mmBCFA population as there are substantially less mmBCFA in *elo-5* RNAi-treated animals than in *elo-7* RNAi-treated animals. This hypothesis is supported by the fact *elo-5* RNAi can be rescued by *B. subtilis*, which predominantly contains anteiso mmBCFAs suggesting that the specific identity of the mmBCFA may not be critical.

It is clear that PAQR-2 plays an important role regulating downstream desaturases to maintain SFA:UFA balance and consequently membrane fluidity; however, analyzing the membrane composition of PAQR-2 mutants revealed a significant decrease in the abundance of mmBCFAs. This suggests that PAQR-2 may also regulate ELO-5 to produce mmBCFAs in response to glucose stress. We were unable to determine if mmBCFAs were specifically compromised in PAQR-2 animals, because our isotope labeling analysis showed a global downregulation in the lipid renewal of all fatty acid species measured. The global decrease in lipid rejuvenation is consistent with the role of PAQR-2 in regulating FAT-7, which we have previously established is required for normal rates of lipid replacement. However, it is also possible that PAQR-2 animals have reduced

food intake due to compromised health. Although it was shown previously that PAQR-2 mutants have a short lifespan (Chen *et al.*, 2019), our data appear to show a more drastic life span impact compared with published studies. We hypothesize that the high mortality might be related to differences in the food sources provided to the worms, since PAQR-2 mutants seem to be strongly affected by the dietary content. In addition to the quantification of lipid metabolism in paqr-2 animals, we found that *B. subtilis*, a diet rich in mmBCFAs, can rescue not only elo-5 animals but also paqr-2 mutants even without glucose exposure. This rescue supports the conclusion that ELO-5 is downstream of PAQR-2.

The identification of ELO-5 as essential for surviving excess dietary glucose required the use of stable isotopes, because GC-MS measurements did not reveal this requirement. Although this finding highlights the unique capabilities of the stable isotope feeding approaches, it is important to note that this technique has some limitations. The stable isotope technique cannot be used to detect PUFA species with more than two double bonds, because it relies on the detection of parent ions, and PUFAs fragment extensively under GC/MS conditions, yielding unreliable results. Also, current stable isotope labeling studies require quantification of the membrane in whole animals to generate sufficient biomass, and it is possible that the response observed could be tissue or organelle specific. Indeed, it has been shown that mmBCFAs are regulated distinctly in different tissues. In mice, the mmBCFAs were ten times more abundant in adipose tissue compared with liver cells (Wallace *et al.*, 2018). The exploration of the role of mmBCFA in individual tissues will be the focus of future work. Additionally, it will be critical to establish the relationship between PAQR-2 and mmBCFAs in more detail and to

identify how mmBCFAs impact survival with glucose. In summary, we have identified a novel role for mmBCFAs under elevated dietary glucose using stable isotopes and mass spectrometry.



### 3.5. Methodologies & Techniques

#### 3.5.1. Bacteria and nematodes growth media and M9 buffer preparation

Bacteria grew using LB and LB+CARB+TET media depending on the type of strain used in the experiments. LB media was used to culture regular bacteria not carrying any antibiotic resistance such as OP50 and *B. subtilis*. LB+CARB+TET was used to grow RNAi bacteria which carried resistant genes against carbenicillin (CARB) and tetracycline (TET) such as L4440. Cultures were prepared by the inoculation of ~2 colonies of bacteria into their respective media.

Nematodes were plated onto HG and NGM+CI media depending on the requirements of each experiment. Glucose was introduced to both media causing the stress desired. High growth (HG) media was used for the maintenance, expansion, and experiments in wildtype and mutant strains. Bacteria not carrying antibiotic resistance were used to seed these plates and feed the nematodes. NGM+CI media was prepared in 3cm and 10cm plates, which were used to carry lifespan (small scale) and membrane lipid testing (large scale) experiments, respectively. This media is used to grow bacteria capable of knockdown genes by RNAi (RNA interference) technique using the inducer called IPTG (Isopropyl  $\beta$ -D-1-thiogalactopyranoside). Carbenicillin is introduced to this media and participate selecting the RNAi antibiotic resistant bacteria used to knockdown and avoiding contamination by unknown bacteria.

Buffer M9 was prepared concentrated 10 times (M9 10x) as a stock solution and diluted to M9 1X when used to transfer nematodes from plates and during wash process. All recipes used to prepare media and buffer solutions were shown in the table below:

**A**

<b>LB + CARB + TET</b>	<b>1 Liters</b>	<b>3 Liters</b>
NaCl	5 g	15 g
Yeast extract	5 g	15 g
Bacto-tryptone	10 g	30 g
Agar	15 g	45 g
NaOH (1M)	1 mL	3 mL
Add following after autoclaving (60 min), 15 min before pouring		
Carbenicillin (100mg/ml)	1 ml	3 ml
Tetracycline (20mg/ml)	0.75 ml	2.25 ml

**B**

<b>NGM + CI plates</b>	<b>1 Liters</b>	<b>3 Liters</b>
Peptone	2.5 g	7.5 g
KH <sub>2</sub> PO <sub>4</sub>	3 g	9 g
K <sub>2</sub> HPO <sub>4</sub>	0.5 g	1.5 g

Agar	25 g	75 g
Add following after autoclaving (60 min), 15 min before pouring		
Cholesterol (8mg/ml)	1 ml	3 ml
Carbenicillin	0.5 ml	1.5 ml
IPTG in 45ml ddH <sub>2</sub> O	1 g	3 g

**C**

HG plates	1 Liters	3 Liters
NaCl	3 g	9 g
Peptone	20 g	60 g
Agar	25 g	75 g
Add following after autoclaving (60 min), 15 min before pouring		
Cholesterol (8mg/ml)	4 ml	12 ml
1 M P.P.B. (pH 6.0)	25 ml	75 ml

**D**

M 10X	1 Liters	3 Liters
Na <sub>2</sub> HPO <sub>4</sub> (Sodium Phosphate-diabasic)	68 g	204 g
KH <sub>2</sub> PO <sub>4</sub> (Potassium Phosphate-mono)	30 g	90 g
NaCl	5 g	15 g
Filter sterilize		

**Table 1: Recipes used to prepare all media. (A)** Media used to grow bacteria culture with and without antibiotic resistance. **(B)** Nematodes growth media (NGM + CI) was used to allow nematodes growth through RNAi experiments in large and small scale, testing membrane composition and lifespan. **(C)** High growth (HG) media was used to grow larger population of nematodes when compared to NGM plates. The higher concentration of bacteria nutrients allows for the growth of a thicker bacteria lawn being able to keep a larger population of nematodes for a longer time. **(D)** M9 10x solution is diluted to M9 1x before it is used to wash and transfer large population of nematodes from regular plates to stress plates. Obs.: During media preparation all volumes and weights were adjusted depending on the final volume required.

### 3.5.2. *C. elegans* and Bacteria Growth and Maintenance

The experiments were conducted using wildtype N2 nematodes as a control, and it was obtained from the *C. elegans* Genetics Center (CGC; MN, USA). PAQR-2 (*tm3410*) and ELO-5 (*gk182*) mutants were also obtained from the *C. elegans* Genetics Center (CGC; MN, USA). To avoid posterior contamination, the nematodes received in NGM (3cm) plates were transferred to new NGM (6cm) plates seeded with OP50. After 24

hours, the nematodes in the plates not showing signs of contamination (fungoes or bacteria) were transferred to large HG (10cm) plates to allow maximum population growth. Nematodes in plates that showed contamination were single picked and the larger number of worms, crawling distant from the contamination spot, were transferred to a new seeded 6cm NGM plate and left growing for another 24 hours. These nematodes were then transferred to seeded 10cm HG plates when no signs of contamination were seen. To synchronize the nematodes, gravid adults were exposed to diluted bleach (table 2) and the washed eggs were left rotating overnight at 20°C in M9 solution not containing food, to prevent the hatched larvae (L1 stage) from beginning their development. After ~18 hours rotating, L1 stage nematodes were plated on three seeded HG plates (5.000/plate) to keep the population growing for future experiments.

For 25ml:	For 100ml:
2.5ml 5N KOH	10ml KOH
5 ml bleach (commercial)	20ml bleach (commercial)
17.5 ml dH <sub>2</sub> O	70ml dH <sub>2</sub> O

**Table 2: Bleach solution.** This table shows the volumes used to prepare a 10% (v/v) bleach solution used to kill and dissolve the adult (D1) nematode’s carcasses. After adding the bleach solution to the tubes containing the nematode’s pellet, we waited around 5 minutes before ending the reaction followed by 3 washes using M9 1x. Note that the 5 minutes bleaching can vary depending on how old is the bleaching solution.

### 3.5.3. Altered Dietary Conditions

Synchronized L4 stage worms (~48 hours growth) grown on HG plates were transferred to +gluc plates for 12 hours. The +gluc plates were made to a final concentration of 15mM, 45mM, 100mM, and 20mM of glucose by adding a filtered glucose solution to cooled autoclaved HG media. The +gluc plates were seeded with regular OP50 bacteria at least 4 day before plating the worms. After the glucose exposure,



animals were labelled using  $^{13}\text{C}$  stable isotopes as described in the following section. For C16:0 stress, L4 animals were transferred to NGM-CI plate (without peptone) inoculated with control or RNAi bacteria. To supplement the SFA in the diet, 2mM of C16:0 was added to the media before the bacteria was inoculated (Devkota et al., 2017). After 18-20 hours growth the bacteria was washed 3 times with fresh liquid media and resuspended in LB or LB+CARB+TET liquid media and spread on the appropriate plate.

#### **3.5.4. RNAi Knockdown**

Knockdown experiments were conducted in large (10 cm) and small (3cm) plates to analyze the membrane composition and lifespan (explained below), respectively. To analyze the membrane composition RNAi strains from the Ahringer library were grown on NGM + CARB + IPTG plates (NGM+CI) (Kamath & Ahringer, 2003). RNAi bacteria along with the control RNAi were plated at a density of 0.15g per 10cm NGM-CI plate. Approximately 8,000 to 10,000 synchronized L1 N2 animals were grown at a density of 2,500 worms per RNAi treatment plate for 48 hours. At L4, the nematodes were transferred to +gluc plates for 12 hours and followed the same protocol of stress described previously in the section 2.3.

*Bacillus subtilis* (sp168) was a kind gift provided by the Walhout lab at UMMAS – Worcester and was cultivated in the same media and following the same protocols used with OP50.

### **3.5.5. Viability Curves and Lifespans**

To quantify survival on +gluc plates, RNAi bacteria or control (empty vector L4440) were seeded onto 3cm NGM+CI plates, and L1 worms were grown for 48 hours. Approximately 50 L4 stage nematodes were then transferred to fresh NGM+CI +gluc plates each day, and the number of dead animals was determined by gently prodding with a pick. *B. subtilis* supplementation started at L1 stage in a mixture prepared with RNAi bacteria (50%:50%) and then continued as described with the RNAi bacteria.

### **3.5.6. Stable Isotope Labeling Strategy**

Animals were labeled with isotopes following the protocols established in (Perez and Van Gilst, 2008). Briefly, isogro media ( $^{13}\text{C}$ ) and LB media ( $^{12}\text{C}$ ) were inoculated with OP50 colonies to allow the growth of bacteria for 16 hours at 37°C. Next, the bacteria were harvested and resuspended in M9 in the concentration of 0.15g/mL. A mixture containing enriched bacteria  $^{13}\text{C}:^{12}\text{C}$  (60%:40%) was transferred to agarose plates and allowed to dry. Nematodes from +gluc plates were harvested, washed three times using M9, and plated onto stable isotope labeling plates containing 800uL of bacteria mixture for 6 hours. Labelled worms were harvested, washed, and stored at -80°C until lipid extraction and analysis by GC/MS.

### **3.5.7. qRT-PCR testing**

The RNAs were extracted using Direct-zol RNA Miniprep kit (Zymo Research Corporation, Cat# R2050) following the manufacturer's instructions. 500 ng of RNAs were reverse-transcribed using M-MuLV reverse transcriptase (NEB, Cat#

M0253S) following the manufacturer's instructions. The resulting cDNAs were diluted 10 times, and 2  $\mu$ L were used for 20  $\mu$ L qPCR reactions, performed using Fast SYBR Green Master Mix (ThermoFischer Scientific, Cat# 4385612) following the manufacturer's instructions, on a QuantStudio 3 Real-Time PCR System (ThermoFisher Scientific, Cat# A28567). Fold changes were quantified using the  $2^{-\Delta\Delta Ct}$  method, and significance was assessed by applying a One-Sample t test (hypothetical value = 1) on GraphPad Prism (v9.0.0).

Enzyme	Primer sequences:
<b>fat-7-298R</b>	accagagacgatgggctccagc
<b>fat-7-195F</b>	cgtcgccgcagccattggactt
<b>fat-6-490R</b>	ctccctctccgacggcagcaat
<b>fat-6-407F</b>	tggtgcatcaacagcgctgctca
<b>fat-5-795R</b>	acctccttctccgactgccgca
<b>fat-5-667F</b>	acggccgccctcttccgttact
<b>elo-6-156R</b>	tgtcatgacagccttgagccca
<b>elo-5-159R</b>	actgagatcgaaggcttttcggt
<b>elo-6-48F</b>	tgagggtgctgacaactgctcca
<b>elo-5-64F</b>	tgccaaagaagttgctcgaggcc

**Table 3: qRT-PCR genes.** This table shows the primers used to test the activity of elongases and desaturases used to produce fatty acids present in the PL membrane. The comparison was made between wildtype and PAQR-2 mutants control in regular plates and glucose stress plates.

### 3.5.8. Lipid Extraction and FAME creation

Total lipid was extracted, and PL and NL populations were separated using solid phase chromatography for GC-MS as described by Perez and Van Gilst (2008) and Dancy et al. (2015). Internal lipid standards, 1,2-diundecanoyl-sn-glycero-3-phosphocholine (Avanti Polar Lipids) and tritridecanoin (Nu-Chek Prep), were added to each sample. To maximize the mass spectrometry analysis and obtain good results, the plate of each sample collected was checked to ensure that enough worms were used in the

lipid extraction. The nematode pallet was transferred to glass culture tube containing a solution of chloroform:methanol (2:1) for 1.5 hours at room temperature to allow total lipid extraction. Dried total lipids in 1mL of chloroform were loaded onto HyperSep Silica SPE columns (100mg capacity, Thermo Scientific), and NLs and PLs were collected. Purified PLs and NLs were dried and resuspended in 1mL of 2.5% H<sub>2</sub>SO<sub>4</sub> in methanol, then incubated for 1 hour at 80°C to create fatty acid methyl esters (FAMES) to run on GC-MS.

### 3.5.9. GC Analysis

We calculate the Relative % of FAs in each sample by using the integrated area under the peaks of each fatty acid species seen in the gas chromatograph and as defined here:  $\text{Relative FA Abundance} = \frac{\text{FA area}}{\text{Total FA area}} * 100$  as in (Perez & Van Gilst, 2008). Labeling with stable isotopes (<sup>13</sup>C) allows for the analysis of the percentage of newly incorporated or Mol Percent Excess (MPE) of most major FA species simultaneously. Briefly, to calculate the MPE the isotopomers were normalized and corrected to the incorporation of natural isotopes. % Newly Incorporated Fatty Acids considers all newly modified fat independent of its source (*de novo* synthesized, elongated or directly absorbed) as described in Dancy et al. Error bars of the lipid composition and <sup>13</sup>C labelling show the standard error of the mean, and *t-tests* were used to identify significant differences between the fatty acids.

## Chapter 4: Targeted Lipidomics Reveals a Novel Role for Glucosylceramide in Glucose Response

Mark A. Xatse<sup>1</sup>, Andre F. C. Vieira<sup>1</sup>, and Carissa Perez Olsen<sup>1</sup>

Submitted to Journal of Lipid Research August 31, 2021

<sup>1</sup>From the Department of Chemistry and Biochemistry, Worcester Polytechnic Institute,  
Worcester, Massachusetts, USA

**Note:** The PL and sphingolipid mass spectrometry data, as well as the mass list and method development, was completed by Mark A. Xatse. The *cgt-3* lifespan data was conducted by Andre F. C. Vieira. Lastly, the *elo-3* lifespan data was a made in collaboration with replicates ran by both authors.

### 4.1. Abstract

The addition of excess glucose to the diet drives a coordinated response of lipid metabolism pathways to tune the membrane composition to the altered diet. Here, we have employed targeted lipidomic approaches to quantify the specific changes in the phospholipid and sphingolipid populations that occur in elevated glucose conditions. The lipids within wildtype *Caenorhabditis elegans* are strikingly stable with no significant changes identified in our global mass spectrometry-based analysis. Previous work has identified ELO-5, an elongase that is critical for the synthesis of monomethyl-branched chain fatty acids, as essential for surviving elevated glucose conditions. Therefore, we performed targeted lipidomics on *elo-5* RNAi fed animals and identified a number of

significant changes in these animals in lipid species that contain mmBCFAs as well as in species that do not contain mmBCFAs. Of particular note, we identified a specific glucosylceramide (GluCer 17:1;O2/22:0;O) that is also significantly upregulated with glucose in wildtype animals. Furthermore, compromising the production of the glucosylceramide pool with *elo-3* or *cgt-3* RNAi leads to premature death in glucose-fed animals. Taken together, the lipid analysis has expanded the mechanistic understanding of metabolic rewiring with glucose feeding and has identified a new role for the GluCer 17:1;O2/22:0;O.

## **4.2. Introduction**

Cell membranes are highly organized and dynamic structures made up of hundreds of unique lipids (Holthuis & Menon, 2014) (van Meer, Voelker & Feigenson, 2008). Perturbations including temperature changes and dietary alterations can alter membrane composition and require regulation of metabolic pathways to adjust the makeup of the membrane and optimize its function in the new conditions (Ernst, Ejsing, & Antonny, 2016) (Levental et al., 2020) (Ma, Sun, & Horvitz, 2015). Of note, elevated concentrations of glucose in the diet of nematodes requires an adaptive response coordinated by the membrane sensor, PAQR-2 which is the homologous to the mammalian adiponectin receptor. In response to glucose stress and the decreased fluidity associated with high glucose, PAQR-2 activates the desaturase FAT-7 which increases the production of unsaturated fatty acids to restore the fluidity of the membrane (Svensk *et al.*, 2016) (Ruiz *et al.*, 2018) (Pilon, 2016). Recently, a novel role for the elongase ELO-5 as part of the response of PAQR-2 to glucose was found using stable isotope labeling and mass

spectrometry approaches. In fact, ELO-5 is required for the production of monomethyl-branched chain fatty acids (mmBCFAs), and RNAi of *elo-5* results in a sensitivity to glucose diets (Vieira *et al.*, 2022). Although the elevated FAT-7 activity results in the production of unsaturated fatty acids to restore membrane fluidity, the impact of ELO- 5 is less clear and does not appear to directly impact fluidity (Svensk *et al.*, 2016) (Vieira *et al.*, 2022).

Distinct from saturated and unsaturated fatty acids, mmBCFAs have a saturated hydrocarbon chain and a methyl group located in the penultimate carbon giving these fatty acids a unique shape (Kniazeva *et al.*, 2004). In *C. elegans*, the major laboratory diet of *E. coli* (OP50) does not contain mmBCFAs and thus they are entirely synthesized de novo via fatty acid synthase, acyl-CoA synthase and two fatty acid elongase enzymes, ELO- 5 and ELO-6 (Perez & Van Gilst, 2008). The mmBCFAs are incorporated into phospholipids (Wallace *et al.*, 2018), and in *C. elegans*, they also serve as precursors for the sphingoid base required for the production of sphingolipids (Cheng *et al.*, 2019) (Mosbech *et al.*, 2013) (Hannich *et al.*, 2017). mmBCFAs production is essential for larval growth and development, and the roles of these fatty acids in adults has recently started to emerge (Kniazeva, Euler & Han, 2008) (Vrablik & Watts, 2012). Recently, it was established that mmBCFAs-derived glucosylceramides (GluCer) are critical to regulate intestinal apical membrane polarity to allow TORC1 activity in response to nutrient signals in the intestine (Kniazeva *et al.*, 2015) (Zhu *et al.*, 2013).

Glucosylceramides are considered sphingolipids and are intermediates of sphingolipid metabolism. Sphingolipids are a highly diverse group of lipid species that contain a sphingoid backbone made up of a linear hydrocarbon chain attached to an

amino and hydroxyl group (Peng *et al.*, 2017). The sphingoid base is amide-linked to long chain fatty acids usually containing 0 or 1 double bond to form ceramides. Ceramides can further be derivatized by the addition of a head group to form more complex sphingolipids such as sphingomyelin (SM), glucosylceramide (GluCer), and more complex glycosphingolipids with higher numbers of sugar residues (Merrill, 2011) (Merrill *et al.*, 2009). Ceramides are not only precursors for complex sphingolipids but also act as a metabolite with roles in stress response, autophagy, apoptosis and signaling (Jiang & Ogretmen, 2014) (Haimovitz-Friedman, Kolesnick, & Fuks, 1997) (Pattingre *et al.*, 2009). These processes are often mediated by specific chain length ceramides that are expressed in distinct subcellular compartments that perform unique functions (Hannun & Obeid, 2011) (Turpin-Nolan & Brüning, 2020). For instance, in *C. elegans*, mmBCFA-derived ceramides are produced by three different ceramide synthases: HYL-1, HYL-2, and LAGR-1. HYL-1 is required for the production of ceramides with very long N-linked fatty acid (C24 to C26), HYL-2 is required for ceramides with long N-linked fatty acids (C20-C22), and LAGR-1 has no major effect on ceramide production (Mosbech *et al.*, 2013) (Menuz *et al.*, 2009).

Glucosylceramides (GluCer) are the precursors to more complex glycosphingolipids (GSL) and are formed by the addition of a UDP-glucose to an existing ceramide molecule by ceramide glucosyltransferase (CGT) (Marza *et al.*, 2009). GSLs impact the structure, localization and activity of raft associated proteins and, in doing so, influence cellular activities including protein-protein interaction and signaling events (Iwabuchi *et al.*, 2010) (Sezgin *et al.*, 2017). In fact, recent studies in *C. elegans* suggest that GSL interacts with cholesterol to form lipid rafts that regulate clathrin localization and signaling processes



involved in stress response (Wang *et al.*, 2021). In *C. elegans*, the production of GluCer is dependent on ELO-3, a recently characterized elongase that produces the very long chain saturated fatty acids included in GluCer. In addition to supplying precursors for glycosphingolipids which have been implicated in stress responses, GluCer have been implicated as important metabolites for aging in *C. elegans* as well (Wang *et al.*, 2021). Because of the crucial roles GSLs play in most organisms, impaired GSL metabolism is linked to many disorders such as cardiovascular diseases, compromised immune response, Gaucher disease and neurodegeneration (Aerts *et al.*, 2019) (D'Angelo *et al.*, 2013) (Okada *et al.*, 2002) (Wu *et al.*, 2011). However, the complexity of these lipid populations has limited the knowledge of how each lipid species impacts cellular function.

*C. elegans* has become a useful model for the study of lipid metabolism through the use of mass spectrometry and genetic approaches (Shi *et al.*, 2016) (Sultana, & Olsen, 2020) (Watts & Ristow, 2017). In addition, the small size of *C. elegans* allows for affordable stable isotope labeling to monitor lipid dynamics. Our lab has developed  $^{15}\text{N}$ - and  $^{13}\text{C}$  - stable isotope feeding strategies in *C. elegans* combined with mass spectrometry to monitor the dynamics of intact phospholipids and fatty acids, respectively (Vieira *et al.*, 2021) (Perez & Van Gilst, 2008) (Dancy *et al.*, 2015). Using a combination of approaches, it has been established that mmBCFAs are essential to the nematode's survival with glucose stress, but it is not known whether this is through a derived lipid, a structural impact on the membrane or an unknown alternate mechanism (Vieira *et al.*, 2021). Here, we use advanced mass spectrometry to profile the changes in the lipids after glucose exposure which allows a more thorough understanding of how glucose impacts the phospholipids of the membrane with a particular focus on the sphingolipids including

GluCer. These lipidomics profiles reveal changes in the ceramide and glucosylceramide populations following glucose exposure that have been corroborated with glucose survival assays.

### **4.3. Results**

Here we present all the results to prove the role played the glucosylceramide d17iso GluCer responding against glucose stress, and also confirm that its synthesis requires the presence of mmBCFAs. In the text we showed all the figures seen in the main body of our paper; however, the supplementary tables and figures will not be included in the body of this Thesis due to the size of the material. To see the supplementary material, you can access the page of the official publication.

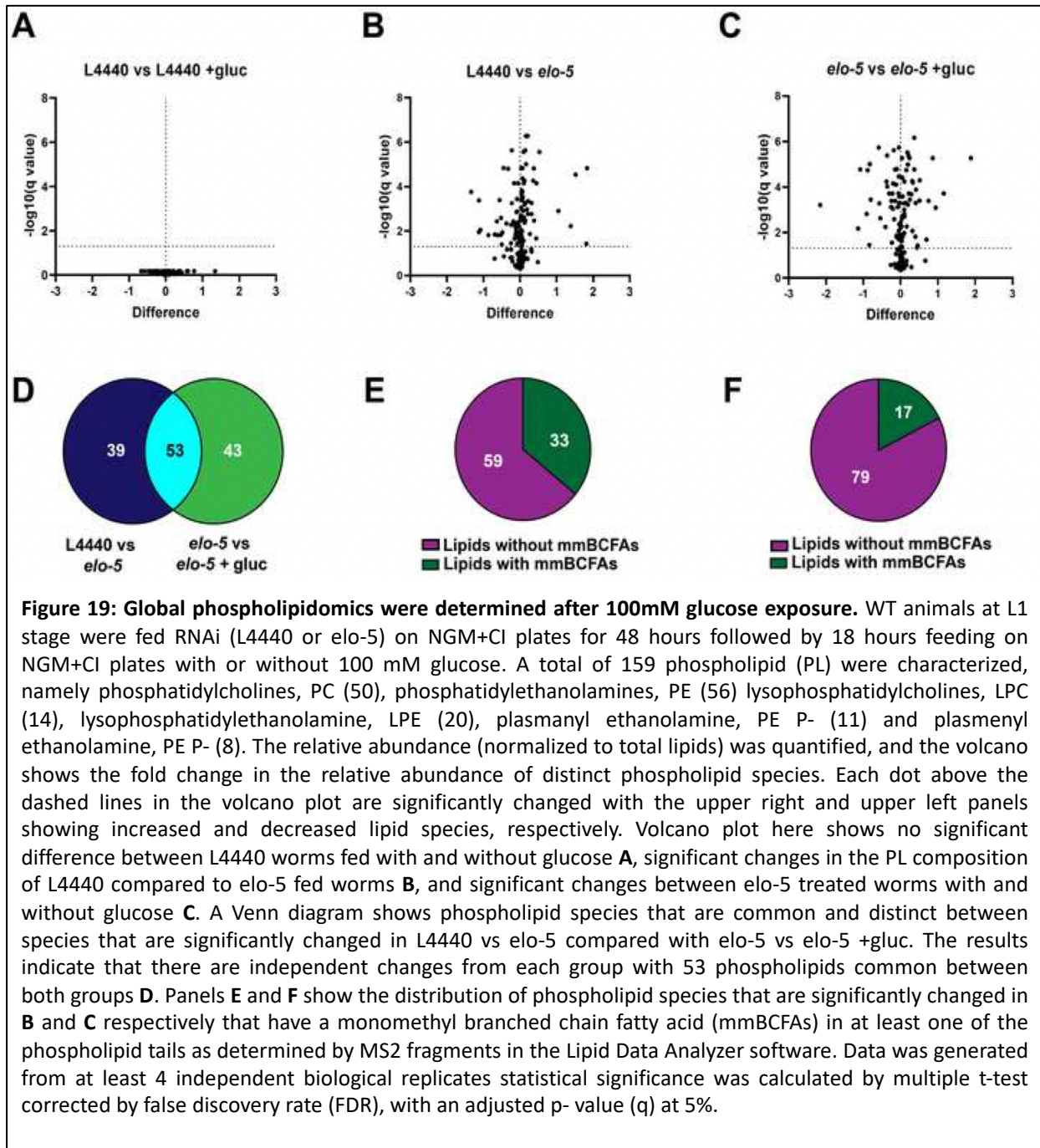
#### **4.3.1. Phospholipid Populations with Glucose Exposure**

Although it is clear that fatty acid metabolism is perturbed with excess dietary glucose, the specific changes in the phospholipids of the animals have not been established. Here, we profiled the phospholipids of control RNAi animals in the presence of 100 mM glucose. Populations of nematodes (L4 stage) were grown with (+gluc) and without 100 mM glucose for 18 hours and the membrane lipids (i.e., phosphatidylcholine (PC), phosphatidylethanolamine (PE), lysophosphatidylcholine (LPC), lysophosphatidylethanolamine (LPE), plasmalogen ethanolamine (PE O-) and plasmalogen ethanolamine (PE P-)) were analyzed using a Q Exactive mass spectrometer (Thermo Scientific, Waltham, MA). The relative abundance of the lipids was determined using Lipid Data Analyzer software and the fold change of distinct lipids under glucose stress

compared. The results showed no significant differences in any of the phospholipids in the target list after 18 hours of glucose exposure ((Fig 19A), complete list found as supplementary Table 1). The lack of significant changes in wildtype nematodes fed glucose is not surprising as it has been established that N2 animals can adapt to high glucose diets (Svensk et al., 2016) (Vieira et al., 2021). Additionally, these populations build the majority of the membrane, and the glucose exposure is relatively short, minimizing the impact of metabolic changes on the entire population due to dilution effects.

We next examined the impact on the phospholipid population when the glucose response is compromised by using an *elo-5* RNAi feeding approach. Here, *elo-5* RNAi was initiated at L1 stage for 48 hours, and then the animals were transferred to plates with and without glucose for 18 hours. First, to establish a baseline comparison, *elo-5* RNAi and control RNAi-fed animals were compared and the results reveal that ~58% of the lipids (92/159) were significantly changed with *elo-5* RNAi (Fig 19B). Next, *elo-5* RNAi treated animals were subjected to 18 hours of glucose exposure. This glucose treatment led to significant changes (~60% of lipids measured) in the phospholipid composition indicating that the ability to maintain membrane composition under glucose stress is compromised with the loss of ELO-5 (Fig 19C). Because there are a significant number of alterations that occur with *elo-5* RNAi feeding with and without glucose, we compared the significant changes and found that only 53 phospholipid species were altered in both conditions (Fig 19D). There are 43 phospholipid species that are significantly impacted when *elo-5* RNAi is combined with glucose treatment implicating these species in the glucose response.

Because ELO-5 is only involved in the production of C15iso and C17iso fatty acids, the impact on this large percentage of membrane lipids implicates ELO-5 or a product of this enzyme in regulating phospholipid metabolism on a larger scale. To interrogate this further, the MS2 scans of the significantly changed species were used to determine if the lipid contains a mmBCFA as one of its tails. In *elo-5* RNAi- fed populations, only 35.8%



of the altered species contain a mmBCFA when compared to L4440 controls (Fig 19E). In *elo-5* RNAi fed animals treated with glucose, only 17.7% of the altered species contain a mmBCFA compared to *elo-5* RNAi without glucose (Fig 19F). Since the majority of the changed species do not directly contain a mmBCFA, the role of ELO-5 in glucose response is more wide-reaching than just the production of these fatty acid species for inclusion in phospholipids.

#### **4.3.2. Analysis of Phospholipid Classes and the Associated Fatty Acid Tails**

To further investigate the impact of ELO-5 across lipid metabolism pathways, the relative distribution of each phospholipid class was determined. In comparing control and *elo-5* RNAi fed animals, there was not a significant difference between the PC and PE headgroups between L4440 and *elo-5* RNAi (Fig 20A). Similarly, there was no change in PC and PE distribution with 100 mM glucose feeding of either control or *elo-5* RNAi (Fig 20A, see supplementary Table 2 for complete list). We next probed lipid populations that are less abundant but play critical roles in signaling and stress response, specifically the lysophospholipids and the plasmalogens (Drechsler *et al.*, 2016) (Hänel, Pendleton, & Witting, 2019) (Hartler *et al.*, 2020) (Tan *et al.*, 2020). The abundance of LPE is significantly lower in *elo-5* RNAi when compared to controls ( $1.24 \pm 0.1\%$  vs  $2.13 \pm 0.20\%$ ). The reduction in the LPC and LPE population in the *elo-5* RNAi treated animals is largely from the depletion of lysophospholipids containing a mmBCFA tail, suggesting that the pool of precursors for mmBCFA-containing fatty acids is severely limited (supplementary Table 1 for full list). The abundance of the LPC and LPE was not altered by glucose exposure in control RNAi and *elo-5* RNAi populations, suggesting that this

reduction in LPE is due to a lack of ELO-5 activity in building the membrane lipids but not in the response to short-term glucose stress (Fig 20B). In analyzing the plasmalogens, we observed an increase in both PE O- and PE P- abundances in *elo-5* RNAi treated animals from  $3.68 \pm 0.50\%$  to  $5.79 \pm 0.67\%$  and  $4.50 \pm 1.3\%$  to  $6.46 \pm 0.46\%$ , respectively (Fig 20B). Despite the elevated PE O- and PE P- levels in untreated *elo-5* RNAi animals, again the glucose exposure does not lead to an additional increase in the *elo-5* RNAi animals suggesting that these animals have a compromised lipid pool, and that plasmalogens are not an induced response to glucose.

The types of fatty acids in each pool have a dramatic impact on lipid metabolism and membrane function (Gianfrancesco, *et al.*, 2018) (Holthuis & Menon, 2014). We analyzed the overall degree of saturation within the PC and PE classes as these glycerophospholipids comprise ~88 % of the total phospholipid population. First, the PC species were binned by the number of total double bonds within the animal to define the overall level of saturation in the phosphatidylcholine lipids in the control RNAi, and the *elo-5* RNAi-fed animals without glucose (Fig 20C). There were alterations in the level of unsaturation *elo-5* RNAi with a significant increase in PC lipids with 2-3 and 6-7 double bonds and a significant decrease in PC lipids with 4-5 and  $\geq 8$  double bonds. Importantly, there is a significant decrease in the 0-1 double bond bin between control RNAi and *elo-5* RNAi which includes mmBCFAs (Fig 20C). The addition of glucose did not alter the level of unsaturation of the majority of PC lipids in control and *elo-5* RNAi worms except for a small but statistically significant increase in the 0-1 double bond bin (Fig 20C). In analyzing the level of unsaturation in the PE population, there were fewer alterations between control RNAi and *elo-5* RNAi than in the PC; however, we did observe a

significant decrease in the 0-1 double bond bin, consistent with mmBCFA loss, and a decrease in 4-5 double bonds. In addition, there was a significant increase in the level of PE lipids with 2- 3 double bonds and 6-7 double bonds (Fig 20D). The addition of glucose did not impact the level of saturation of control animals, but interestingly the addition of glucose significantly increased the levels of lipids with 2-3 double bonds and significantly decreased lipids with  $\geq 4$  double bonds in *elo-5* RNAi treated worms (Fig 20D). Overall, the phospholipidomic analysis indicates that the majority of differences in *elo-5* RNAi treated animals is due to loss of the enzyme, but there is a significant role for *elo-5* in the alterations of PE lipids in animals treated with glucose. The biophysical properties of phospholipids are also impacted by the chain length of the associated fatty acid tails (Klose, Surma, & Simons, 2013) (Sampaio *et al.*, 2011). Therefore, we performed a similar analysis, but binning based on chain length (i.e.,  $\leq 32$ , 33-34, 35-36, etc. carbons in both fatty acid chains). Similar to the double bond analysis, there are multiple significant changes between control RNAi and *elo-5* RNAi fed animals in the PC (Fig 20E) and the PE classes (Fig 20F), specifically decreases in  $\leq 32$  and 33-34 carbons. Interestingly, these decreases are offset in each lipid class differently with an increase in 37-38 for PC and in 35-36, 37-38 and 39-40 for PE, indicating that the regulation is not occurring in the fatty acid pool but in phospholipid metabolism pathways. The addition of glucose shows no impact on the chain length in control animals; however, there are a number of significant changes in *elo-5* treated animals fed high glucose diets. Here, the chain length changes are the same in both PC (Fig 20E) and PE (Fig 20F): elevated  $\leq 32$ , 33-34 and 35-36 bins and decreased 37-38 and 39-40 bins. These changes cannot be explained by

the reduced capacity to produce mmBCFA and further support that ELO-5 plays roles in regulating metabolism perhaps through impacting signaling lipids.

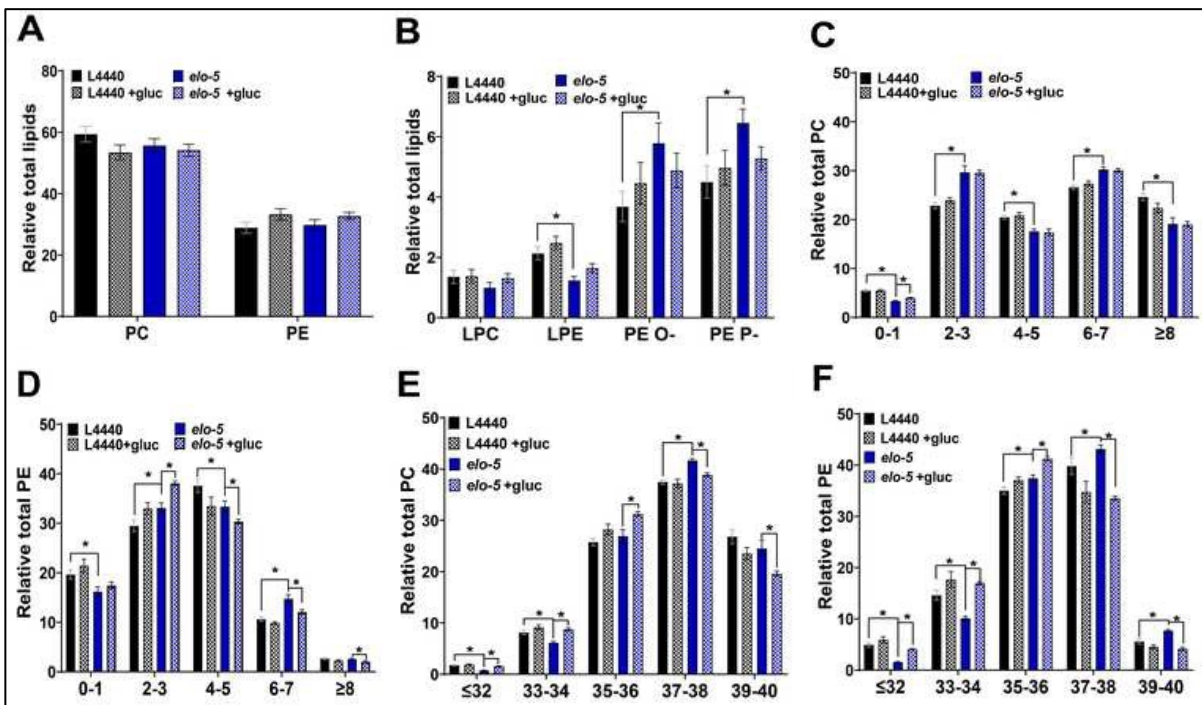


**Figure 20: Glucose feeding impacts fatty acid saturation and length in phospholipids.** **A**, The relative distribution of the major PL class- PC and PE for L4440 (black), L4440 +gluc (black and checked), *elo-5* (blue) and *elo-5* +gluc (blue and checked) was generated by targeted lipidomic analysis. **B**, The distribution of the less abundant lipid classes- LPC, LPE, PE O- and PE P- was generated for the same populations of animals. The results show a significant decrease in the LPE population and a significant increase in the plasmalogen (PE O- and PE P-) species in L4440 compared to *elo-5* RNAi. Glucose stress did not significantly impact the distribution of each lipid class. **C**, PC phospholipids were binned by the total number of double bonds associated with their fatty acids for each treatment group. The result shows a significant decrease in PL with a total of 0- 1, 4-5 and 8 or more double bonds and an increase in lipids with 2-3 and 6-7 double bonds in L4440 compared to *elo-5* RNAi. Glucose stress did not greatly alter the distribution of double bonds apart from a significant increase in PC species with 0-1 double bonds in *elo-5* glucose-stressed animals. **D**, Similarly, the double bond distribution of PE lipids was quantified. The results showed a significant increase in PE species with 6-7 and 2-3 double bonds and a decrease in lipids with 0- 1 and 4-5 double bonds in L4440 compared to *elo-5*. Glucose stress did not alter the PE double distribution in control animals but led to a significant increase in PE species with 2-3 double bonds and a significant decrease in species with 4 or more double bonds in *elo-5* animals stressed with glucose. **E**, PC lipids were binned according to the total number of carbons in the fatty acid tails. The results indicate that the loss of *elo-5* significantly increased lipids with a total fatty acid tail of 37-38 and a significant decrease in lipids with a relatively shorter chain (less than 36 carbon). Glucose did not impact the chain length of control animals but led to significant increase in shorter chain lipids (less than 36) and a decrease in longer chains (36 carbon or more). **F**, Similarly, PE lipids were binned according to chain length show a significant decrease in lipids with shorter chain length (less than 36 carbons) and a significant increase in lipids with longer carbon chains (36 or more) in *elo-5* RNAi worms compared to controls (L4440). Contrastingly, the presence of glucose showed a significant increase in lipids with relatively shorter carbon chains (36 carbons or less) and a significant decrease in lipids with longer carbon chains (more than 36 carbons) in *elo-5* worms stressed with 100 mM glucose while controls remained unchanged. Data was generated from at least 4 independent biological replicates. Statistical significance was calculated by multiple t-test corrected by false discovery rate (FDR), with an adjusted p- value (q) at 5%



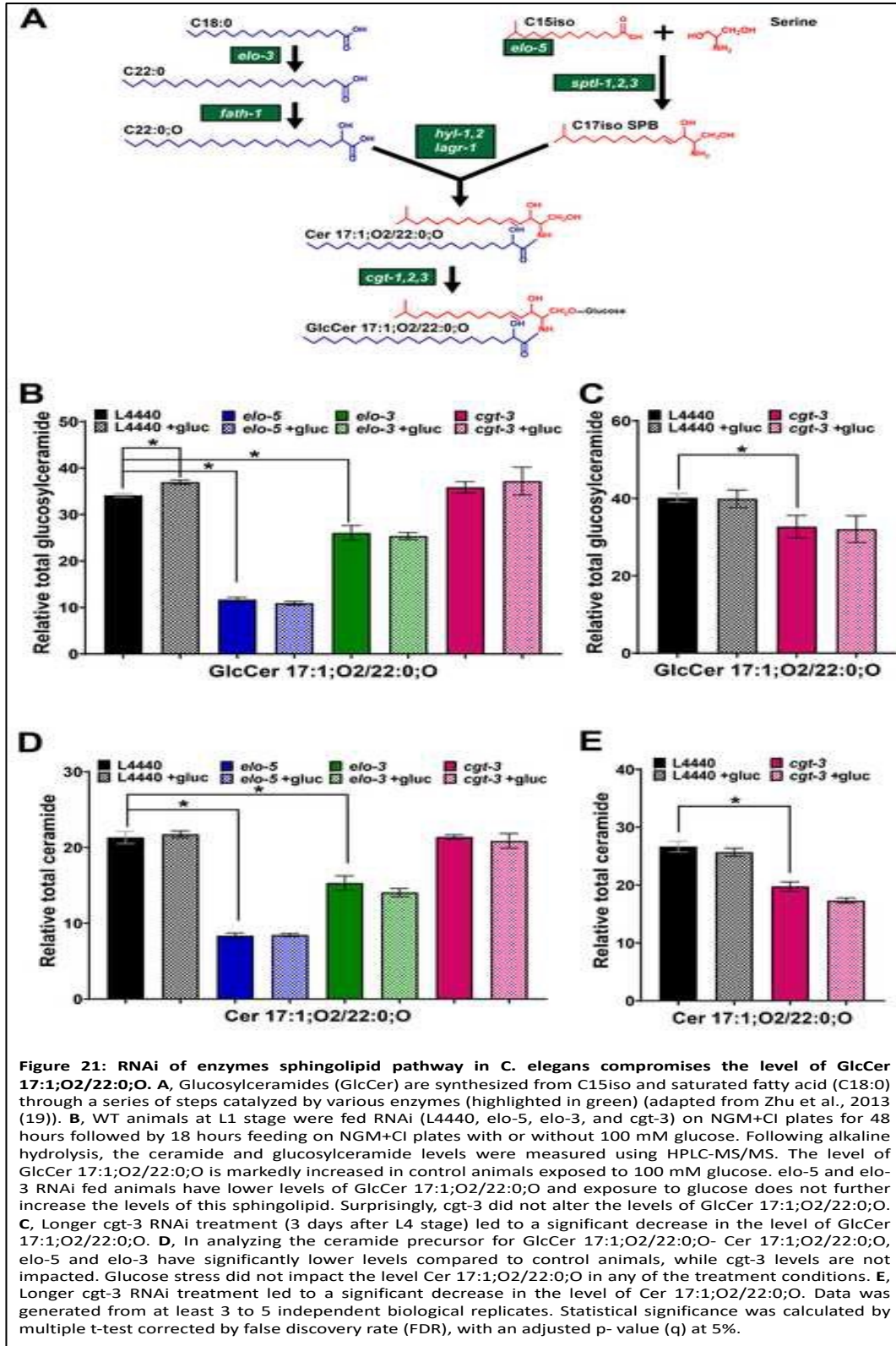
### 4.3.3. Glycolipid Populations Respond to Glucose Diets

The glucosylceramide population is of particular interest in *elo-5* treated animals as the mmBCFA population provides precursors for their synthesis. In particular, GluCer 17:1;O2/22:0;O is a critical metabolite that is responsible for regulating postembryonic growth and development but has not been implicated in response to glucose(19). Here, we use the Lipid Maps nomenclature for sphingolipids GluCer XX/YY where GluCer represents the headgroup, XX represents the sphingoid base and YY represents the N-linked FA (Liebisch *et al.*, 2020). GluCer 17:1;O2/22:0;O synthesis requires ELO-5 to produce the mmBCFA backbone and ELO-3 to produce saturated very long chain fatty acids (SVLCFAs) which are both further processed before ultimately being joined by a ceramide glucosyl transferase (CGT) to produce GluCer 17:1;O2/22:0;O (Fig 21A) (19, 32). In order to determine if GluCer 17:1;O2/22:0;O has a role in glucose response, we first established an assay by HPLC-MS/MS to quantify the abundance of this species based on a method previously developed (Cheng *et al.*, 2019) (Hänel, Pendleton, & Witting, 2019). Although our method does not distinguish between the isomeric hexosylceramides (HexCer), GluCer and galactosylceramide (GalCer), there is no data available currently about the presence of GalCer in *C. elegans*. The HexCer measured in *C. elegans* in previous studies is GluCer (Cheng *et al.*, 2019) (Zhu *et al.*, 2013) (Marza *et al.*, 2009) (Wang *et al.*, 2021) and for the rest of the paper, we assume that the HexCer measured here is GluCer. Animals treated with *elo-3* RNAi were included as a control as ELO-3 is required to produce GluCer 17:1;O2/22:0;O and indeed the abundance of this lipid was significantly reduced from  $34.12 \pm 0.40\%$  in control animals to  $26.07 \pm 1.59\%$

with *elo-3* RNAi validating the methodology (Fig 21B, supplementary Table 3). Similarly, *elo-5* RNAi led to strongly reduced GluCer 17:1;O2/22:0;O to  $11.69 \pm 0.0.47\%$  (Fig 21B).

*C. elegans* has three ceramide glucosyltransferase- *cgt-1,2,3*. We tested the impact of *cgt-3* RNAi because CGT-3 protein was previously shown to have the highest CGT activity compared with *cgt-1* and *cgt-2* (Nomura *et al.*, 2011) and has also been recently shown to be important for stress response (Wang *et al.*, 2021). Interestingly, there was no significant reduction in GluCer 17:1;O2/22:0;O with *cgt-3* RNAi (Fig 21B). We hypothesized that this lack of reduction may be a result of the relatively short-term RNAi exposure. To test this, we extended the RNAi period to 3 days at which point we observed significant death within the *cgt-3* RNAi treated animals. In these longer term *cgt-3* RNAi treated animals, we were able to quantify significantly reduced GluCer 17:1;O2/22:0;O but not to the same extent as with *elo-5* and *elo-3* RNAi which we hypothesize is a result of the death of the animals with the most reduced levels (Fig 21C, supplementary Table 4). Because of the power of HPLC-MS/MS, the levels of Cer 17:1;O2/22:0;O, the immediate precursor to GluCer 17:1;O2/22:0;O, were also quantified. The same trends were observed in this population with significantly reduced Cer 17:1;O2/22:0;O in *elo-5*, *elo-3* and long-term *cgt-3* RNAi treatment (Fig 21D and 21E).

Once the assays were validated, the abundance of GluCer 17:1;O2/22:0;O was quantified after 100 mM glucose exposure, and there was a significant increase from  $34.12 \pm 0.40\%$  to  $36.96 \pm 0.48\%$  in control animals (Fig 21B). There was no increase in GluCer 17:1;O2/22:0;O in *elo-3*, *elo-5* or long-term *cgt-3* RNAi treatment indicating that this elevation with glucose treatment is due to increased synthesis of GluCer 17:1;O2/22:0;O and not reduced consumption or degradation (Fig 21B and Fig 21C).



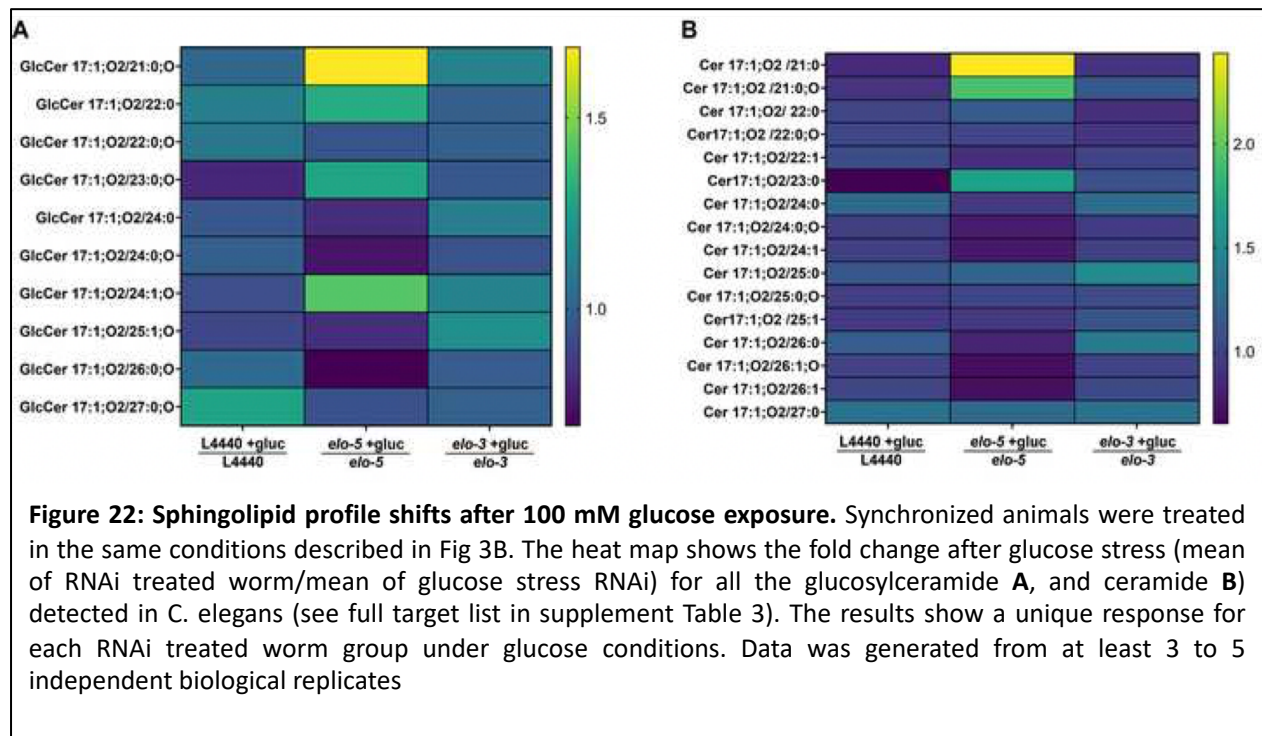
Interestingly, glucose exposure did not lead to an increase in the production of GluCer 17:1;O2/22:0;O with long-term glucose treatment in control populations implicating the

increased production as a short-term impact that will be modulated with time. Similarly, there is no change in the Cer 17:1;O2/22:0;O pool in controls treated with glucose (Fig 21D) suggesting that there is an immediate role for GCT in funneling precursors to GluCer 17:1;O2/22:0;O production.

#### **4.3.4. Ceramide and Glucosylceramide Pools Change with High Glucose Diets**

Although GluCer 17:1;O2/22:0;O has been implicated in other phenotypes of mmBCFA deficiency, there are many other glucosylceramide and ceramide species within the nematode. We expanded our criteria and surveyed all the major glucosylceramides and ceramides in control animals and detected 16 ceramide species and 10 GluCer species (supplementary Table 3 for full list). Here, we focused on the species that changed with glucose exposure in L4440 RNAi animals and found that the majority of ceramides and glucosylceramides are stable except there were significant decreases in Cer 17:1;O2/23:0, and significant increases in GluCer 17:1;O2/22:0. Overall, this suggests that the response to glucose in the diet alters sphingolipid metabolism to keep the levels of most individual species relatively stable (Fig 22A and Fig 22B).

We next interrogated how these lipid populations are impacted without the ability to synthesize new sphingolipid molecules. Because *elo-5* RNAi had the greatest impact of the GluCer 17:1;O2/22:0;O pool, we first compared the sphingolipid profiles in *elo-5* RNAi fed animals that were also subjected to high glucose diets. There were significant alterations in 8/16 ceramides specifically Cer 17:1;O2/21:0, Cer 17:1;O2/21:0;O, Cer 17:1;O2/22:0, Cer 17:1;O2/23:0, Cer 17:1;O2/24:1, Cer 17:1;O2/24:0;O, Cer 17:1;O2/26:0, and Cer 17:1;O2/26:0;O. Many of the corresponding GluCer (6/10) were

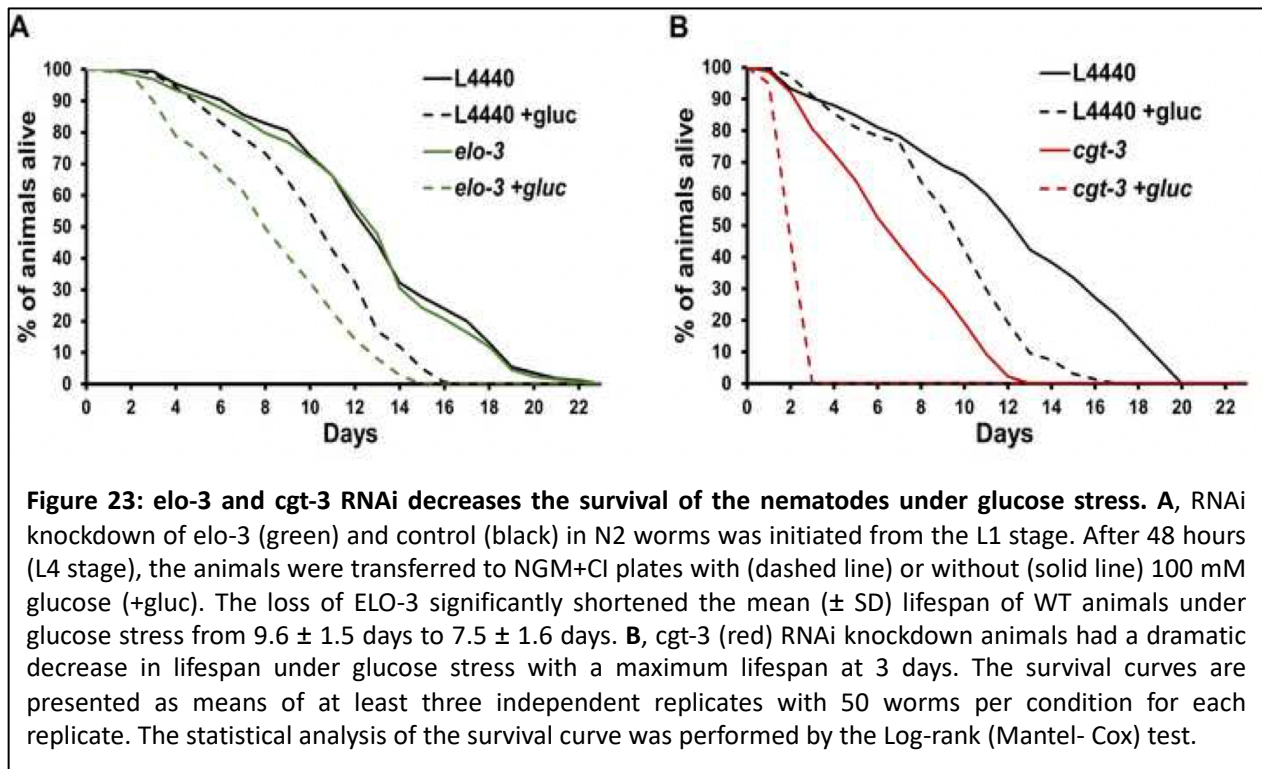


also significantly different from controls including GluCer17:1;O2/24:1, GluCer 17:1;O2/21:0;O, GluCer 17:1;O2/23:0;O, GluCer 17:1;O2/24:0;O, GluCer 17:1;O2/25:0;O and GluCer 17:1;O2/26:0;O (Fig 22A and 22B). Glucose does not have a major impact in *elo-3* RNAi animals under glucose stress with the only significant change being a decrease in Cer 17:1;O2/25:0. In summary, the impact of glucose stress on the ceramide and glucosylceramide is more severe in *elo-5* fed RNAi compared to control and *elo-3* fed RNAi animals.

#### 4.3.5. Spingolipid Synthesis is Critical for Survival in Elevated Glucose Conditions

Because of the altered GluCer pool observed in the *elo-3* RNAi animals similar to *elo-5* animals, we examined whether *elo-3* RNAi also caused glucose sensitivity. Synchronized L1 animals were fed control or *elo-3* RNAi. After 48 h, L4 stage animals

were transferred to RNAi plates with or without 100 mM glucose. The results show that *elo-3* RNAi significantly decreased the median lifespan of WT animals under glucose stress from 11 days to 8 days (Figure 23A). Similarly, the survival of the nematodes under glucose stress was monitored with *cgt-3* RNAi. Interestingly, *cgt-3* RNAi dramatically shortened the lifespan of the animals under glucose stress with a maximum lifespan of 3 days (Figure 23B). This dramatic decrease in lifespan was more severe than shortened lifespan observed previously in *elo-5* RNAi animals. This result suggests a critical role of glucosylceramide production in the survival of glucose stress.



#### 4.4. Discussion

In this study, we have established GluCer 17:1;O2/22:0;O as a critical mediator of the response to glucose in *C. elegans*. The monomethyl branched chain fatty acids and this derived glucosylceramide has been previously implicated in post-embryonic development

and foraging in *C. elegans* (Kniazeva *et al.*, 2015) (Zhu *et al.*, 2013). Here, we define a new role for this sphingolipid in participating in the nematode's response to high glucose diets. In doing so, ELO-5, ELO-3 and CGT-3, all enzymes involved in GluCer 17:1;O2/22:0;O production, have been established as participants in the system of metabolic pathways that are critical for surviving high glucose diets. The response network to glucose stress in *C. elegans* has been developing over the last decade, and our work here expands the knowledge of how this response acts mechanistically.

One of the striking features of these glucose-response targeted lipidomic datasets is the lack of significant changes in wildtype animals. In fact, we find no significant changes in animals fed 100 mM glucose in our initial global comparison, highlighting the rewiring of metabolic pathways with glucose. This maintenance of overall phospholipid composition is somewhat unexpected as a few changes in fatty acid composition have been documented (Vieira *et al.*, 2021) (Lee *et al.*, 2015). We believe that the existence of so many individual phospholipid species dilutes the impact of the fatty acid changes on any given lipid. The adjustment in metabolic pathways can be observed by compromising the genes in pathways required for the response including the membrane sensor, PAQR-2. PAQR-2 has been established as a critical mediator of the transcriptional changes that occur with glucose exposure including increased expression of desaturases and elongases required to produce unsaturated fatty acids and monomethyl-branched chain fatty acids (Svensk *et al.*, 2016) (Vieira *et al.*, 2021). Here, we have found that the role of mmBCFAs in this response is in providing the precursors for glucosylceramide synthesis; thus, the PAQR-2 sensor is further connected to sphingolipid metabolism. This is of particular interest as GluCer is a mediator of TOR activity in other conditions (Zhu *et al.*,

2013), though further studies would be needed to confirm the role of TOR in glucose response.

The study revealed an interesting membrane remodeling seen in *elo-5* RNAi fed animals under glucose. In general, the results show that *elo-5* fed RNAi worms under glucose stress had relatively less double bonds and an overall shorter chain length. This shift is characteristic of an adaptation of the membrane to a phospholipid composition that is resistant to oxidative stress as highly polyunsaturated fatty acids are most susceptible to damage by reactive oxygen species (Reis *et al.*, 2011) (Hulbert, Kelly, & Abbott, 2014). This shift would be protective against the higher levels of oxidative species seen in high glucose diets (Alcántar-Fernández *et al.*, 2018) (Schlotterer *et al.*, 2009). Although it has been hypothesized that glucose supplementation results in excess saturated fatty acid in the membrane (Svensk *et al.*, 2016) (Pilon, 2016), we believe that the extra glucose is increasing the oxidative load in the animal and this shift lends support to that model.

RNAi of ceramide glucosyltransferase led to a perturbation in GluCer populations and a dramatically shortened lifespan on glucose. We were intrigued by the fact that CGT-3 RNAi needed a longer timeframe to see significant decreases in sphingolipid populations while compromised survival happens readily. In fact, the longer RNAi period required for the lipidomic analysis results in a significant death of the treated animals with only  $80 \pm 3.1$  % animals remaining at time of collection. We hypothesize that the role of GluCer in glucose response may be required only in a specific subset of cells within the intestine. Studies in the nematode have found that mutations in any of the three ceramide glucosyltransferase (CGT) genes can be rescued by expression in a small subset of



intestinal cells (Marza *et al.*, 2009). Many lipid signaling pathways have been found to work in cell nonautonomous manner and it is likely that the GluCer response to glucose follows that pattern.

Our study here also highlights the power of mass spectrometry in the genetic organism, *C. elegans*. Stable isotope labeling originally identified mmBCFA as implicated in the response to glucose. In fact, this role was only observed using stable isotopes as the populations of these fatty acids are not significantly altered in wildtype nematodes (9). The stability of lipid populations is a common trend in wildtype worms; however, by combining stable isotope and genetic approaches, it is clear that multiple pathways are required to maintain the membrane populations under these stressed conditions. In fact, reduction or elimination of these pathways including ELO-5 and CGT-3 led to reduced survival under high glucose diets. Overall, the utilization of mass spectrometry methods combined with genetic tools has identified a novel and specific role for a particular glucosylceramide in membrane adaptation.

## **4.5. Methodologies & Techniques**

### **4.5.1. Strains and RNAi treatment**

All experiments were conducted using wild-type N2 nematodes obtained from the *C. elegans* Genetics Center (CGC). For RNAi experiments, RNAi bacteria clones from the Ahringer library (L4440 (empty vector), *elo-5*, *elo-3* and *cgt-3*) were grown on NGM + Carbenicillin + IPTG plates (NGM+CI) (Kamath & Ahringer, 2003).

#### **4.5.2. Nematode Growth and Elevated Glucose Feeding Protocols**

In order to synchronize the nematodes, gravid adults were exposed to dilute bleach, and the washed eggs were left rotating overnight at 20 °C in M9 solution. Approximately 5,000-6,000 synchronized L1 animals were grown at a density of 2,000 worms per 10 cm RNAi treatment plate for 48 hours. At L4, nematodes were transferred to NGM+CI plates with (referred to as +gluc plates) or without glucose for an additional 18 hours.

The glucose stress was carried out as previously described (Vieira *et al.*, 2022). Briefly, the glucose plates were made to a final concentration of 100 mM glucose by adding a filtered glucose solution to cooled autoclaved NGM+CI media. The glucose plates were seeded with RNAi bacteria at least 4 days before plating the worms. RNAi bacteria along with the control RNAi were seeded on plates at a density of 0.15 g per 10 cm NGM+CI plate.

#### **4.5.3. Extraction and Detection of Phospholipids by LC-MS/MS**

Total lipids were extracted from frozen nematodes via chloroform/methanol (2:1 v/v) solvent system as previously described (Dancy *et al.*, 2015) (Drechsler *et al.*, 2016). A 1,2-diundecanoyl-sn-glycerco-3-phosphocholine standard was added for relative quantification later as described previously (Avanti Polar Lipids). Briefly, total lipid extracts were dried under nitrogen and then dissolved in 200 µL of acetonitrile/2-propanol/water (65:30:5 v/v/v) dilution buffer. Next, 10 µL of resuspended lipids were injected onto the LC-MS/MS system for the negative ion scanning mode analysis. Lipids samples were separated using an HPLC system (Dionex UHPLC UltiMate 3000) equipped with a C18 Hypersil Gold 2.1 x 50mm, 1.9µm column (25002-052130; Thermo Scientific) equipped

with a 2.1 mm ID, 5  $\mu$ m Drop-In guard cartridge (25005–012101; Thermo Scientific). The column was connected to an Dionex UltiMate 3000 RS quaternary pump, a Dionex UltiMate 3000 RS autosampler, and a Q Exactive Orbitrap mass spectrometer from Thermo Scientific coupled with a heated electrospray ionization (HESI) source.

The HPLC phospholipid separation was carried out with mobile phase A and B consisting of 60:40, water (H<sub>2</sub>O): acetonitrile (ACN) plus 10 mM ammonium formate (NH<sub>4</sub>COOH) and 0.1% formic acid and 90:10, isopropyl alcohol (IPA): acetonitrile (ACN) with 10 mM ammonium formate (NH<sub>4</sub>COOH) and 0.1% formic acid, respectively. The gradient method began with 32% B over 0-1.5 min; 32-45% B from 1.5-4 min; 45-52% B from 4-5 min; 52-58% B from 5-8 min; 58-66% B from 8-11min; 66-70% B from 11-14 min; 70-75% B from 14-18 min; 75-97% B from 18-21 min; 97% B up to 25 min; 97-32% B from 25-26 min; 32% B is maintained until 30 min for column equilibration.

The following parameters were used for the HPLC and MS conditions: column oven temperature was maintained at 50 °C and autosampler was set 10 °C with mobile phase flow rate at 300  $\mu$ L/min and MS scan range between m/z 300-1200. The capillary temperature was set at 325 °C, the sheath gas flow rate at 45 units, the auxiliary gas flow at 10 units, the source voltage was 3.2 kV and the AGC target  $10^6$ . The acquisition was carried out with full scan data dependent MS<sub>2</sub> (ddMS<sub>2</sub>) mode. For MS<sub>1</sub> profiling, scans were run at a resolution of 70k. MS<sub>2</sub> analyses were performed using 6 scan events, where the top five ions were chosen from an initial MS<sub>1</sub> scan. For fragmentation, a normalized collision energy of 35 was used. MS<sub>1</sub> spectra were collected in profile mode where MS<sub>2</sub> collected in centroid mode.

#### 4.5.4. Extraction and Detection of Sphingolipids by LC-MS/MS

Sphingolipid extraction was conducted based on previous studies (Cheng *et al.*, 2019) (Hänel *et al.*, 2019) (Peng *et al.*, 2017). Briefly, total lipids were extracted from nematodes with 2:1 chloroform:methanol for 1.5 hours. Ceramide/sphingoid internal standard mixture II (Avanti Polar Lipids) was added prior to extraction. Extracted lipids were dried under nitrogen and 50  $\mu$ L of 1M KOH in methanol was added. The mixture was vortexed briefly and incubated at 37 °C for 2 hours. After incubation, the sample was neutralized with 2-3  $\mu$ L of glacial acetic acid. After phase separation with 450  $\mu$ L methanol, 1000  $\mu$ L chloroform and 500  $\mu$ L of water, the sphingolipid fraction (organic phase) was dried under nitrogen and dissolved in 200  $\mu$ L of isopropanol/chloroform/methanol (90:5:5, v/v/v).

The sphingolipids (10  $\mu$ L injection) were separated and analyzed using the same instrument used for PL with the following modification to the instrument method adapted from a recent study (Hartler *et al.*, 2020). The mobile phase A consisted of water containing 1% formic acid and 10 mM ammonium formate while the mobile phase B consisted of 5:2 (v/v) acetonitrile/isopropanol containing 1% formic acid and 10 mM ammonium formate. The gradient method started at 50% mobile phase B, rising to 100% B over 15 min, held at 100% B for 10 min, and the column was then re-equilibrated with 50% B for 8 min before the next injection. The flow rate was 0.150 mL/min. For MS analysis, sphingolipids were analyzed in the positive mode with the following parameters the capillary temperature was set at 275 °C, the sheath gas flow rate at 45 units, the auxiliary gas flow at 10 units, the source voltage was 3.2 kV and the AGC target  $10^6$ . The acquisition was carried out with full scan data dependent MS2 (ddMS2) mode. For MS1 profiling, scans were run at a resolution of 70k. MS2 analyses were performed using 5

scan events, where the top five ions were chosen from an initial MS1 scan. For fragmentation, a normalized collision energy of 50 was used. MS1 spectra were collected in profile mode where MS2 collected in centroid mode (Harter 2020).

#### **4.5.5. Phospholipid and Sphingolipidomic Analysis**

Lipid analysis of the LC-MS/MS data was conducted using the software Lipid Data Analyzer (LDA) Version 2.8.1. The LDA utilizes a 3D algorithm relying on the exact mass, predicted isotopic distribution from full scan MS, retention time, and MS/MS spectra for reliable analysis of the lipids (Hartler *et al.*, 2020). During LDA analysis, a 0.1% relative peak cutoff value was applied to the RAW files in order to focus on the major lipid species. LDA mass lists were generated for phospholipids based on a previous study in our lab (Dancy *et al.*, 2015). A relative quantification was used to compare between samples; however, the lipids were not normalized, so an absolute quantitation was not done.

LDA mass lists for ceramide and glucosylceramide were created by combining the carbon length of the sphingoid backbone in *C. elegans* (C17iso SPB) (Hannich *et al.*, 2017) (Hänel, Pendleton, & Witting, 2019), with N-linked fatty acid tail ranging from a chain length of 16-28 with degrees of saturation of 0 and 1 which is common for sphingolipids (Merrill, 2011). MS2 scans were manually verified on Xcalibur version 4.1.31.9 for the sphingoid base fragment specific for *C. elegans* of 250.25.

Statistical analysis for all the studies were performed using GraphPad Prism 9.4.1 software. Multiple t-test (unpaired) with corrected by false discovery rate (FDR), with an adjusted p-value (q) at 5% was used to compare two conditions in the lipidomics data.

#### **4.5.6. Survival Analysis**

Lifespan was performed with 50 synchronized L4 animals on NGM+CI plates with or without glucose. Worms were transferred every day onto fresh plates, and the number of dead animals was confirmed by prodding each animal and recorded daily. For lifespan data, statistical analysis was performed using a log-rank (Cox-Mantel) test.

## Chapter 5: Conclusions and future work

### 5.1. Overall conclusion

The adaptation of membrane composition responding to different stimuli is thought to be mediated by different signaling pathways; however, just a few of these mechanisms have been properly tested. Because the replacement of consumed and/or damaged FAs, also called membrane dynamics, plays an important role in maintaining membrane composition; here, we aimed to experimentally understand how membrane dynamics are participating in the response against glucose stress. Glucose was shown to be capable of increasing the levels of saturated fat available in the system and possibly damaging susceptible molecules such as PUFAs via increased oxidative stress. In humans, aberrant membrane composition is associated with many diseases such as Alzheimer's, cancer, and diabetes suggesting a role for membrane composition in health; however, it is not clear how membrane composition impacts these conditions. Studies such as those completed in this thesis will expand the knowledge of the genes and pathways that control membrane composition. This understanding will allow for possible biomarker discovery, novel therapeutic targets and improved drug delivery capability.

In addition to the basal membrane composition, membrane composition also impacts flux through metabolic pathways. Specifically, our data found that the dynamics of specific fatty acids such as SFA, UFA, and mmBCFAs participate in the response to glucose stress. One of required responses for survival with glucose stress is the direct regulation of membrane saturation levels by the activity of FAT-7. Because the response seen in FAT-7 is likely linked to the regulation of membrane fluidity, this finding will help

to inform the mechanisms that result in the rigidification of membranes, as a result of SFA accumulation, which is present in diseases such as diabetes and cancer.

In addition to FAT-7 upregulation, the activity of ELO-5 is also vital for survival on glucose and appears to help in the production of a glucosylceramide that does not regulate fluidity but could participate in regulating the oxidative stress caused by glucose. Interestingly, the accumulation of glucose in diabetic patients was shown to elevate oxidative stress in the cells and consequently induce apoptosis. Thus, if further studies confirm the participation of this molecule in regulating oxidative stress, we could use it as a targeted treatment for diabetic patients, avoiding oxidative stress and controlling apoptosis. Although we still do not know the complete mechanisms regulating membranes undergoing challenging conditions such as glucose stress. The work done here confirms that there is a network of responses that are essential for survival.

### **5.1.1. Conclusion chapter 2**

The activity of transmembrane proteins such as membrane sensors, and cytosolic transcription factors controlling fatty acid production were important discoveries to indicate that lipids play an important role in the organism's homeostasis. Here and in the literature, PAQR-2 was found to coordinate a response to high glucose levels by elevating the expression of desaturases and elongases. Each one of these enzymes produces a specific fatty acid species to maintain optimal membrane composition. As shown in the literature, the upregulation of FAT-7 maintains the saturated and unsaturated fatty acid balance in glucose stress nematodes. Our results also confirmed that metabolic pathways are constantly active during the stress maintaining UFA levels; however, the removal of



stress allows the animals to recover which ultimately caused a decrease in C18:1n9 and C18:2n6. We hypothesize that this reduction reflects the channeling of these fatty acids to PUFA synthesis. Adaptation to fatty acid metabolism pathways seems to be more effective in longer stress periods, suggesting that the rewiring of metabolism requires time to complete.

Although this first work was focused on the responses in PUFAs, we also observed an unexpected increase in mmBCFAs dynamics, suggesting that they were participating in the overall response to high glucose stress. mmBCFAs were previously shown to participate in the correct development of nematodes but never responding to glucose stress. Therefore, understanding the importance of these FAs could open many new possibilities to create new treatments to mitigate alterations caused by glucose stress.

### **5.1.2. Conclusion chapter 3**

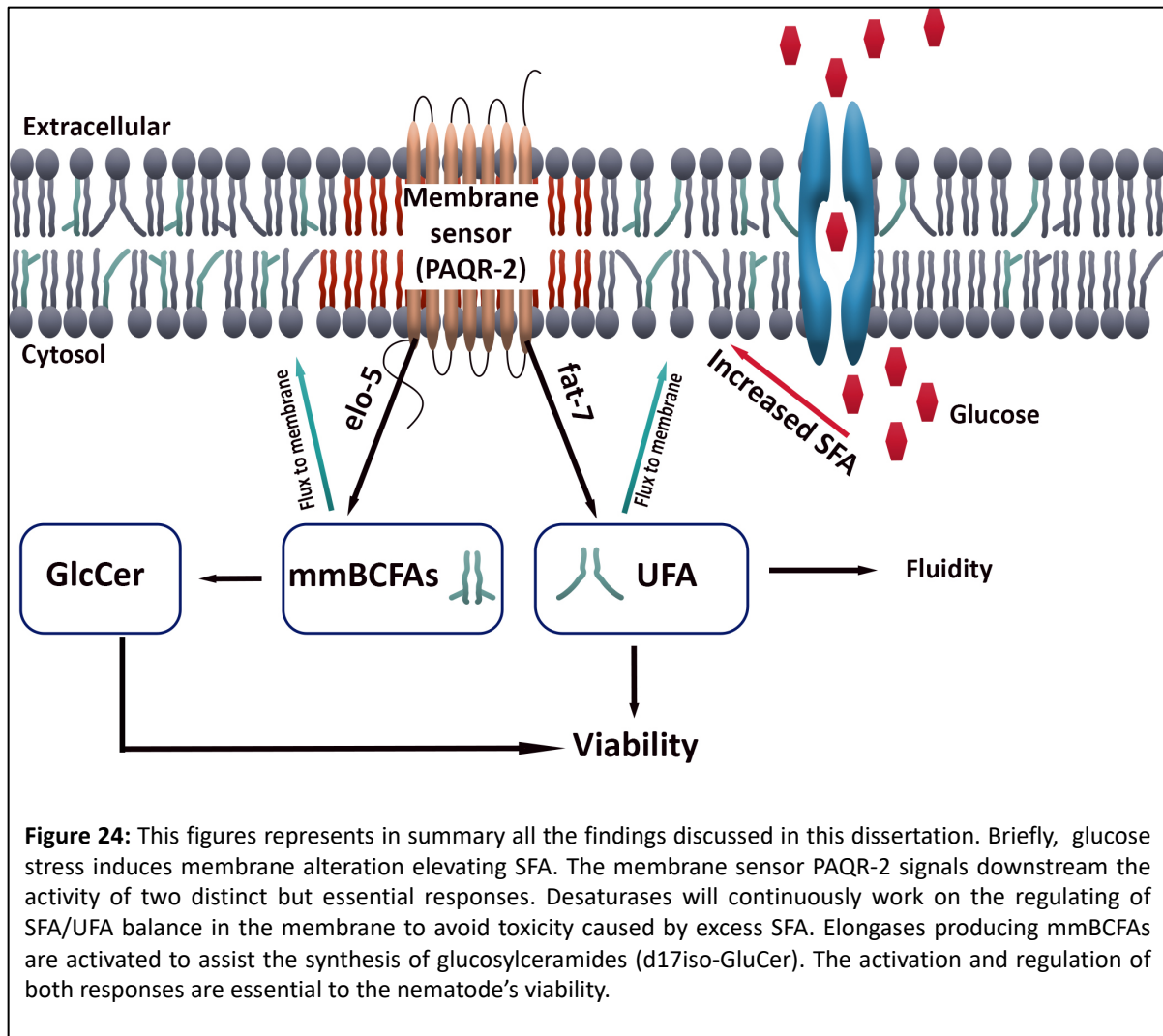
The mmBCFAs present in the membrane of *C. elegans* are saturated fatty acids that contain 15 and 17 carbons and a methyl group attached to the penultimate carbon. In *C. elegans*, these fatty acids are essential for nematode development; and in humans, low levels of mmBCFAs were correlated to the poor activity of insulin (Kniazeva et al., 2004) (Su *et al.*, 2015). Our data found that *elo-5* activity, producing C15iso and C17iso, is essential to survive the excess glucose in the diet. Moreover, this response acts downstream of PAQR-2 signals, but it is not directly linked to the regulation of membrane fluidity. Further studies are needed to investigate the complete pathway by which these FAs are responding to glucose stress and to dissect the role of glucosylceramide in promoting resistance to glucose stress.

### 5.1.3. Conclusion chapter 4

Reduced *elo-5* expression determined that nematodes do not survive glucose stress if mmBCFAs are not synthesized; however, ELO-5 was not essential for surviving increased saturated fatty acid levels which suggested this role was at least not directly regulating membrane fluidity. Therefore, we investigated other mechanisms that could explain the role of mmBCFAs. A literature review revealed a glucosylceramide called d17iso GluCer, which requires the presence of C15iso and a glucose molecule to synthesize its structure. This glucosylceramide promotes proper foraging behavior and participates in the apical membrane localization in nematodes (Zhu *et al.*, 2013) (Zhu *et al.*, 2015). Therefore, we hypothesized that d17iso GluCer could potentially explain the role of mmBCFAs in the glucose response.

To better understand what mechanisms required mmBCFAs to respond to glucose stress, we used HPLC combined with tandem mass spectrometry to characterize the phospholipid population with an eventual focus on d17iso GluCer. First, we determined that mmBCFA activity is more wide-reaching than the production of these fatty acid species for inclusion in phospholipids. Next, we showed that d17iso GluCer is actively responding to glucose stress and that this lipid requires *elo-5* and *elo-3* activity for production. Finally, the lifespan of *elo-3*, *elo-5*, and *cgt-3* RNAi confirmed that mmBCFAs and C18:0 producing the d17iso GluCer is essential to survive glucose stress. Overall, our data indicated that the response to glucose stress involves a large cascade of events that will maintain optimal membrane composition through PAQR-2 signaling and glucosylceramide signaling.

**Figure 24: Model representation of the findings in this dissertation:**



#### 5.1.4. Future directions

One important find in our work established the importance of fatty acids regulation, more especially SFA, UFA, and mmBCFAs, to the overall maintenance of membrane composition and organism homeostasis. Interestingly, the dysregulation of both mmBCFA and UFA was also shown in diseases such as diabetes. Their aberrant membranes showed rigidification caused by the unbalance of SFA/UFA favoring the

accumulation of saturated fat, and a positive correlation with the activity of insulin depending on the levels of mmBCFAs in the membrane. Therefore, it would be important to use more complex diabetes models like rats and mice to further investigate the importance of UFAs and mmBCFAs. An extensive lipidomic analysis in the pancreatic cells of this models, focusing on the alterations that we found here, could help in the development of diagnostic techniques and treatments for diabetic patients focused on membrane regulation.

The results presented in this work are not limited just to the regulation of membrane balance responding to glucose, which could lead to the idea that only diabetic patients could be favored. The response of mmBCFAs/d17iso GluCer does not appear to be directly related to SFA/UFA balance but could be responding to the regulation of oxidative stress damage caused by glucose. Reactive oxygen species (ROS) emerged as a key factor driving Alzheimer's disease and other neurodegenerative conditions. Therefore, a more profound investigation into the importance of mmBCFAS/d17iso GluCer responding to ROS could help in the development of treatment of these diseases.

## Chapter 6: References

- Aerts, J. M. F. G., Artola, M., van Eijk, M., Ferraz, M. J., and Boot, R. G. (2019) Glycosphingolipids and Infection. Potential New Therapeutic Avenues. *Front. Cell Dev. Biol.* 7, 324.
- Alberts B, Johnson A, Lewis J, et al. *Molecular Biology of the Cell*. 4th edition. New York: Garland Science; 2002. The Lipid Bilayer. Available from: <https://www.ncbi.nlm.nih.gov/books/NBK26871/>
- Alcántar-Fernández J, Navarro RE, Salazar-Martínez AM, Pérez-Andrade ME, Miranda-Ríos J. Caenorhabditis elegans respond to high-glucose diets through a network of stress-responsive transcription factors. *PLoS ONE*. 2018;13(7). doi: 10.1371/journal.pone.0199888.
- Assies J, Mocking RJ, Lok A, Ruhé HG, Pouwer F, Schene AH. Effects of oxidative stress on fatty acid- and one-carbon-metabolism in psychiatric and cardiovascular disease comorbidity. *Acta Psychiatr Scand*. 2014 Sep;130(3):163-80. doi: 10.1111/acps.12265. Epub 2014 Mar 21. PMID: 24649967; PMCID: PMC4171779.
- Ayala A, Muñoz MF, Argüelles S. Lipid peroxidation: production, metabolism, and signaling mechanisms of malondialdehyde and 4-hydroxy-2-nonenal. *Oxid Med Cell Longev*. 2014;2014:360438. doi: 10.1155/2014/360438. Epub 2014 May 8. PMID: 24999379; PMCID: PMC4066722.
- Bandet CL, Tan-Chen S, Bourron O, Le Stunff H, Hajdúch E. Sphingolipid Metabolism: New Insight into Ceramide-Induced Lipotoxicity in Muscle Cells. *Int J Mol Sci*. 2019;20(3):479. Published 2019 Jan 23. doi:10.3390/ijms20030479

- Bandu, R., Mok, H. J., & Kim, K. P. (2018). Phospholipids as cancer biomarkers: Mass spectrometry-based analysis. *Mass Spectrometry Reviews*, 37(2), 107-138. doi:10.1002/mas.21510
- Bianco CM, Fröhlich KS, Vanderpool CK. Bacterial Cyclopropane Fatty Acid Synthase mRNA Is Targeted by Activating and Repressing Small RNAs. *J Bacteriol*. 2019 Sep 6;201(19):e00461-19. doi: 10.1128/JB.00461-19. PMID: 31308070; PMCID: PMC6755755.
- Bieberich E. Sphingolipids and lipid rafts: Novel concepts and methods of analysis. *Chem Phys Lipids*. 2018;216:114-131. doi:10.1016/j.chemphyslip.2018.08.003
- Borkman M, Storlien LH, Pan DA, Jenkins AB, Chisholm DJ, Campbell LV. The relation between insulin sensitivity and the fatty-acid composition of skeletal-muscle phospholipids. *N Engl J Med*. 1993 Jan 28;328(4):238-44. doi: 10.1056/NEJM199301283280404. PMID: 8418404.
- Braverman NE, Moser AB. Functions of plasmalogen lipids in health and disease. *Biochim Biophys Acta*. 2012 Sep;1822(9):1442-52. doi: 10.1016/j.bbadis.2012.05.008. Epub 2012 May 22. PMID: 22627108.
- Budin, I., de Rond, T., Chen, Y., Chan, L. J. G., Petzold, C. J., & Keasling, J. D. (2018). Viscous control of cellular respiration by membrane lipid composition. *Science (American Association for the Advancement of Science)*, 362(6419), 1186-1189. doi:10.1126/science.aat7925
- Byerly L, Cassada RC, Russell RL. The life cycle of the nematode *Caenorhabditis elegans*. I. Wild-type growth and reproduction. *Dev Biol*. 1976 Jul 1;51(1):23-33. doi: 10.1016/0012-1606(76)90119-6. PMID: 988845.

- Cajka T, Fiehn O. Comprehensive analysis of lipids in biological systems by liquid chromatography-mass spectrometry. *Trends Analyt Chem.* 2014 Oct 1;61:192-206. doi: 10.1016/j.trac.2014.04.017. PMID: 25309011; PMCID: PMC4187118.
- Cao Z, Mak HY. Married at Birth: Regulation of Cellular Fat Metabolism by ER–Lipid Droplet Crosstalk. *Contact.* 2020;3. doi:10.1177/2515256420934671
- Carman GM, Han GS. Regulation of phospholipid synthesis in the yeast *Saccharomyces cerevisiae*. *Annu Rev Biochem.* 2011;80:859-883. doi:10.1146/annurev-biochem-060409-092229
- Casares D, Escribá PV, Rosselló CA. Membrane Lipid Composition: Effect on Membrane and Organelle Structure, Function and Compartmentalization and Therapeutic Avenues. *Int J Mol Sci.* 2019 May 1;20(9):2167. doi: 10.3390/ijms20092167. PMID: 31052427; PMCID: PMC6540057.
- Cerbon J, Calderon V. 1995. Generation modulation and maintenance of the plasma membrane asymmetric phospholipid composition in yeast cells during growth: their relation to surface potential and membrane protein activity. *Biochim. Biophys. Acta* 1235:100–106. 10.1016/0005-2736(94)00311-C
- Chandel NS. Carbohydrate Metabolism. *Cold Spring Harb Perspect Biol.* 2021 Jan 4;13(1):a040568. doi: 10.1101/cshperspect.a040568. PMID: 33397651; PMCID: PMC7778149.
- Chaurasia B & Summers SA. Ceramides in Metabolism: Key Lipotoxic Players. *Annu Rev Physiol.* 2021;83:303-330. doi:10.1146/annurev-physiol-031620-093815
- Che H, Li Q , Zhang T , Ding L , Zhang L , Shi H , Yanagita T , Xue C , Chang Y , Wang Y . A comparative study of EPA-enriched ethanolamine plasmalogen and EPA-enriched

phosphatidylethanolamine on A $\beta$ <sub>42</sub> induced cognitive deficiency in a rat model of Alzheimer's disease. *Food Funct.* 2018 May 23;9(5):3008-3017. doi: 10.1039/c8fo00643a. PMID: 29774334.

- Chen YL, Tao J, Zhao PJ, Tang W, Xu JP, Zhang KQ, Zou CG. Adiponectin receptor PAQR-2 signaling senses low temperature to promote *C. elegans* longevity by regulating autophagy. *Nat Commun.* 2019 Jun 13;10(1):2602. doi: 10.1038/s41467-019-10475-8. PMID: 31197136; PMCID: PMC6565724.
- Cheng M, Bhujwalla ZM, Glunde K. Targeting Phospholipid Metabolism in Cancer. *Front Oncol.* 2016;6:266. Published 2016 Dec 27. doi:10.3389/fonc.2016.00266
- Cheng, X., Jiang, X., Tam, K. Y., Li, G., Zheng, J., and Zhang, H. Sphingolipidomic analysis of *C. elegans* reveals development-and environment-dependent metabolic features. *Int. J. Biol. Sci* 2019 15, 2897–2910.
- Chiu HH, Kuo CH. Gas chromatography-mass spectrometry-based analytical strategies for fatty acid analysis in biological samples. *J Food Drug Anal.* 2020 Jan;28(1):60-73. doi: 10.1016/j.jfda.2019.10.003. Epub 2019 Nov 27. PMID: 31883609.
- Cybulski LE, Ballering J, Moussatova A, Inda ME, Vazquez DB, Wassenaar TA, et al. Activation of the bacterial thermosensor DesK involves a serine zipper dimerization motif that is modulated by bilayer thickness. *Proc Natl Acad Sci U S A.* 2015;**112**:6353–8. doi: 10.1073/pnas.1422446112.
- D'Angelo, G., Capasso, S., Sticco, L., and Russo, D. Glycosphingolipids: synthesis and functions. *FEBS J* 2013 280, 6338–6353.
- Daleke D. L. Regulation of transbilayer plasma membrane phospholipid asymmetry. *J. Lipid Res.* 2003 44, 233–242. 10.1194/jlr.R200019-JLR200



- Dancy, B. C. R., Chen, S., Drechsler, R., Gafken, P. R., & Olsen, C. P. 13C- and 15N-labeling strategies combined with mass spectrometry comprehensively quantify phospholipid dynamics in *C. elegans*. *PloS One*, 2015 10(11), e0141850. doi:10.1371/journal.pone.0141850
- Dashty M. A quick look at biochemistry: carbohydrate metabolism. *Clin Biochem*. 2013 Oct;46(15):1339-52. doi: 10.1016/j.clinbiochem.2013.04.027. Epub 2013 May 14. PMID: 23680095.
- Dawidowicz E. A. Dynamics of membrane lipid metabolism and turnover. *Annual Review of Biochemistry* 1987 56:1, 43-57
- de Carvalho CCCR, Caramujo MJ. The Various Roles of Fatty Acids. *Molecules*. 2018 Oct 9;23(10):2583. doi: 10.3390/molecules23102583. PMID: 30304860; PMCID: PMC6222795.
- Delgado A, Fabriàs G, Casas J, Abad JL. Natural products as platforms for the design of sphingolipid-related anticancer agents. *Adv Cancer Res*. 2013;117:237-81. doi: 10.1016/B978-0-12-394274-6.00008-X. PMID: 23290782.
- Delmonte P. Evaluation of poly(90% biscyanopropyl/10% cyanopropylphenyl siloxane) capillary columns for the gas chromatographic quantification of trans fatty acids in non-hydrogenated vegetable oils. *J Chromatogr A*. 2016 Aug 19;1460:160-72. doi: 10.1016/j.chroma.2016.07.019. Epub 2016 Jul 18. PMID: 27470095.
- Devkota R, Svensk E, Ruiz M, Ståhlman M, Borén J, Pilon M. The adiponectin receptor AdipoR2 and its *Caenorhabditis elegans* homolog PAQR-2 prevent membrane rigidification by exogenous saturated fatty acids. *PLoS genetics*. 2017;13(9):e1007004. <https://www.ncbi.nlm.nih.gov/pubmed/28886012>. doi: 10.1371/journal.pgen.1007004.

- Diot C, García-González AP, Vieira AF, Walker M, Honeywell M, Doyle H, Ponomarova O, Rivera Y, Na H, Zhang H, Lee M, Olsen CP, Walhout AJM. Bacterial diet modulates tamoxifen-induced death via host fatty acid metabolism. *Nat Commun.* 2022 Sep 23;13(1):5595. doi: 10.1038/s41467-022-33299-5. PMID: 36151093; PMCID: PMC9508336.
- Drechsler, R., Chen, S. W., Dancy, B. C. R., Mehrabkhani, L., and Olsen, C. P. HPLC-Based mass spectrometry characterizes the phospholipid alterations in ether-linked lipid deficiency models following oxidative stress. *PLoS One* 2016 11, 1–22.
- Edwards C, Canfield J, Copes N, Brito A, Rehan M, Lipps D, Brunquell J, Westerheide SD, Bradshaw PC. Mechanisms of amino acid-mediated lifespan extension in *Caenorhabditis elegans*. *BMC Genet.* 2015 Feb 3;16(1):8. doi: 10.1186/s12863-015-0167-2. PMID: 25643626; PMCID: PMC4328591.
- Eibler, D., Abdurahman, H., Ruoff, T., Kaffarnik, S., Steingass, H., & Vetter, W. Unexpected formation of low amounts of (R)-configured anteiso-fatty acids in rumen fluid experiments. *PloS One*, 2017 12(1), e0170788. doi:10.1371/journal.pone.0170788
- Ernst, R., Ejsing, C. S., and B. Antonny. Homeoviscous Adaptation and the Regulation of Membrane Lipids. *J. Mol. Biol* 2016 428, 4776–4791.
- Esther Dalfó, PhD, Manuel Portero-Otín, MD, PhD, Victoria Ayala, PhD, Anna Martínez, Reinald Pamplona, MD, PhD, Isidre Ferrer, MD, PhD, Evidence of Oxidative Stress in the Neocortex in Incidental Lewy Body Disease, *Journal of Neuropathology & Experimental Neurology*, Volume 64, Issue 9, September 2005, Pages 816–830, <https://doi.org/10.1097/01.jnen.0000179050.54522.5a>

- Fabiani C, Antollini SS. Alzheimer's Disease as a Membrane Disorder: Spatial Cross-Talk Among Beta-Amyloid Peptides, Nicotinic Acetylcholine Receptors and Lipid Rafts. *Front Cell Neurosci.* 2019 Jul 18;13:309. doi: 10.3389/fncel.2019.00309. PMID: 31379503; PMCID: PMC6657435.
- Fanning, S., Haque, A., Imberdis, T., Baru, V., Barrasa, M. I., Nuber, S., . . . Selkoe, D. (2019). Lipidomic analysis of  $\alpha$ -synuclein neurotoxicity identifies stearoyl CoA desaturase as a target for parkinson treatment. *Molecular Cell*, 73(5), 1001-1014.e8. doi:10.1016/j.molcel.2018.11.028
- Farine L, Niemann M, Schneider A, Bütikofer P. Phosphatidylethanolamine and phosphatidylcholine biosynthesis by the Kennedy pathway occurs at different sites in *Trypanosoma brucei*. *Scientific Reports.* 2015;5:16787. doi:10.1038/srep16787.
- Farkas, T.; Fodor, E.; Kitajka, K.; Halver, J.E. Response of fish membranes to environmental temperature. *Aquacult. Res.* 2001, 32, 645–655.
- Fecchio, C., Palazzi, L., & de Laureto, P. P. (2018). A-synuclein and polyunsaturated fatty acids: Molecular basis of the interaction and implication in neurodegeneration. *Molecules (Basel, Switzerland)*, 23(7), 1531. doi:10.3390/molecules23071531
- Ferguson MA. "Lipid anchors on membrane proteins". *Current Opinion in Structural Biology.* August 1991;1 (4): 522–9. doi:10.1016/s0959-440x(05)80072-7
- Fujino T, Yamada T, Asada T, et al. Efficacy and Blood Plasmalogen Changes by Oral Administration of Plasmalogen in Patients with Mild Alzheimer's Disease and Mild Cognitive Impairment: A Multicenter, Randomized, Double-blind, Placebo-controlled Trial. *EBioMedicine.* 2017;17:199-205. doi:10.1016/j.ebiom.2017.02.012

- Gianfrancesco, M. A., Paquot, N., Piette, J., & Legrand-Poels, S. (2018). Lipid bilayer stress in obesity-linked inflammatory and metabolic disorders. *Biochemical Pharmacology*, 153, 168-183. doi:10.1016/j.bcp.2018.02.022
- Gibellini F, Smith TK. The Kennedy pathway--De novo synthesis of phosphatidylethanolamine and phosphatidylcholine. *IUBMB Life*. 2010 Jun;62(6):414-28. doi: 10.1002/iub.337. PMID: 20503434.
- Glickman MS, Cahill SM, Jacobs WR Jr. The Mycobacterium tuberculosis cmaA2 gene encodes a mycolic acid trans-cyclopropane synthetase. *J Biol Chem*. 2001 Jan 19;276(3):2228-33. doi: 10.1074/jbc.C000652200. Epub 2000 Nov 22. PMID: 11092877.
- Haimovitz-Friedman, A., Kolesnick, R. N., and Fuks Z. (1997) Ceramide signaling in apoptosis. *Br. Med. Bull* 53, 539–553.
- Hänel, V., Pendleton, C., and Witting, M.. (2019) The sphingolipidome of the model organism *Caenorhabditis elegans*. *Chem. Phys. Lipids*. 222, 15–22.
- Hannich, T. J., Mellal, D., Feng, S., Zumbuehl, A., and Riezman, H. (2017) Structure and conserved function of iso-branched sphingoid bases from the nematode: *Caenorhabditis elegans*. *Chem. Sci* 8, 3676–3686.
- Hannun, Y. A., and Obeid L. M. (2011) Many Ceramides . *J. Biol. Chem* 286, 27855–27862. Turpin-Nolan, S. M., and Brüning J. C. (2020) The role of ceramides in metabolic disorders: when size and localization matters. *Nat. Rev. Endocrinol* 16, 224–233.
- Hartler, J., Armando, A. M., Trötz Müller, M., Dennis, E. A., Köfeler, H. C., and Quehenberger, O. (2020) Automated Annotation of Sphingolipids including Accurate Identification of Hydroxylation Sites Using MS<sup>n</sup> Data. *Anal. Chem* 92, 14054–14062.

- Hedger, G., & Sansom, M. S. P. (2016). Lipid interaction sites on channels, transporters and receptors: Recent insights from molecular dynamics simulations. *Biochimica Et Biophysica Acta. Biomembranes*, 1858(10), 2390-2400. doi:10.1016/j.bbamem.2016.02.037
- Holthuis JC, Menon AK Lipid landscapes and pipelines in membrane homeostasis. *Nature*. 2014; 510:48–57. doi:10.1038/nature13474.
- Horton JD, Goldstein JL, Brown MS. SREBPs: activators of the complete program of cholesterol and fatty acid synthesis in the liver. *J Clin Invest*. 2002;109(9):1125-1131. doi:10.1172/JCI15593
- Hulbert, A. J., Kelly, M. A., and Abbott, S. K. (2014) Polyunsaturated fats, membrane lipids and animal longevity. *J. Comp. Physiol. B Biochem. Syst. Environ. Physiol* 184, 149–166.
- Iwabuchi, K., Nakayama, H., Iwahara, C., and Takamori, K. (2010) Significance of glycosphingolipid fatty acid chain length on membrane microdomain-mediated signal transduction. *FEBS Letter* 584, 1642–1652.
- Jiang, W., and Ogretmen. B. (2014) Autophagy paradox and ceramide. *Biochim. Biophys. Acta - Mol. Cell Biol. Lipids* 1841, 783–792.
- Jung Y, Kwon S, Ham S, Lee D, Park HH, Yamaoka Y, Jeong DE, Artan M, Altintas O, Park S, Hwang W, Lee Y, Son HG, An SWA, Kim EJE, Seo M, Lee SV. *Caenorhabditis elegans* Lipin 1 moderates the lifespan-shortening effects of dietary glucose by maintaining  $\omega$ -6 polyunsaturated fatty acids. *Aging Cell*. 2020 Jun;19(6):e13150. doi: 10.1111/accel.13150. Epub 2020 May 31. PMID: 32475074; PMCID: PMC7294780.

- Kaletta T, Hengartner MO. Finding function in novel targets: *C. elegans* as a model organism. *Nat Rev Drug Discov.* 2006 May;5(5):387-98. doi: 10.1038/nrd2031. PMID: 16672925.
- Kamath, R. S., & Ahringer, J. (2003). *Genome-wide RNAi screening in caenorhabditis elegans* Elsevier BV. doi:10.1016/s1046-2023(03)00050-1
- Kingsley SF, Seo Y, Allen C, Ghanta KS, Finkel S, Tissenbaum HA. Bacterial processing of glucose modulates *C. elegans* lifespan and healthspan. *Sci Rep.* 2021;11(1):5931. Published 2021 Mar 15. doi:10.1038/s41598-021-85046-3
- Klose, C., Surma, M. A., and Simons, K. (2013) Organellar lipidomics-background and perspectives. *Curr. Opin. Cell Biol* 25, 406–413.
- Kniazeva M, Crawford QT, Seiber M, Wang CY, Han M. Monomethyl branched-chain fatty acids play an essential role in *Caenorhabditis elegans* development. *PLoS Biol.* 2004;2(9):E257. doi:10.1371/journal.pbio.0020257
- Kniazeva, M., Euler, T., & Han, M. (2008). A branched-chain fatty acid is involved in post-embryonic growth control in parallel to the insulin receptor pathway and its biosynthesis is feedback-regulated in *C. elegans*. *Genes & Development*, 22(15), 2102-2110. doi:10.1101/gad.1692008
- Kniazeva, M., Zhu, H., Sewell, A. K., & Han, M. (2015). A lipid-TORC1 pathway promotes neuronal development and foraging behavior under both fed and fasted conditions in *C. elegans*. *Developmental Cell*, 33(3), 260-271. doi:10.1016/j.devcel.2015.02.015
- Koshy, C., & Ziegler, C. (2015). Structural insights into functional lipid–protein interactions in secondary transporters. *Biochimica Et Biophysica Acta. General Subjects*, 1850(3), 476-487. doi:10.1016/j.bbagen.2014.05.010

- Lai CH, Chou CY, Ch'ang LY, Liu CS, Lin W. Identification of novel human genes evolutionarily conserved in *Caenorhabditis elegans* by comparative proteomics. *Genome Res.* 2000 May;10(5):703-13. doi: 10.1101/gr.10.5.703. PMID: 10810093; PMCID: PMC310876.
- Lee D, Jeong DE, Son HG, Yamaoka Y, Kim H, Seo K, Khan AA, Roh TY, Moon DW, Lee Y, Lee SJ. SREBP and MDT-15 protect *C. elegans* from glucose-induced accelerated aging by preventing accumulation of saturated fat. *Genes Dev.* 2015 Dec 1;29(23):2490-503. doi: 10.1101/gad.266304.115. PMID: 26637528; PMCID: PMC4691952.
- Levental, K. R., Malmberg E., Symons J. L., Fan Y.Y., Chapkin, R. S., Ernst R., and Levental. I. (2020) Lipidomic and biophysical homeostasis of mammalian membranes counteracts dietary lipid perturbations to maintain cellular fitness. *Nat. Commun* 11, 1–13
- Li Z, Agellon LB, Allen TM, Umeda M, Jewell L, Mason A, Vance DE. The ratio of phosphatidylcholine to phosphatidylethanolamine influences membrane integrity and steatohepatitis. *Cell Metab.* 2006 May;3(5):321-31. doi: 10.1016/j.cmet.2006.03.007. PMID: 16679290.
- Liebisch, G., Fahy, E., Aoki, J., Dennis, E. A., Durand, T., Ejsing, C. S., Fedorova, M., Feussner, I., Griffiths, W. J., Köfeler, H., Merrill, A. H., Murphy, R. C., O'Donnell, V. B., Oskolkova, O., Subramaniam, S., Wakelam, M. J. O., and Spener, F. (2020) Update on LIPID MAPS classification, nomenclature, and shorthand notation for MS-derived lipid structures. *J. Lipid Res.* 61, 1539–1555.
- Lim YJ, Dial EJ, Lichtenberger LM. Advent of novel phosphatidylcholine-associated nonsteroidal anti-inflammatory drugs with improved gastrointestinal safety. *Gut Liver.*

2013 Jan;7(1):7-15. doi: 10.5009/gnl.2013.7.1.7. Epub 2012 Nov 13. PMID: 23423874; PMCID: PMC3572323.

- Ling J, Chaba T, Zhu LF, Jacobs RL, Vance DE. Hepatic ratio of phosphatidylcholine to phosphatidylethanolamine predicts survival after partial hepatectomy in mice. *Hepatology*. 2012 Apr;55(4):1094-102. doi: 10.1002/hep.24782. Epub 2012 Feb 29. PMID: 22095799.
- Lunn J, Theobald H.E. The health effects of dietary unsaturated fatty acids. *Nutrition bulletin*. 2006 25 August 2006 <https://doi.org/10.1111/j.1467-3010.2006.00571.x>
- Martin ML, Barceló-Coblijn G, de Almeida RF, Noguera-Salvà MA, Terés S, Higuera M, Liebisch G, Schmitz G, Busquets X, Escribá PV. The role of membrane fatty acid remodeling in the antitumor mechanism of action of 2-hydroxyoleic acid. *Biochim Biophys Acta*. 2013 May;1828(5):1405-13. doi: 10.1016/j.bbamem.2013.01.013. Epub 2013 Jan 27. PMID: 23360770.
- Marza, E., Simonsen, K. T., Færgeman, N. J., and Lesa, G. M. (2009) Expression of ceramide glucosyltransferases, which are essential for glycosphingolipid synthesis, is only required in a small subset of *C. elegans* cells. *J. Cell Sci* 122, 822–833.
- McMahon HT, Boucrot E. (2015) Membrane curvature at a glance. *J Cell Sci*. Mar 15;128(6):1065-70. doi: 10.1242/jcs.114454. PMID: 25774051; PMCID: PMC4359918.
- Menuz, V., Howell, K. S., Gentina, S., Epstein, S., Riezman, I., Fornallaz-Mulhauser, M., Hengartner, M. O., Gomez, M., Riezman, H., and Martinou J. C. (2009) Protection of *C. elegans* from Anoxia by HYL-2 ceramide synthase. *Science* 324, 381–384.
- Merrill, A. H. (2011) Sphingolipid and glycosphingolipid metabolic pathways in the era of sphingolipidomics. *Chem. Rev* 111, 6387–6422.



- Merrill, A. H., Stokes, T. H., Momin, A., Park, H., Portz, B. J., Kelly, S., Wang, E., M. C., and Sullards, M. D. (2009). Sphingolipidomics: A valuable tool for understanding the roles of sphingolipids in biology and disease. *J. Lipid Res* 50, 97–102.
- Mosbech, M. B., Kruse, R., Harvald, E. B., Olsen, A. S. B., Gallego, S. F., Hannibal-Bach, H. K., Ejsing, C. S., and Færgeman, N. J. (2013) Functional Loss of Two Ceramide Synthases Elicits Autophagy-Dependent Lifespan Extension in *C. elegans*. *PLoS One* 8, e70087.
- Mueller-Roeber B, Pical C. Inositol Phospholipid Metabolism in Arabidopsis. Characterized and Putative Isoforms of Inositol Phospholipid Kinase and Phosphoinositide-Specific Phospholipase C. *Plant Physiology*. 2002;130(1):22-46. doi:10.1104/pp.004770.
- Muschiol D, Schroeder F, Traunspurger W. Life cycle and population growth rate of *Caenorhabditis elegans* studied by a new method. *BMC Ecol*. 2009 May 16;9:14. doi: 10.1186/1472-6785-9-14. PMID: 19445697; PMCID: PMC2696410.
- Nomura, K. H., Murata, D., Hayashi, Y., Dejima, K., Mizuguchi, S., Kage-Nakadai, E., Gengyo- Ando, K., Mitani S., Hirabayashi, Y., Ito, M., and Nomura, K. (2011) Ceramide glucosyltransferase of the nematode *Caenorhabditis elegans* is involved in oocyte formation and in early embryonic cell division. *Glycobiology* 21, 834–848.
- Oguntibeju OO. Type 2 diabetes mellitus, oxidative stress and inflammation: examining the links. *Int J Physiol Pathophysiol Pharmacol*. 2019 Jun 15;11(3):45-63. PMID: 31333808; PMCID: PMC6628012.
- Okada, M., Itoh, M. I., Haraguchi, M., Okajima, T., Inoue, M., Oishi, H., Matsuda, Y., Iwamoto, T., Kawano, T., Fukumoto, S., Miyazaki, H., Furukawa, K., Aizawa, S., and

Furukawa, K. (2002) b-series Ganglioside deficiency exhibits no definite changes in the neurogenesis and the sensitivity to Fas-mediated apoptosis but impairs regeneration of the lesioned hypoglossal nerve. *J. Biol. Chem* 277, 1633–1636.

- Olsen Anne S. B. & Færgeman Nils J. Sphingolipids: membrane microdomains in brain development, function and neurological diseases. *Open Biol.* 2017;7170069170069 <http://doi.org/10.1098/rsob.170069>.
- Papackova Z, Cahova M. Fatty acid signaling: the new function of intracellular lipases. *Int J Mol Sci.* 2015;16(2):3831-3855. Published 2015 Feb 10. doi:10.3390/ijms16023831
- Patingre, S., Bauvy, C., Levade, T., Levine, B., and Codogno, P. (2009) Ceramide-induced autophagy: To junk or to protect cells? *Autophagy* 5, 558.
- Peng C, Ma J, Gao X, Tian P, Li W, Zhang L. High glucose induced oxidative stress and apoptosis in cardiac microvascular endothelial cells are regulated by FoxO3a. *PLoS One.* 2013 Nov 18;8(11):e79739. doi: 10.1371/journal.pone.0079739. PMID: 24260294; PMCID: PMC3832590.
- Peng, B., Weintraub S. T., Coman, C., Ponnaiyan, S., Sharma, R., Tews, B., Winter, D., and Ahrends, R.. (2017) A Comprehensive High-Resolution Targeted Workflow for the Deep Profiling of Sphingolipids. *Anal. Chem* 89, 12480–12487.
- Perez, C. L., & Van Gilst, M. R. (2008). A <sup>13</sup>C isotope labeling strategy reveals the influence of insulin signaling on lipogenesis in *C. elegans*. *Cell Metabolism*, 8(3), 266-274. doi:10.1016/j.cmet.2008.08.007
- Pilon M. Paradigm shift: the primary function of the "Adiponectin Receptors" is to regulate cell membrane composition. *Lipids Health Dis.* 2021 Apr 30;20(1):43. doi: 10.1186/s12944-021-01468-y. PMID: 33931104; PMCID: PMC8088037.

- Pilon, M. (2016). Revisiting the membrane-centric view of diabetes. *Lipids in Health and Disease*, 15(1), 167. doi:10.1186/s12944-016-0342-0
- Poojari, C.S., Scherer, K.C. & Hub, J.S. Free energies of membrane stalk formation from a lipidomics perspective. *Nat Commun* 12, 6594 (2021). <https://doi.org/10.1038/s41467-021-26924-2>
- Poole CF. Ionization-based detectors for gas chromatography. *J Chromatogr A*. 2015 Nov 20;1421:137-53. doi: 10.1016/j.chroma.2015.02.061. Epub 2015 Feb 24. PMID: 25757823.
- Poss AM, Maschek JA, Cox JE, et al. Machine learning reveals serum sphingolipids as cholesterol-independent biomarkers of coronary artery disease. *J Clin Invest*. 2020;130(3):1363-1376. doi:10.1172/JCI131838
- Rachdi, L., Balcazar, N., Osorio-Duque, F., Elghazi, L., Weiss, A., Gould, A., . . . Bernal-Mizrachi, E. (2008). Disruption of Tsc2 in pancreatic cells induces cell mass expansion and improved glucose tolerance in a TORC1-dependent manner. *Proceedings of the National Academy of Sciences*, 105(27), 9250-9255. doi:10.1073/pnas.0803047105
- Rao V, Fujiwara N, Porcelli SA, Glickman MS. Mycobacterium tuberculosis controls host innate immune activation through cyclopropane modification of a glycolipid effector molecule. *J Exp Med*. 2005;201(4):535-543. doi:10.1084/jem.20041668
- Reis, R. J. S., Xu, L., Lee, H., Chae, M., Thaden, J. J., Bharill, P., Tazearslan, C., Siegel, E., Alla, R., Zimniak, P., and Ayyadevara, S. (2011) Modulation of lipid biosynthesis contributes to stress resistance and longevity of *C. elegans* mutants. *Aging* 3, 125–147.
- Rilfors, L. (1984). Difference in packing properties between iso and anteiso methyl-branched fatty acids as revealed by incorporation into the membrane lipids of *A*

choleplasma laidlawii strain A. *Biochimica et Biophysica Acta* 813 (1985) 151-160: Elsevier.

- Rui L. Energy metabolism in the liver. *Compr Physiol.* 2014;4(1):177-197. doi:10.1002/cphy.c130024
- Ruiz M, Bodhicharla R, Svensk E, Devkota R, Busayavalasa K, Palmgren H, Ståhlman M, Boren J, Pilon M. Membrane fluidity is regulated by the *C. elegans* transmembrane protein FLD-1 and its human homologs TLCDC1/2. *Elife.* 2018 Dec 4;7:e40686. doi: 10.7554/eLife.40686. PMID: 30509349; PMCID: PMC6279351.
- Ruiz M, Ståhlman M, Borén J, Pilon M. AdipoR1 and AdipoR2 maintain membrane fluidity in most human cell types and independently of adiponectin. *J Lipid Res.* 2019 May;60(5):995-1004. doi: 10.1194/jlr.M092494. Epub 2019 Mar 19. PMID: 30890562; PMCID: PMC6495173.
- Sampaio, J. L., Gerl, M. J., Klose, C., Ejsing, C. S., Beug, H., Simons, K., and Shevchenko, A. (2011) Membrane lipidome of an epithelial cell line. *Proc. Natl. Acad. Sci. U. S. A* 108, 1903– 1907.
- Samuel, V., & Shulman, G. (2012). Mechanisms for insulin resistance: Common threads and missing links. *Cell (Cambridge)*, 148(5), 852-871. doi:10.1016/j.cell.2012.02.017
- Schlotterer, A., Kukudov, G., Bozorgmehr, F., Hutter, H., Du, X., Oikonomou, D., Ibrahim, Y., Pfisterer, F., Rabbani, N., Thornalley, P., Sayed, A., Fleming, T., Humpert, P., Schwenger, V., Zeier, M., Hamann, A., Stern, D., Brownlee, M., Bierhaus, A., Nawroth, P., and Morcos, M. (2009) *C. elegans* as model for the study of high glucose-mediated life span reduction. *Diabetes* 58, 2450–2456.

- Sezgin, E., Levental, I., Mayor, S., and Eggeling, C. (2017) The mystery of membrane organization: composition, regulation and roles of lipid rafts. *Nat. Rev. Mol. Cell Biol* 18, 361– 374.
- Shi YN, Liu YJ, Xie Z, Zhang WJ. Fructose and metabolic diseases: too much to be good. *Chin Med J (Engl)*. 2021;134(11):1276-1285. Published 2021 May 18. doi:10.1097/CM9.0000000000001545
- Shi, X., Tarazona, P., Brock, T. J., Browse, J., Feussner, I., and Watts, J. L. (2016) A *Caenorhabditis elegans* model for ether lipid biosynthesis and function. *J. Lipid Res* 57, 265–275.
- Siliakus, M. F., van der Oost, J., & Kengen, S. W. M. (2017). Adaptations of archaeal and bacterial membranes to variations in temperature, pH and pressure. *Extremophiles : Life Under Extreme Conditions*, 21(4), 651-670. doi:10.1007/s00792-017-0939-x
- Snowden MB, Steinman LE, Bryant LL, Cherrier MM, Greenlund KJ, Leith KH, Levy C, Logsdon RG, Copeland C, Vogel M, Anderson LA, Atkins DC, Bell JF, Fitzpatrick AL. Dementia and co-occurring chronic conditions: a systematic literature review to identify what is known and where are the gaps in the evidence? *Int J Geriatr Psychiatry*. 2017 Apr;32(4):357-371. doi: 10.1002/gps.4652. Epub 2017 Feb 1. PMID: 28146334; PMCID: PMC5962963.
- Snowden SG, Ebshiana AA, Hye A, An Y, Pletnikova O, O'Brien R, Troncoso J, Legido-Quigley C, Thambisetty M. Association between fatty acid metabolism in the brain and Alzheimer disease neuropathology and cognitive performance: A nontargeted metabolomic study. *PLoS Med*. 2017 Mar 21;14(3):e1002266. doi: 10.1371/journal.pmed.1002266. PMID: 28323825; PMCID: PMC5360226.

- Sodt AJ, Pastor RW. Molecular modeling of lipid membrane curvature induction by a peptide: more than simply shape. *Biophys J*. 2014 May 6;106(9):1958-69. doi: 10.1016/j.bpj.2014.02.037. PMID: 24806928; PMCID: PMC4017297.
- Spector, A. A., & Yorek, M. A. (1985). Membrane lipid composition and cellular function. *Journal of Lipid Research*, 26(9), 1015-1035. Retrieved from <http://www.jlr.org/cgi/content/abstract/26/9/1015>
- Su, X., Magkos, F., Zhou, D., Eagon, J. C., Fabbrini, E., Okunade, A. L., & Klein, S. (2015). Adipose tissue monomethyl branched-chain fatty acids and insulin sensitivity: Effects of obesity and weight loss. *Obesity (Silver Spring, Md.)*, 23(2), 329-334. doi:10.1002/oby.20923
- Sultana, N., & Olsen, C. P. (2020). Using stable isotope tracers to monitor membrane dynamics in *C. elegans*. *Chemistry and Physics of Lipids*, 233, 104990. doi:10.1016/j.chemphyslip.2020.104990
- Svensk E, Ståhlman M, Andersson CH, Johansson M, Borén J, Pilon M. PAQR-2 regulates fatty acid desaturation during cold adaptation in *C. elegans*. *PLoS Genet*. 2013;9(9):e1003801. doi: 10.1371/journal.pgen.1003801. Epub 2013 Sep 12. PMID: 24068966; PMCID: PMC3772066.
- Svensk, E., Devkota, R., Ståhlman, M., Ranji, P., Rauthan, M., Magnusson, F., . . . Pilon, M. (2016). *Caenorhabditis elegans* PAQR-2 and IGLR-2 protect against glucose toxicity by modulating membrane lipid composition. *PLoS Genetics*, 12(4), e1005982. doi:10.1371/journal.pgen.1005982
- Tan, S. T., Ramesh T., Toh, X. R., and Nguyen, L. N. (2020) Emerging roles of lysophospholipids in health and disease. *Prog. Lipid Res* 80, 101068.

- Tappy L, Rosset R. Health outcomes of a high fructose intake: the importance of physical activity. *J Physiol.* 2019;597(14):3561-3571. doi:10.1113/JP278246
- Thorens B, Rodriguez A, Cruciani-Guglielmacci C, Wigger L, Ibberson M, Magnan C. Use of preclinical models to identify markers of type 2 diabetes susceptibility and novel regulators of insulin secretion - A step towards precision medicine. *Mol Metab.* 2019;27S(Suppl):S147-S154. doi:10.1016/j.molmet.2019.06.008
- Thurnhofer S, Vetter W. A gas chromatography/electron ionization-mass spectrometry-selected ion monitoring method for determining the fatty acid pattern in food after formation of fatty acid methyl esters. *J Agric Food Chem.* 2005 Nov 16;53(23):8896-903. doi: 10.1021/jf051468u. PMID: 16277380.
- Tomczyk MM, Dolinsky VW. The Cardiac Lipidome in Models of Cardiovascular Disease. *Metabolites.* 2020;10(6):254. Published 2020 Jun 17. doi:10.3390/metabo10060254
- van de Vossenberg JL, Driessen AJ, da Costa MS, Konings WN (1999) Homeostasis of the membrane proton permeability in *Bacillus subtilis* grown at different temperatures. *Biochim Biophys Acta* 1419: 97–104.
- van der Veen JN, Kennelly JP, Wan S, Vance JE, Vance DE, Jacobs RL. The critical role of phosphatidylcholine and phosphatidylethanolamine metabolism in health and disease. *Biochim Biophys Acta Biomembr.* 2017 Sep;1859(9 Pt B):1558-1572. doi: 10.1016/j.bbamem.2017.04.006. Epub 2017 Apr 11. PMID: 28411170.
- Van Gilst MR, Hadjivassiliou H, Jolly A, Yamamoto KR. Nuclear hormone receptor NHR-49 controls fat consumption and fatty acid composition in *C. elegans*. *PLoS Biol.* 2005;3(2):e53. doi:10.1371/journal.pbio.0030053

- van Meer G, Voelker DR, Feigenson GW. Membrane lipids: where they are and how they behave. *Nature reviews Molecular cell biology*. 2008;9(2):112-124. doi:10.1038/nrm2330.
- Valderrama MJ, Monteoliva-Sanchez M, Quesada E, Ramos-Cormenzana A. Influence of salt concentration on the cellular fatty acid composition of the moderately halophilic bacterium *Halomonas salina*. *Res Microbiol*. 1998 Oct;149(9):675-9. doi: 10.1016/s0923-2508(99)80015-1. PMID: 9826923.
- Vance, J. E. & Tasseva, G. Formation and function of phosphatidylserine and phosphatidylethanolamine in mammalian cells. *Biochim. Biophys. Acta* 1831, 543–554 (2013).
- Vieira, A. F. C., Xatse, M. A., Tifeki, H., Diot, C., Walhout, A. J. M., and Olsen., C. P. (2022) Monomethyl branched-chain fatty acids are critical for *Caenorhabditis elegans* survival in elevated glucose conditions. *J. Biol. Chem* 298, 101444.
- Volpe CMO, Villar-Delfino PH, Dos Anjos PMF, Nogueira-Machado JA. Cellular death, reactive oxygen species (ROS) and diabetic complications. *Cell Death Dis*. 2018 Jan 25;9(2):119. doi: 10.1038/s41419-017-0135-z. PMID: 29371661; PMCID: PMC5833737.
- Vrablik, T. L., and Watts. J. L. (2012) Emerging roles for specific fatty acids in developmental processes. *Genes Dev* 26, 631–637.
- Walker AK, Jacobs RL, Watts JL, Rottiers V, Jiang K, Finnegan DM, Shioda T, Hansen M, Yang F, Niebergall LJ, Vance DE, Tzoneva M, Hart AC, Näär AM. A conserved SREBP-1/phosphatidylcholine feedback circuit regulates lipogenesis in metazoans. *Cell*. 2011 Nov 11;147(4):840-52. doi: 10.1016/j.cell.2011.09.045. Epub 2011 Oct 27. PMID: 22035958; PMCID: PMC3384509.



- Wallace, M., Green, C. R., Roberts, L. S., Lee, Y. M., Mccarville, J. L., Sanchez-Gurmaches, J., . . . Metallo, C. M. (2018). *Enzyme promiscuity drives branched-chain fatty acid synthesis in adipose tissues* Springer Science and Business Media LLC. doi:10.1038/s41589-018-0132-2
- Wallach DF, Zahler PH. Protein conformations in cellular membranes. *Proc Natl Acad Sci U S A*. 1966 Nov;56(5):1552-9. doi: 10.1073/pnas.56.5.1552. PMID: 5230314; PMCID: PMC220029.
- Wang X, Zhang L, Zhang L, Wang W, Wei S, Wang J, Che H, Zhang Y. Effects of excess sugars and lipids on the growth and development of *Caenorhabditis elegans*. *Genes Nutr*. 2020 Jan 29;15:1. doi: 10.1186/s12263-020-0659-1. PMID: 32015763; PMCID: PMC6988283.
- Wang, F., Dai, Y., Zhu, X., Chen, Q., Zhu, H., Zhou, B., Tang, H., and Pang, S. (2021) Saturated very long chain fatty acid configures glycosphingolipid for lysosome homeostasis in long-lived *C. elegans*. *Nat. Commun*, 12, 1–14.
- Warner SO, Yao MV, Cason RL, Winnick JJ. Exercise-Induced Improvements to Whole Body Glucose Metabolism in Type 2 Diabetes: The Essential Role of the Liver. *Front Endocrinol (Lausanne)*. 2020;11:567. Published 2020 Aug 28. doi:10.3389/fendo.2020.00567
- Watts JL, Browse J. Genetic dissection of polyunsaturated fatty acid synthesis in *Caenorhabditis elegans*. *Proc Natl Acad Sci U S A*. 2002;99(9):5854–5859. doi:10.1073/pnas.092064799

- Watts JL. Using *Caenorhabditis elegans* to Uncover Conserved Functions of Omega-3 and Omega-6 Fatty Acids. *J Clin Med*. 2016 Feb 2;5(2):19. doi: 10.3390/jcm5020019. PMID: 26848697; PMCID: PMC4773775.
- Watts, J. L., & Ristow, M. (2017). Lipid and carbohydrate metabolism in *caenorhabditis elegans*. *Genetics*, 207(2), 413-446. doi:10.1534/genetics.117.300106
- Wu N, Shen H, Liu H, Wang Y, Bai Y, Han P. Acute blood glucose fluctuation enhances rat aorta endothelial cell apoptosis, oxidative stress and pro-inflammatory cytokine expression in vivo. *Cardiovasc Diabetol*. 2016 Aug 5;15(1):109. doi: 10.1186/s12933-016-0427-0. PMID: 27496150; PMCID: PMC4974767.
- Wu, G., Lu, Z. H., Kulkarni, N., Amin, R., and Ledeen, R. W. (2011) Mice lacking major brain gangliosides develop Parkinsonism. *Neurochem. Res* 36, 1706–1714.
- Yang X, Sheng W, Sun GY, Lee JC. Effects of fatty acid unsaturation numbers on membrane fluidity and  $\alpha$ -secretase-dependent amyloid precursor protein processing. *Neurochem Int*. 2011 Feb;58(3):321-9. doi: 10.1016/j.neuint.2010.12.004. Epub 2010 Dec 22. PMID: 21184792; PMCID: PMC3040984.
- Yuan-Li Chen, Jun Tao, Pei-Ji Zhao, Wei Tang, Jian-Ping Xu, Ke-Qin Zhang, & Cheng-Gang Zou. (2019). Adiponectin receptor PAQR-2 signaling senses low temperature to promote *C. elegans* longevity by regulating autophagy. *Nature Communications*,1-10. Retrieved from <https://www.nature.com/articles/s41467-019-10475-8>
- Yudkin J, Kang SS, Bruckdorfer KR. Effects of high dietary sugar. *Br Med J*. 1980;281(6252):1396. doi:10.1136/bmj.281.6252.1396
- Zhang Y, Tobias HJ, Auchus RJ, Brenna JT, Comprehensive 2-dimensional gas chromatography fast quadrupole mass spectrometry (GC  $\times$  GC-qMS) for urinary steroid

profiling: Mass spectral characteristics with chemical ionization, *Drug Test. Anal*, 3 (2011) 857–867. [PubMed: 22147458]

- Zheng J, Gao C, Wang M, Tran P, Mai N, Finley JW, Heymsfield SB, Greenway FL, Li Z, Heber D, Burton JH, Johnson WD, Laine RA. Lower Doses of Fructose Extend Lifespan in *Caenorhabditis elegans*. *J Diet Suppl*. 2017 May 4;14(3):264-277. doi: 10.1080/19390211.2016.1212959. Epub 2016 Sep 28. PMID: 27680107; PMCID: PMC5225670.
- Zhu, H., Shen, H., Sewell, A. K., Kniazeva, M., & Han, M. (2013). A novel sphingolipid-TORC1 pathway critically promotes postembryonic development in *caenorhabditis elegans*. *eLife*, 2, e00429. doi:10.7554/elife.00429
- Zhu H, Sewell AK, Han M. Intestinal apical polarity mediates regulation of TORC1 by glucosylceramide in *C. elegans*. *Genes Dev*. 2015 Jun 15;29(12):1218-23. doi: 10.1101/gad.263483.115. PMID: 26109047; PMCID: PMC4495394.
- Zoeller RA, Lake AC, Nagan N, Gaposchkin DP, Legner MA, Lieberthal W. Plasmalogens as endogenous antioxidants: somatic cell mutants reveal the importance of the vinyl ether. *Biochem J*. 1999;338 (Pt 3)(Pt 3):769-776.